MAREES TERRESTRES

BULLETIN D'INFORMATIONS

N°80

15 fevrier 1979

Association Internationale de Geodesie

Commission Permanente des Marees Terrestres

Editeur Prof. Paul MELCHIOR
Observatoire royal de Belgique
Avenue Circulaire 3
1180 Bruxelles

TABLE DES MATIERES N° 80

Ce Bulletin contient les articles distribués mais non présentés lors du VIII^{ème} Symposium International des Marées Terrestres (Bonn, septembre, 1977).

THE EFFECT OF EARTH LATERAL HETEROGENEITIES UPON THE TIDES

S.M. MOLODENSKY

On the basis of the results obtained earlier working formulas are received which permit to calculate the effect of small lateral heterogeneities in the elastic properties of the Earth upon the tidal waves on the Earth's surface. In the case of diurnal and semi-diurnal tidal waves the effect is manifested in the variation of amplitudes and in the phase lag. Phase lags are different in the different points of surface and contain (together with the amplitudes of tidal waves) the information about Earth's lateral heterogeneity.

Recently the lateral heterogeneity of the mantle was extensively studied on the basis of eigenfrequency splitting data / Dahlen, 1968, Zharkov, Lubimov, 1970, Madariaga, Aki, 1972, Luh, 1974, Dahlen, 1974, 1976 /.

Up to now tidal data don't contain reliable information about the lateral heterogeneity of the Earth. For instance, the differences of the factor δ, which were obtained on the frequency M_2 in Western Europe do not exceed the errors of measurements after excluding the influence of the ocean tide / Pertsev, Ivanova, 1975 /. The same situation takes place for measurements on the territory of the USSR / Pariisky et al., 1975 /. The measurements of Kuo et al., 1970 along the profile, crossing North America in west-east direction after including the corrections for the ocean tide give an anomal value of δ only in a few points / Pertsev, 1976 /.

Nevertheless it must be pointed out that with the improvement of measurements accuracy and the accuracy of cotidal maps the tidal data may give an important new information about the Earth's lateral heterogeneity. The principal advantages of tidal data comparing with the eigenfrequency splitting data are as follows:

1. Tidal measurements allow to expose the heterogeneity in the neighbourhood of the point of measurements, whereas eigenfrequencies give an information about the averaged heterogeneities.
2. The influence of the Earth lateral heterogeneity upon the eigenfrequencies as upon the tides depends on the orientation of heterogeneities relative to the wave. In the case of free oscillations determination of the waves orientation presents a rather difficult independent problem. This problem is complicated, in particular, by the rotational splitting of eigenfrequencies which excites the rotation of the tesseral waves relatively to the lateral heterogeneities. In contrast to the case of free oscillations, the orientation of tidal waves is known exactly at every moment of time. As the consequence of it, the investigation of the local heterogeneities and the determination of geographical coordinates of heterogeneities is more simple while using tidal data.

In this work the theory, connecting the Earth's lateral heterogeneities with the amplitudes and phase lags of tidal waves is studied. Because of the lack of data we shall not do any numerical computations, however the final expressions have the final form convenient for the computations.

1. Let's consider the statical tides in the laterally heterogeneous Earth which at the fixed moment of time are generated by the tidegenerating potential of the form:

$$V_e = V_{e_o} \left(\frac{r}{a}\right)^{n_o} Y_{n_o}^{m_o}(\theta,\phi), \tag{1}$$

where θ, ϕ are colatitude and longitude, $Y_{n_o}^{m_o}$ - spherical harmonic. The terms corresponding to $n_o = 3, 4 \ldots$ are small and practical interest offers the case $n_o = 2$, $m_o = 0, 1, 2$.

The potential (1) generates on the Earth's surface waves which in general case must be presented in the form:

$$\vec{u}(a) = \frac{\vec{r}}{r} H_{n_o}^{m_o}(a)\, Y_{n_o}^{m_o}(\theta,\phi) + T_{n_o}^{m_o}(a)\, \nabla Y_{n_o}^{m_o}(\theta,\phi) + \sum_{n=0}^{\infty} \sum_{m=-n}^{n} \frac{\vec{r}}{r} H_n^{m*}(a)\, Y_n^m(\theta,\phi) + T_n^{m*}(a)\, \nabla Y_n^m(\theta,\phi);$$

$$R(a) = R_{n_o}^{m_o}(a)\, Y_{n_o}^{m_o}(\theta,\phi) + \sum_{n=0}^{\infty} \sum_{m=-n}^{n} R_n^{m*}(a)\, Y_n^m(\theta,\phi), \tag{2}$$

where $\vec{u}$ is a displacement and R is a variation of potential. The first term in (2) corresponds to the tide in the spherically symmetric Earth and other waves determine the influence of the lateral heterogeneities. The simplest way of all the amplitudes in (2) determination is the application of Betti's

reciproical theorem to the equations of the statical equilibrium of spherically symmetric Earth.

Let (u°, R°) and (u^j, R^j) be the solutions of the elastic-gravitational equilibrium equations of the laterally homogeneous Earth with the hydrostatical initial stress, corresponding to different boundary conditions:

$$L_i(\vec{u}^\circ, R^\circ) = 0 \tag{3a}$$

$$L_i(\vec{u}^j, R^j) = 0 \tag{3b}$$

where

$$L_i(\vec{u}, R) = \rho\left[\frac{\partial}{\partial x_i}(R + (\vec{u}, \nabla V)) - \operatorname{div}\vec{u}\,\frac{\partial V}{\partial x_i}\right] + \frac{\partial \sigma_{ik}}{\partial x_k} \tag{3c}$$

$$\sigma_{ik} = \mu\left(\frac{\partial u_i}{\partial x_k} + \frac{\partial u_k}{\partial x_i}\right) + \lambda \operatorname{div}\vec{u}\,\delta_{ik} \tag{3d}$$

ρ, λ, μ - density and Lame's parameters, V - the potential of a Earth in the initial state, δ_{ik} - Kronekker, s symbol, R satisfies Poisson's equation:

$$\Delta R^\circ = 4\pi\chi \operatorname{div}(\rho\vec{u}^\circ); \tag{4a}$$

$$\Delta R^j = 4\pi\chi \operatorname{div}(\rho\vec{u}^j); \tag{4b}$$

Δ - Laplace's operator, χ - the gravitational constant. Then the work of elastic-gravitational forces $L_i(\vec{u}^\circ, R^\circ)$ on the displacements $(\vec{u}^j, R^j)$ is equal to the work of forces $L_i(\vec{u}^j, R^j)$ on the displacements $(\vec{u}^\circ, R^\circ)$:

$$\iiint_V \left[u_i^j L_i(\vec{u}^\circ, R^\circ) - u_i^\circ L_i(\vec{u}^j, R^j)\right] dv =$$

$$\iint_s \left[(u_i^j \sigma_{ik}^\circ - u_i^\circ \sigma_{ik}^j)\frac{\chi_k}{r} + R^j P^\circ - R^\circ P^j\right] ds = 0, \tag{5}$$

where v is volume which occupies the Earth and s its surface.

Further we shall use the length unit which is equal to averaged Earth's radius. Then v, s are the unit sphere and its surface. The components $\sigma_{ik}^\circ \frac{\chi_k}{r}$ and $\sigma_{ik}^j \frac{\chi_k}{r}$ (here and further we use iterational sum rule) determine the forces which act on the Earth's surface. We suppose that these forces are determined by some boundary conditions for solutions (u°, R°) and (u^j, R^j). P^j, P° is the value of a simple layer on the surface which is determined by the boundary conditions too. The values P°, P^j are connected with the outer and inner derivatives of R°, R^j and with the radial components H°, H^j of displacement in the form:

$$P^\circ = \frac{1}{4\pi\chi}\,(R^{\circ\prime}_{int.} - R^{\circ\prime}_{out.} - 4\pi\chi\rho\, H^\circ);$$
$$P^j = \frac{1}{4\pi\chi}\,(R^{j\prime}_{int.} - R^{j\prime}_{out.} - 4\pi\chi\rho\, H^j). \qquad (6)$$

The equality of a volume integral to zero in (5) is a trivial consequence of eq. (3a, b); the second part of this equation may be proved with the help of partial integration of a volume integral / S.M. Molodensky, 1977a /. The equation (5) for the surface integral points out to the existance of connections between the solutions which are determined by different boundary conditions (the connection of Love numbers and loading Love numbers, / S.M. Molodensky, 1977b /).

Let then the solution (u°, R°) describe a statical tide in the laterally homogeneous Earth which is generated by the potential (1). Then

$$\sigma^\circ_{ik}\,\frac{\chi_k}{r} = 0;$$
$$P^\circ = \frac{2n+1}{4\pi\chi}\,V_e \quad (a) \qquad (7)$$

Let the operator L has a small variation δL corresponding to the change from a laterally homogeneous to a heterogeneous Earth model. Then instead of (3a), (4a) we have for the perturbation of the solution:

$$\delta L_i(\vec{u}^\circ, R^\circ) + L_i\,(\delta\vec{u}, \delta R) = 0; \qquad (8a)$$

$$\Delta(\delta R) = 4\pi\chi\ \mathrm{div}\,(\delta\rho\,\vec{u}^\circ + \rho\,\delta\,\vec{u}), \qquad (8b)$$

where $\delta\vec{u}$, δR - the variations of the solution. Then the connection of type (5) for the pair of $(\delta\vec{u}, \delta R)$ and $(\vec{u}^j, R^j)$ may be obtained by excluding from (5) $L_i\,(\delta\vec{u}, \delta R)$ with the help of (8a) using the boundary conditions and the connection (8b). Finally we get: / S.M. Molodensky, 1977 a /:

$$\iint_S (\delta u_i\ \sigma^j_{ik}\,\frac{\chi_k}{r} + \delta R\ P^j)\ ds = F^j\,(\delta\rho, \delta\mu, \delta\lambda) \qquad (9)$$

where

$$F^j(\delta\rho, \delta\mu, \delta\lambda) = \iiint_V \left\{ \delta\rho(u^\circ, \nabla R^j) + u^j_i\,\delta L_{i\rho}(\vec{u}^\circ, R^\circ) - \delta\mu\left(\frac{\partial u^\circ_i}{\partial\chi_k} + \frac{\partial u^\circ_k}{\partial\chi_i}\right)\frac{\partial u^j_i}{\partial\chi_k} - \delta\lambda\ \mathrm{div}\,\vec{u}^\circ\ \mathrm{div}\,\vec{u}^j \right\} d\tau;$$

$\delta L_{i\rho}$ is a variation of i-th component of the operator L connected with the density's variation.

Determining the auxiliary solutions (u^j, R^j) in (9) by different boundary conditions we can obtain the serched values $\delta \vec{u}$, δR in every point of Earth's surface.

Indeed, supposing

1) $j = 1$,

$$\sigma^j_{ik} \frac{\chi_k}{r} = f_1 \frac{\chi_i}{r} \frac{\delta(\theta-\theta_o)\ \delta(\phi-\phi_o)}{\sin\phi}, \qquad (11a)$$

$$P^j = 0,$$

(where f_1 is a unit force which is normal to the surface and acts in the point with the coordinates (θ_o, ϕ_o)): and then integrating the left side of (9) with respect to θ, ϕ we obtain:

$$\delta u_r\ (\theta_o, \phi_o) = F^j\ (\delta\rho, \delta\mu, \delta\lambda)\ /_{j=1},$$

where δu_r is a radial component of $\vec{u}$ on the surface. By analogy, determining $\sigma^j_{ik} \frac{\chi_k}{r}$ by the unit tangential force, we shall obtain $\delta u_{\text{tangential}}\ (\theta_o, \phi_o)$. Finally, putting

3) $j = 3$,

$$\sigma^j_{ik} \frac{\chi_k}{r} = 0; \qquad (11b)$$

$$P^j = P^o \frac{\delta(\theta-\theta_o)\ \delta(\phi-\phi_o)}{\sin\phi},$$

we obtain

$$\delta R(\theta_o, \phi_o) = F^j\ (\delta\rho, \delta\mu, \delta\lambda)/_{j=3}$$

The solutions which are determined by the boundary conditions (11) may be obtained numerically by means of development of δ - function into a spherical harmonics $Y^m_n\ (\theta,\phi)$ integrating the equations of the statical equilibrium of the laterally homogeneous Earth for every n and summarizing the obtained solutions, completely in the same manner, as it is made for the calculation of the oceans influence upon the tides / Pertsev, 1976, et al./.

Then the substitution of every spherical harmonic into (9) determines one coefficient of development of tidal displacements or potential variations.

Indeed, putting (u^j, R^j) in the form

$$u_i^j = H_n^j(r)\frac{x_i}{r}Y_n^m(\theta,\phi) + T_n^j(r)\frac{\partial}{\partial x_i}Y_n^m(\theta,\phi);$$
$$R^j = R_n^j(r)\,Y_n^m(\theta,\phi) \qquad (12)$$

we obtain:

$$\sigma_{ik}^j\frac{x_k}{r}\Big/_s = N_n^j(1)\frac{x_i}{r}Y_n^m(\theta,\phi) + M_n^j(1)\frac{\partial}{\partial x_i}Y_n^m(\theta,\phi);$$
$$P^j\Big/_s = \frac{L_n^j(1) + (n+1)R_n^j(1)}{4\pi\chi}Y_n^m(\theta,\phi) \qquad (13)$$

where, following the notations / M.S. Molodensky, 1953 /,

$$N_n^j = (\lambda + 2\mu)H_n^{j\prime} + \lambda\left(\frac{2}{r}(H_n^j)' - \frac{n(n+1)}{r^2}T_n^j\right);$$
$$M_n^j = r^2\mu\left((T_n^j)' + H_n^j - \frac{2}{r}T_n^j\right); \qquad (14)$$
$$L_n^j = r^2\left((R_n^j)' - 4\pi\chi\rho H_n^j\right);$$
$$r/_s = a = 1.$$

Defining the auxiliary solutions by the boundary conditions:

1) $j=1$ $\quad N_n^j(1) = 1;\quad M_n^j(1) = 0;\quad P_n^j(1) = 0;$

2) $j=2$ $\quad N_n^j(1) = 0;\quad M_n^j(1) = 1;\quad P_n^j(1) = 0;$

3) $j=3$ $\quad N_n^j(1) = 0;\quad M_n^j(1) = 0;\quad P_n^j(1) = 1;$

substituting (2), (13) into (9), we obtain after integration over the angular variables:

$$F_{nm}^j(\delta\rho,\ \delta\mu,\ \delta\lambda) = c\begin{cases} H_n^{m*}(1) & \text{if } j=1 \\ T_n^{m*}(1) & \text{if } j=2 \\ R_n^{m*}(1) & \text{if } j=3 \end{cases} \qquad (16)$$

where

$$c = \iint_S \left(Y_n^m(\theta,\phi)\right)^2 ds = \frac{2\pi\varepsilon\,(n+m)!}{(2n+1)\,(n-m)!} \tag{16a}$$

$$\varepsilon = \begin{cases} 1 & \text{if} \quad m \neq 0 \\ 0 & \text{if} \quad m = 0 \end{cases}$$

2. So, both the tidal displacements and the variation of the potential on the Earth's surface are determined by the values of integral (10) which must be calculated for the various n, m and j = 1, 2, 3. The relation (16) is correct for the arbitrary variations of $\delta\rho$, $\delta\lambda$, $\delta\mu$. But the effect of density's lateral heterogeneities cannot be exactly computed, if we know the density's heterogeneities only. Indeed, if the density has a laterally heterogeneous part, then the initial stress is nonhydrostatical and the operator L obtains the additional terms, connected with the initial stress field / Dahlen, 1972 /. Thus the variation $\delta L: \rho$ in eq. (10) contains 1) the known terms, which are connected with the density's and gravity's variations and 2) unknown terms which are connected with the initial stress field.

The relative accuracy of modern tidal measurements is less, than the average variations of density (estimated on the ground of gravity anomalies). Owing to this the lateral heterogeneity of density may be neglected in the first approximation. Further we shall consider the effect of parameters λ, μ only.

Let's write (10) in the form convenient for the computations. Following the method which is used in the eigen-frequency theory, let's present the lateral heterogeneity in the form of infinite spherical harmonic series

$$\delta\mu(\theta, \phi, r) = \sum_{\ell=1}^{\infty} \sum_{p=-\ell}^{\ell} \mu_{\ell p}^{(r)}\, Y_\ell^p(\theta, \phi);$$

$$\delta\lambda(\theta, \phi, r) = \sum_{\ell=1}^{\infty} \sum_{p=-\ell}^{\ell} \lambda_{\ell p}^{(r)}\, Y_\ell^p(\theta, \phi). \tag{17}$$

Then the part of (10), which is connected with $\delta\lambda$ comes at once to the integral including three spherical harmonics:

$$F_{nm}^j(\delta\lambda) = -\iiint \left[\sum_{\ell=1}^{\infty} \sum_{p=-\ell}^{\ell} \lambda_{\ell p}^{(r)} \mathscr{D}_{n_o}(r) \mathscr{D}_n^j(r)\right.$$

$$\cdot\, Y^{p}(\theta,\phi)\, Y^{m_o}_{n_o}(\theta,\phi)\, Y^{m}_{n}(\theta,\phi)\Big]\, dv = \tag{18}$$

$$= \sum_{\ell=1}^{\infty}\sum_{p=-\ell}^{\ell} A_{\ell p n m n_o m_o} \int_0^i r^2\, \lambda_{\ell p}(r)\, \mathscr{D}_{n_o}(r)\cdot$$

$$\mathscr{D}^{j}_{n}(r)\, dr,$$

where

$$\mathscr{D}_{n_o}(r) = H'_{n_o} + \frac{2}{r} H_{n_o} - \frac{n_o(n_o+1)}{r^2} T_{n_o};$$

$$\mathscr{D}^{j}_{n}(r) = (H^{j}_{n})' + \frac{2}{r} H^{j}_{n} - \frac{n(n+1)}{r^2} T^{j}_{n};$$

$$\operatorname{div} \vec{u}^{\circ} = \mathscr{D}_{n_o}(r)\, Y^{m_o}_{n_o}(\theta,\phi); \tag{19}$$

$$\operatorname{div} \vec{u}^{j}\, \mathscr{D}^{j}_{n}(r)\, Y^{m}_{n}(\theta,\phi);$$

$$A_{\ell p n m n_o m_o} = \iint_s Y^{p}_{\ell}(\theta,\phi)\, Y^{m}_{n}(\theta,\phi)\, Y^{m_o}_{n_o}(\theta,\phi)\, ds.$$

For the integrals (19) there are the analytical expressions / Edmonds, 1957, Luh, 1974 /. We shall not give this expression here because of its unwieldity. It must be pointed out only, that (19) is equal to zero if the indexes 1, n, n_o do not satisfy the triangle inequality. Thus, in (19) the index 1 has in fact five values only:

$$1 = n-2,\ n-1,\ n,\ n+1,\ n+2$$

The index p has two values only:

$$p = m - m_o; \qquad p = m + m_o$$

So, every partial wave in development (2) depends on ten coefficients $\lambda_{\ell p}(r)$ only.

If the development (17) is finite ($1 \le l_o$, where l_o is some fixed value), than the series (2) do not contain the terms with $n > l_o+2$.

To calculate $F^{j}_{nm}(\delta\mu)$ let's introduce some new variables h^{j}_{n}, t^{j}_{n} with the help of which we shall write expression (12) in more compact form:

$$u^{j}_{i} = h^{j}_{n}(r)\, \chi_i\, \omega^{m}_{n} + t^{j}_{n}(r)\, \frac{\partial\, \omega^{m}_{n}}{\partial \chi_i} \tag{20}$$

where $\omega^{m}_{n} = r^{n}\, Y^{m}_{n}(\theta,\phi)$ is the harmonic polynom of degree n which satisfies the equations:

$$\Delta\,\omega_n^m = 0;$$
$$\chi_i \frac{\partial\,\omega_n^m}{\partial \chi_i} = n\,\omega_n^m; \tag{21}$$

h_n^j, t_n^j are connected with H_n^j, T_n^j by the simple relations:

$$h_n^j = \frac{H_n^j}{r^{n+1}} - \frac{n\,T_n^j}{r^{n+2}};$$
$$t_n^j = \frac{T_n^j}{r^n} \tag{22}$$

In this notation we obtain:

$$\frac{\partial u_i^j}{\partial \chi_k} + \frac{\partial u_k^j}{\partial \chi_i} = 2(h_n^j)'\,\frac{\chi_i\,\chi_k}{r}\,\omega_n^m + 2\,h_n^j\,\omega_n^m\,\delta_{ik} + \left(h_n^j + \frac{(t_n^j)'}{r}\right)$$
$$(\chi_i\,\nabla_k\,\omega_n^m + \chi_k\,\nabla_i\,\omega_n^m) + 2t_n^j\,\nabla_i\,\nabla_k\,\omega_n^m;$$

$$-F_{nm}^j\,(\delta\mu) = \frac{1}{2}\left(\frac{\partial\,u_i^o}{\partial\,\chi_k} + \frac{\partial\,u_k^o}{\partial\,\chi_i}\right)\left(\frac{\partial\,u_i^j}{\partial\,\chi_k} + \frac{\partial\,u_k^j}{\partial\,\chi_i}\right) =$$
$$= h'_{n_o}\,\omega_{n_o}^{m_o}\,\frac{1}{r}\left[2(h_n^j)'\,r^3\,\omega_n^m + 2r^2\,h_n^j\,\omega_n^m + 2\left(h_n^j + \frac{(t_n^j)'}{r}\right)r^2\,n\,\omega_n^m +\right.$$
$$\left. + 2\,t_n^j\,\chi_i\,\chi_k\,\nabla_i\,\nabla_k\,\omega_n^m\right] + h_{n_o}\,\omega_{n_o}^{m_o}\left[2(h_n^j)'\,r\,\omega_n^m + 6\,h_n^j\,\omega_n^m +\right.$$
$$\left. + 2\left(h_n^j + \frac{(t_n^j)'}{r}\right)n\,\omega_n^m + 2\,t_n^j\,\nabla^2\,\omega_n^m\right] + (h_{n_o} + t'_{n_o}/r)\cdot$$
$$\cdot\,(\chi_i\,\nabla_k\,\omega_{n_o}^{m_o} + \chi_k\,\nabla_i\,\omega_{n_o}^{m_o})\left[h_n^j\,\frac{\chi_i\,\chi_k}{r}\,\omega_n^m + h_n^j\,\omega_n^m\,\delta_{ik} +\right.$$
$$\left. + \frac{1}{2}\left(h_n^j + \frac{(t_n^j)'}{r}\right)(\chi_i\,\nabla_k\,\omega_n^m + \chi_k\,\nabla_i\,\omega_n^m) + t_n^j\,\nabla_i\,\nabla_k\,\omega_n^m\right] +$$
$$+ t_{n\cdot}\,\nabla_i\,\nabla_k\,\omega_{n_o}^{m_o}\left[2(h_n^j)'\,\frac{\chi_i\,\chi_k}{r}\,\omega_n^m + 2h_n^j\,\omega_n^m\,\delta_{ik} +\right.$$
$$\left. + \left(h_n^j + \frac{(t_n^j)'}{r}\right)(\chi_i\,\nabla_k\,\omega_n^m + \chi_k\,\nabla_i\,\omega_n^m) + t_n^j\,\nabla_i\,\nabla_k\,\omega_n^m\right].$$

Using the relations (21), we get:

$$(\chi_i\,\nabla_k\,\omega_{n_o}^{m_o})\,(\nabla_i\,\nabla_k\,\omega_n^m) = \nabla_i\,(\chi_k\,\nabla_i\,\omega_{n_o}^{m_o}\,\nabla_k\,\omega_n^m) -$$

$$- \nabla_k \omega_n^m (\chi_k \nabla^2 \mu_{n_o}^{m_o} + \nabla_i \omega_{n_o}^{m_o} \delta_{ik}) = (n-1)(\nabla \omega_n^m, \nabla \omega_{n_o}^{m_o});$$

$$\omega_n^m \chi_i \chi_k \nabla_i \nabla_k \omega_{n_o}^{m_o} = \nabla_i (\nabla_k \omega_{n_o}^{m_o} \chi_i \chi_k \omega_n^m) -$$

$$- \nabla_k \omega_{n_o}^{m_o} (\chi_i \chi_k \nabla_i \omega_n^m + 3 \chi_k \omega_n^m + \chi_i \delta_{ik} \omega_n^m) =$$

$$= \nabla_i (n_o \omega_{n_o}^{m_o} \chi_i \omega_n^m) - n n_o \omega_n^m \omega_{n_o}^{m_o} - 4 n_o \omega_n^m \omega_{n_o}^{m_o} =$$

$$= 3 n_o \omega_{n_o}^{m_o} \omega_n^m + n_o^2 \omega_n^m \omega_{n_o}^{m_o} + n n_o \omega_n^m \omega_{n_o}^{m_o} = n_o (n_o - 1) \omega_n^m \omega_{n_o}^{m_o}.$$

And so,

$$-F_{nm}^j(\delta\mu) = \sum_{\ell=1}^{\infty} \sum_{p=-\ell}^{\ell} \iiint_V \left\{ \omega_\ell^p \omega_n^m \omega_{n_o}^{m_o} f_{nn_o}^{(1)\ell p}(r) + \right.$$

$$\left. + \omega_\ell^p (\nabla \omega_n^m, \nabla \omega_{n_o}^{m_o}) f_{nn_o}^{(2)\ell p}(r) + \omega_\ell^p \nabla_i \nabla_k \omega_n^m \cdot \nabla_i \nabla_k \omega_{n_o}^{m_o} f_{nn_o}^{(3)\ell p}(r) \right\} dv,$$

where

$$f_{nn_o}^{(1)\ell p}(r) = \frac{2\mu_\ell p(r)}{r^\ell} \left\{ r^2 (h_n^j)' h'_{n_o} + r(h_n^j)' h_{n_o} + \right.$$

$$+ r h_n^j h'_{n_o} + n r h'_{n_o} \left(h_n^j + \frac{(t_n^j)'}{r} \right) + n_o r (h_n^j)' \left(h_{n_o} + \frac{t'_{n_o}}{r} \right) +$$

$$+ \frac{n(n-1)}{r} h'_{n_o} t_n^j + \frac{n_o(n_o-1)}{r} (h_n^j)' t_{n_o} + 3 h_n^j h_{n_o} +$$

$$\left. + n h_{n_o} \left(h_n^j + \frac{(t_n^j)'}{r} \right) + n_o h_n^j \left(h_{n_o} + \frac{(t n_o)'}{r} \right) + \frac{1}{2} \left(h_{n_o} + \frac{(t_{n_o})'}{r} \right) \left(h_n^j + \frac{(t_n^j)'}{r} \right); \right. \quad (23)$$

$$f_{nn_o}^{(2)\ell p}(r) = \frac{\mu_\ell p(r)}{r^\ell} r^2 h_{n_o} + \frac{t'_{n_o}}{r} h_n^j + \frac{(t_n^j)'}{r} +$$

$$+ 2(n-1) t_n^j h_{n_o} + \frac{t'_{n_o}}{r} + 2(n_o - 1) t_{n_o} h_n^j + \frac{(t_n^j)'}{r};$$

$$f_{nn_o}^{(3)\ell p}(r) = \frac{2\mu_\ell p(r)}{r^\ell} t_n^j t_{n_o}.$$

We have further

$$\iiint_V f_{nn_o}^{(1)\ell p}(r) \omega_\ell^p \omega_n^m \omega_{n_o}^{m_o} dv = A_{\ell p n m n_o m_o} \int_0^i r^{\ell+n+n_o+2} f_{nn_o}^{(1)\ell p}(r) dr, \quad (24)$$

where $A_{\ell pnmn_o m_o}$ is determined by (19). The integration over the angular variables is somewhat more difficult in the second and the third terms of (22). For their calculation let's first calculate the integrals

$$I^{\ell p\ (1)}_{n_o m_o nm} = \iiint_V \omega^p_\ell\ (\nabla\ \omega^m_n,\ \nabla\ \omega^{m_o}_{n_o})\ dv$$

and

$$I^{\ell p\ (2)}_{n_o m_o nm} = \iiint_V \omega^p_\ell\ \nabla_i\ \nabla_k\ \omega^m_n\ \nabla_i\ \nabla_k\ \omega^{m_o}_{n_o}\ dv.$$

Partially integrating $I^{\ell p\ (1)}_{n_o m_o nm}$ and using (21) we obtain

$$I^{\ell p\ (1)}_{n_o m_o nm} + I^{n_o m_o\ (1)}_{\ell pnm} = n\ A_{\ell pnmn_o m_o} \qquad (25)$$

and two other identities which may be obtained from (25) by a transposition of ω^p_ℓ, ω^m_n, $\omega^{m_o}_{n_o}$. Solving these equations, we obtain:

$$I^{\ell p(1)}_{nmn_o m_o} = \frac{1}{2}\ (n + n_o - \ell)\ A_{\ell pnmn_o m_o} \qquad (25a)$$

Partially integrating $I^{\ell p\ (2)}_{n_o m_o nm}$, we get:

$$I^{\ell p\ (2)}_{n_o m_o nm} = \iint \chi_i\ (\omega^p_\ell\ \nabla_k\ \omega^m_n\ \nabla_i\ \nabla_k\ \omega^{m_o}_{n_o})\ ds - I^{n_o m_o (3)}_{\ell pnm},$$

where

$$I^{n_o m_o\ (3)}_{\ell p\ n\ m} = \iiint_V \nabla_i\ \omega^p_\ell\ \nabla_k\ \omega^m_n\ \nabla_i\ \nabla_k\ \omega^{m_o}_{n_o}.$$

Using (21), we have:

$$\chi_i\ \nabla_i\ \nabla_k\ \omega^{m_o}_{n_o} = \nabla_k\ (\chi_i\ \nabla_i\ \omega^{m_o}_{n_o}) - \nabla_i\ \omega^{m_o}_{n_o}\ \delta_{ik} = (n_o - 1)\ \nabla_k\ \omega^{m_o}_{n_o}$$

and

$$\iint_S \chi_i\ \omega^p_\ell\ \nabla_k\ \omega^m_n\ \nabla_k\ \omega^{m_o}_{n_o}\ ds = (n_o - 1) \iint \omega^p_\ell\ (\nabla\ \omega^m_n,\ \nabla\ \omega^{m_o}_{n_o})\ ds = (n_o - 1)(\ell + n + n_o + 1) \qquad (27)$$

$$I^{\ell p\ (1)}_{nmn_o m_o} = \frac{1}{2}\ (n_o - 1)(n_o + n - \ell)(\ell + n + n_o + 1)\ A_{\ell pnmn_o m_o}$$

After the partial integration of $I^{n_o m_o}_{\ell pnm}$ we obtain:

$$I^{n_o m_o (3)}_{\ell pnm} + I^{nm\ (3)}_{\ell pn_o m_o} = \iint_S \chi_i\ \nabla_i\ \omega^p_\ell\ (\nabla\ \omega^m_n,\ \nabla\ \omega^{m_o}_{n_o})\ ds = \ell(\ell + n + n_o + 1)\ I^{\ell p(1)}_{n_o m_o nm}.$$

Making a cyclical transposition of indexes $(l, p) \to (n, m) \to (n_o, m_o)$ in this relation and solving the obtained system of three equations with three variables, we get:

$$I^{n_o m_o (3)}_{\ell p n m} = \frac{1}{2}(\ell+n+n_o+1)\left(-n_o I^{n_o m_o (1)}_{\ell p n m} + \ell I^{\ell p (1)}_{n m n_o m_o} + n I^{n m (1)}_{\ell p n_o m_o}\right),$$

or, substituting (25a),

$$I^{n_o m_o (3)}_{\ell p n m} = \frac{1}{4}(\ell+n+n_o+1)(n_o^2-n^2-\ell^2+2n\ell). \tag{28}$$

$$A_{\ell p n m n_o m_o}.$$

Substituting (27), (28) into (26), we obtain:

$$I^{\ell p (2)}_{n_o m_o n m} = \frac{1}{4}(\ell+n+n_o+1)(n_o+n-\ell). \tag{29}$$

$$.(n_o+n-\ell-2).\ A_{\ell p n m n_o m_o}$$

With the help of integrals (25a), (29) we can integrate (22) over the angular variables, taking into account that a radial part of the function which is under the integration in (22), (29) is homogeneous polynom of the degree $\ell+n+n_o-2$ or $\ell+n+n_o-4$.

If we denote

$$I = \iiint_V r^N X(\theta,\phi)\, dv,$$

then, obviously

$$\iiint_V f(r)\, r^N X(\theta,\phi) dv = (N+3)\, I \int_0^1 f(r)\, r^{N+2}\, dr.$$

Using this relation and the integrals (25a), (29), we obtain:

$$\iiint_V \omega^p_\ell \left(\nabla \omega^m_n, \nabla \omega^{m_o}_{n_o}\right) f^{(2)}_{n n_o \ell p}(r)\, dv = \frac{1}{2}(\ell+n+n_o+1)(n+n_o-\ell).\ A_{\ell p n m n_o m_o} \tag{30}$$

$$\int_0^1 f^{(2)}_{n n_o \ell p}(r)\, r^{\ell+n+n_o}\, dr;$$

$$\iiint_V \omega^p_\ell\, \nabla_i \nabla_k \omega^{m_o}_{n_o}\, \nabla_{ik} \nabla_k \omega^m_n\, f^{(3)}_{n n_o \ell p}(r)\, dv = \frac{1}{4}(\ell+n+n_o-1)(\ell+n+n_o+1)(n_o+n-\ell)(n_o+n-\ell-2) \tag{31}$$

$$\int_0^1 f^{(3)}_{n n_o \ell p}(r)\, r^{\ell+n+n_o-2}\, dr$$

and finally we lead the expression (22) to the form:

$$-F^{j}_{nm}(\delta\mu) = \sum_{\ell=1}^{\infty}\sum_{p=-\ell}^{\ell} A_{\ell p n m n_o m_o}\int_o^1 r^{\ell+n+n_o}\,dr.$$
$$\Big\{ r^2 f^{(1)}_{nn_o\ell p}(r) + \frac{1}{2}(\ell+n+n_o+1)(n+n_o-\ell). \qquad (32)$$
$$f^{(2)}_{nn_o\ell p}(r) + \frac{1}{4}(\ell+n+n_o+1)(\ell+n+n_o-1).$$
$$(n+n_o-\ell)(n_o+n-\ell-2).\frac{1}{r^2} f^{(3)}_{nn_o\ell p}(r)\Big\}.$$

So, $F^{j}_{nm}(\delta\mu)$ as well as $F^{j}_{nm}(\delta\lambda)$ is expressed from the integral (19). It means that sum (32) as well as (18) in fact contains no more than ten terms (ℓ=n-2, n-1, n, n+1, n+2, p=m-m_o or p=m+m_o).

The series (2) don't contain the terms with $n > \ell_o+2$ if the development of $\delta\mu(r,\theta,\phi)$ (17) does not contain the terms with $\ell > \ell_o$.

For the large values n all the integrals (19) decrease to the Earth's centre as r^n. It means that the waves of a high order are dependent upon the lateral heterogeneities in the layer which is close to the Earth surface and has an effective thickness $a - r \sim \frac{a}{n}$.

In the simplest case $\ell = p = 0$ the relations (16), (18), (32) determine the dependence of Love numbers upon the small variations of the density and Lame's parameters in the spherically symmetric Earth. In this case the relations obtained here coincide with the appropriate relations /S.M. Molodensky, 1976/.

3. Up to now we considered the amplitudes of the statical tides on the surface of the laterally heterogeneous Earth at some fixed momentum of time. Let's discuss the consequences of the obtained results for semidiurnal, diurnal and the zonal tidal waves. Accounting the dependence upon the time the tidegenerating potential (1) may be presented in the form:

$$V_e = V_{eo}\left(\frac{r}{a}\right)^{n_o} P^{m_o}_{n_o}(\cos\theta)\cos(\sigma f - m_o\phi) =$$
$$= V_{eo}\left(\frac{r}{a}\right)^{n_o}\left[Y^{m_o}_{n_o}(\theta,\phi)\cos\sigma f + Y^{-m_o}_{n_o}(\theta,\phi)\sin\sigma f\right] \qquad (33)$$

where t - time, σ - angular frequency of the tide,

$$Y^{m_o}_{n_o}(\theta,\phi) = P^{m_o}_{n_o}(\cos\theta)\cos m_o\phi;$$
$$Y^{-m_o}_{n_o}(\theta,\phi) = P^{m_o}_{n_o}(\cos\theta)\sin m_o\phi.$$

In the case of the zonal ($m_o = 0$) tides the expression (35) differs from (1) by the multiplier cos σf only. The non-perturbing solution (u^o, R^o) differs from the statical one by the same multiplier. Assuming that the auxiliary solutions (u^j, R^j) don't

depend upon the time as well as in (12) from the relation (9) we obtain that the values δu, $\delta R/_s$ are dependent upon the time as well as $\cos \sigma t$. So, the tidal waves which are generated by a zonal (longperiodical) tide-generating wave have the same phase and frequency on the Earth's surface as the tidegenerating potential. The lateral heterogeneity is manifested in the dependence of the factors δ, γ upon the point of measurements on the Earth's surface only. After the calculation of the coefficients $H_n^{m^*}(a)$, $R_n^{m^*}(a)$ with the help of the relations (18), (32) and (16) the dependence of δ and γ upon θ, ϕ may be determined by the simple way:

$$\Delta\delta(\theta,\phi) = \frac{1}{Y_{n_o}^{m_o}(\theta,\phi)} \sum_{n=o}^{\infty} \sum_{m=-n}^{n} \left[H_n^{m^*}(a) - \frac{n+1}{2} R_n^{m^*}(a) \right] Y_n^m(\theta,\phi); \tag{34}$$

$$\Delta\gamma(\theta,\phi) = \frac{1}{Y_{n_o}^{m_o}(\theta,\phi)} \sum_{n=o}^{\infty} \sum_{m=-n}^{n} \left[R_n^{m^*}(a) - H_n^{m^*}(a) \right] Y_n^m(\theta,\phi),$$

where $Y_{n_o}^{m_o}(\theta,\phi) = \frac{3}{2}\cos^2\theta - \frac{1}{2}$ in case $m_o=0$.

If the dependence of δ and γ upon θ, ϕ is known from the measurements it is possible to put the inverse problem: namely, resolving $\Delta g(\theta,\phi)$, or tilt (θ,ϕ) into the series of spherical harmonics, we can determine the coefficients $H_n^{m^*}(a)$, $R_n^{m^*}(a)$, which are equal to F_{nm}^j for $j=1$ or $j=3$. Then it is possible to solve the equations (18), (32) and to determine the coefficients $\lambda_{\ell p}(r)$, $\mu_{\ell p}(r)$. Then every value of F_{nm}^j gives one integral (with respect to r) condition on serched coefficients. The choice of an initial meridian is obviously unimportant: the coefficients $\lambda_{\ell p}(r)$, $\mu_{\ell p}(r)$ are determined in the same system of coordinates which we choose for the development of $\delta(\theta,\phi)$, $\gamma(\theta,\phi)$.

Let's consider now the waves which are generated by a diurnal or semi-diurnal ($m_o=1,2$) tidegenerating potential.

The amplitudes of the tidal waves are determined in this case at every fixed momentum of time by the same development (2). However, the disfiguration of the tidal bulge by the lateral heterogeneities and the rotation of the tidal wave in case $m \neq 0$ leads to the new effect - the influence of the lateral heterogeneities upon the phase lag. For its estimation let's write the solution of the statical tidal equilibrium equations for the spherically-symmetric Earth corresponding to the tidegenerating potential (35):

$$\vec{\zeta}^a = \frac{\vec{r}}{r} H_{n_o}^{m_o}(r) \left(Y_{n_o}^{m_o}(\theta,\phi) \cos\sigma t + Y_{n_o}^{-m_o}(\theta,\phi) \sin\sigma t + T_{n_o}^{m_o}(r) \left[\cos\sigma t \, \nabla Y_{n_o}^{m_o}(\theta,\phi) + \sin\sigma t \, \nabla Y_{n_o}^{-m_o}(\theta,\phi) \right] \right); \tag{35}$$

$$R^{\circ} = R_{n_o}^{m_o}(r)\left[Y_{n\bar{o}}^{m_o}(\theta,\phi)\cos\sigma t + Y_{n_o}^{-m_o}(\theta,\phi)\sin\sigma t\right].$$

We shall assume the auxiliary solutions (u^j, R^j) to be independent upon the time. Substituting (35), (12) into (10), we obtain:

$$F_{nm}^{j}(\delta\lambda, \delta\mu, t) = F_{nm}^{j(1)}(\delta\lambda, \delta\mu)\cos\sigma t + F_{nm}^{j(2)}(\delta\lambda, \delta\mu)\sin\sigma t = F_{nm}^{j(1)}(\delta\lambda, \delta\mu)\sqrt{1 + tg^2\,\psi_{nm}}\cos(\sigma t - \psi_{nm}). \tag{36}$$

where $F_{nm}^{j(1)}(\delta\lambda, \delta\mu)$ is determined by (18), (32) for $m_o = 1$ or 2 and $F_{nm}^{j(2)}(\delta\lambda, \delta\mu)$ is determined by the same relations for $m_o = -1$ or $m_o = -2$, consequently,

$$tg\,\psi_{nm} = \frac{F_{nm}^{j(2)}}{F_{nm}^{j(1)}} \tag{37}$$

Using (37), we can see that the phase of every partial wave differs essentially from phase of the tidegenerating potential. Indeed, the amplitude value of tidegenerating potential (33) on the initial longitude (ϕ=0) corresponds to the momentum of time $t = 0$. The coefficients F_{nm}^{j} (which are connected with the displacements and the potential variations in accordance with (16) have an amplitude value at the momentum

$$t = \frac{\psi_{nm}}{\sigma}$$

The value ψ_{nm} is not a small one in general case. For instance, in the simplest case, when the lateral heterogeneities in (17) are presented by one term only with $\ell = \ell_o$, $p = p_o$, we obtain from (18), (32):

$$tg\,\psi_{nm} = \frac{A_{\ell_o p_o nmn_o - m_o}}{A_{\ell_o p_o nmn_o m_o}}$$

This ratio alters from 0 to $\pm\infty$ for different n, m, ℓ_o, p_o and does not decrease when $\lambda_{\ell_o p}$, $\mu_{\ell_o p}$ decrease. The small value of the whole phase lag is a consequence of the smallness of the partial waves amplitudes, but not the consequence of the smallness of the phase lag for the partial waves. So, we may assume that phase lag in general case is the value of the same order of smallness as the ratio of the partial waves amplitudes to the amplitude of the principal waves and the variations of the factors δ, γ on the Earth's surface.

Summarizing the partial waves (2), it is possible to determine the whole values of the amplitudes and phase lags on the Earth's surface. For the tidal variations of the gravity we obtain:

$$\Delta g\ (\theta,\phi) = -\frac{2V_{eo}}{a}\left\{\left[\delta_{n_o}\, P_{n_o}^{m_o}\ (\cos\theta)\cos m_o\phi + \chi_1\ (\theta,\phi)\right]\cos\sigma t + \right.$$

$$\left.\left[\delta_{n_o}\, P_{n_o}^{m_o}\ (\cos\theta)\sin m_o\phi + \chi_2\ (\theta,\phi)\right]\sin\sigma t\right\}, \qquad (38)$$

where

$$\chi_1\ (\theta,\phi) = \frac{1}{C}\sum_{n=1}^{\infty}\sum_{m=-n}^{n}\left(F_{nm}^{(j=1)(1)} - \frac{n+1}{2}F_{nm}^{(j=3)(1)}\right)Y_n^m\ (\theta,\phi);$$

$$\chi_2\ (\theta,\phi) = \frac{1}{C}\sum_{n=1}^{\infty}\sum_{m=-n}^{n}\left(F_{nm}^{(j=1)(2)} - \frac{n+1}{2}F_{nm}^{(j=3)(2)}\right)Y_n^m\ (\theta,\phi);$$

C is determined by the formula (16a).

For the tilts the value $2V_{eo}/a$ must be substituted for $\varphi_o\gamma$, where φ_o is the tilt's amplitude on the surface of an absolute rigid Earth, $\gamma = 1 + k - h$, and the values χ_1, χ_2 must be substituted for $\tilde{\chi}_1$, $\tilde{\chi}_2$, where

$$\tilde{\chi}_1\ (\theta,\phi) = \frac{1}{C}\sum_{n=1}^{\infty}\sum_{m=-n}^{n}Y_n^m\ (\theta,\phi)\left[F_{nm}^{(j=1)(1)} - F_{nm}^{(j=1)(1)}\right];$$

$$\tilde{\chi}_2\ (\theta,\phi) = \frac{1}{C}\sum_{n=1}^{\infty}\sum_{m=-n}^{n}Y_n^m\ (\theta,\phi)\left[F_{nm}^{(j=3)(2)} - F_{nm}^{(j=1)(2)}\right] \qquad (39a)$$

With the accuracy of the order of χ_1, χ_2, $\tilde{\chi}_1$, $\tilde{\chi}_2$ the expression (38) may be presented in the form:

$$\delta g(\theta,\phi) = -\frac{2V_{eo}}{a}\left[\delta_{n_o}\, P_{n_o}^{m_o}\ (\cos\theta) + \alpha(\theta,\phi)\right]\cdot\cos\left(\sigma t - m_o\phi - \beta(\theta,\phi)\right),$$

where

$$\alpha(\theta,\phi) = \chi_1(\theta,\phi)\cos m_o\phi + \chi_2\ (\theta,\phi)\sin m_o\phi;$$

$$\beta\ (\theta,\phi) = \frac{\cos m_o\phi\ \chi_2(\theta,\phi) - \sin m_o\phi\ \chi_1(\theta,\phi)}{\delta_{n_o} P_{n_o}^{m_o}\ (\cos\theta)}$$

and by analogy (after the commutation of $\frac{2}{a}V_{\ell_o}\delta$ on $\varphi_o\gamma$, χ_1 on $\tilde{\chi}_1$, χ_2 on $\tilde{\chi}_2$) for the tilts.

So, the amplitudes and phase lags for the diurnal and semi-diurnal tidal waves are completely determined too. As well as in the case of zonal waves, the choice of the initial meridian in the development (39) is determined by the choice of the initial meridian in the development of the lateral heterogeneities (17).

If the functions $\alpha(\theta,\phi)$, $\beta(\theta,\phi)$ are known from the measurements, it is possible to determine $\chi_1(\theta,\phi)$, $\chi_2(\theta,\phi)$(or $\tilde{\chi}_1(\theta,\phi)$, $\tilde{\chi}_2(\theta,\phi)$) with the help of (41) and then, with the help of (39) - to determine the coefficients $F_{nm}^{j(1)}$, $F_{nm}^{j(2)}$ for j=1, 3. Then the relations (18), (32) as well as in the case of zonal waves may be used for the determination of $\lambda_{\ell p}(r)$, $\mu_{\ell p}(r)$.

In the case of diurnal and semidiurnal waves the information about the Earth's lateral heterogeneities give not only the amplitudes of the tidal waves, but the phase lags too.

REFERENCES

DAHLEN F.A., 1968 The normal modes of a rotating, elliptical Earth
Geophys. J.R. astr. Soc., 16, 329-367.

DAHLEN F.A., 1972 Elastic dislocation theory for a self gravitating elastic configuration with an initial static stress field
Geophys. J.R. astr. Soc., 28, 357-383.

DAHLEN F.A., 1974 Inference of the lateral heterogencity of the Earth from the eigenfrequency spectrum: a linear inverse problem
Geophys. J.R. astr. Soc., 38, 143-167.

DAHLEN F.A., 1967 Models of the lateral heterogeneity of the Earth consistent with eigenfrequency splitting data
Geophys. J.R. astr. Soc., 44, 77-105.

EDMONDS A.R., 1957 Angular momentum in quantum mechanics
Princeton University Press

KUO J.T., JACHENS R.C., WHITE C., EWING M., 1970 Tidal gravity measurements along a transcontinental profile across the United States
Comm. Obs. Roy. Belg. Série Géophys. A9.

LUH P.C.H., 1973 The normal modes of the rotating self-gravitating inhomogeneous Earth, Ph. D. thesis, Univ. of California, San Diego

MADARIAGA R., AKI K., 1972 Spectral splitting of toroidal-free oscillations due to lateral heterogeneity of the Earth's structure
J. Geophys. Res. 77, 4421-4431.

MOLODENSKY M.S., 1953 Earth's tides, free nutation and some problems of the Earth's inner structure
Trudi geophizicheskogo instituta AN SSSR, n°19(146) p.p. 3-52 Moscow

MOLODENSKY S.M., 1976 On the Green's function for the equations of the Earth's spheroidal deformations
Izv. (Bull.) of Acad. Sci. USSR, N°11

MOLODENSKY S.M., 1977a On the influence of lateral heterogeneity of the manth on the amplitudes of tidal waves
Izv. (Bull.) of Acad. Sci. USSR, N°2

MOLODENSKY S.M., 1977b On the connection between Love numbers and loading Love numbers
Izv. (Bull.) of Acad. Sci. USSR, N°3

PARIYSKY N.N. et AL. A note concerning regional variations in the gravity factor δ
Proceedings of the seventh Int. Symp. on earth tides Sopron 1976

PERTSEV B.P., IVANOVA M.V., 1975 The corrections for the influence of the ocean tides for the tidal measurements in Europe
Izv. (Bull.) of Acad. Sci. USSR, N°12

PERTSEV B.P., 1976 Influence des marées océaniques des zones proches sur les observations de marées terrestres
Marées terrestres Bull. d'Inf., N°74, 4259-4274

ZHARKOV V.N., LUBIMOV V.M., 1970 The theory of the spheroidal free oscillations of laterally heterogeneous Earth
Izv. (Bull.) of Acad. Sci. USSR, N°10

LE CALCUL DE L'EFFET DE CAVITE DANS LES MAREES TERRESTRES

L.E. KHASSILEV

1. INTRODUCTION

La dispersion considérable des caractéristiques de marée de la croûte terrestre γ et $\Delta\phi$ et des nombres Love et Shida h et ℓ apparaît dans les résultats des observations dans les galeries et les mines à l'aide des clinomètres et les déformographes. En interprétant ces observations, on explique ordinairement cette dispersion par l'influence de différents effets indirects. En 1973, King et Bilham {5} ont émis l'hypothèse d'une altération des inclinaisons de la croûte terrestre enregistrées par la courbure des murs de la chambre dans laquelle les appareils enregistreurs ont été installés. On appelle ordinairement ces perturbations "effet de cavité". On connait quelques séries d'observations qui confirment cette hypothèse qualitativement, par exemple {6,7}. Les résultats de calculs précis des valeurs de l'effet de cavité pour les chambres sphériques et cylindriques sont publiés dans l'article {8}. Les résultats des calculs suivant la méthode des éléments finis pour une chambre ayant une section carrée sont publiés dans l'article {9}.

Dans l'article présent nous avons calculé d'une manière analytique l'angle de l'écart de la normale et des déplacements le long de la limite d'une galerie horizontale. Les sections transversales avaient des formes de trois rectangles, d'une voûte et d'un demi-cercle. Outre cela, nous avons calculé les corrections de ces valeurs dues à l'influence de la surface libre de la Terre. Les méthodes de calculs que nous avons utilisées sont exposées en détail dans les monographies de N.I. Mouskhelichvili {1} et de G.N. Savine {2}.

Nous considérons la croûte terrestre comme un corps homogène isotrope élastique caractérisé par les constantes de Lamé λ et μ. La longueur de la galerie est beaucoup plus grande que ses dimensions transversales. Nous considérons le problème d'élasticité à l'approximation statique.

2. LA METHODE DE CALCUL.

Dans le calcul nous utiliserons les coordonnées rectangulaires : l'axe X_1 est dirigé perpendiculairement à l'axe de la galerie, l'axe X_2 verticalement vers le haut et l'axe X_3 le long de l'axe longitudinal de la galerie (figure 1). Nous admettons la dépendance entre le tenseur des déformations de marée ε_{ik}, où i, k = 1, 2, 3, et le tenseur des tensions de marée σ_{ik} suivant la loi de Hooke pour un corps solide isotrope. Nous pouvons poser que les tensions et les déformations ne dépendent pas de la coordonnée X_3 parce que la longueur de la galerie le long de l'axe X_3 est très grande en comparaison de ses dimensions transversales. En utilisant cette hypothèse on peut montrer la constance de la composante du tenseur de déformation ε_{33} sur tout le plan X_1, X_2. Alors, nous obtiendrons pour les tensions σ_{11}, σ_{22} et σ_{12} un système d'équations bi-dimensionnel de l'élasticité. Les conditions à l'infini et les conditions limites sur la surface libre de la section transversale de la galerie seront les conditions limites pour ce problème bi-dimensionnel.

Utilisons les expressions des tensions à deux dimensions σ_{11}, σ_{22}, σ_{12} à l'aide de la fonction des tensions (fonction d'Airy). Ensuite, représentons la fonction biharmonique des tensions à l'aide de deux fonctions régulières $\phi(Z)$, $\psi(Z)$ de la variable complexe $z = x_1 + ix_2$:

$$\frac{\partial F}{\partial X_1} - i\frac{\partial F}{\partial X_2} = \psi(Z) + \overline{Z}\,\phi'(Z) + \overline{\phi(Z)} \qquad (1)$$

Ici le "prime" indique la dérivée par rapport à z, $\overline{z} = x_1 - ix_2$. Les conditions limites s'expriment sur la surface libre :

$$\frac{\partial F}{\partial X_1} - i\frac{\partial F}{\partial X_2} = \text{const.} \qquad (2)$$

A une distance de la galerie beaucoup plus grande que ses dimensions, les perturbations des tensions dues à la galerie disparaissent :

$$\sigma_{12} \to 0, \quad \sigma_{22} \to 0, \quad \sigma_{11} \to T \qquad (3)$$

Pour trouver les fonctions ϕ et ψ à l'aide de l'équation (1), des conditions limites (2) et de la condition à l'infini (3), nous utiliserons la représentation conforme de l'extérieur du cercle unitaire sur l'extérieur de la section transversale de la galerie. Dans le cas d'une section rectangulaire la formule Christoffel - Schwarz nous donne la représentation nécessaire. Le développement en série de Laurent a la forme :

$$Z = \omega(\xi) = C\left[\xi + \frac{\beta}{2}\frac{1}{\xi} + \frac{\beta^2-4}{24}\frac{1}{\xi^3} + \frac{\beta(\beta^2-4)}{80}\frac{1}{\xi^5} + \frac{(\beta^2-4)(5\beta^2-4)}{896\,\xi^7} + \ldots\right] \qquad (4)$$

Le paramètre β détermine la relation des côtés d'un rectangle : quand β = 1, 0, -1, nous obtiendrons approximativement la relation des côtés 3,2:1, 1:1, 1:3,2 respectivement. Les représentations conformes pour les sections à la voûte et du demi-cercle sont données dans la monographie {2}. Dans le plan de la variable complexe ξ les fonctions $\phi(\omega(\xi))$ et $\psi(\omega(\xi))$ seront régulières hors du cercle unitaire. Alors, on peut les représenter ici en séries de Laurent. Les coefficients de ces séries sont déterminés à l'aide des équations (1 - 3), si nous posons les coefficients des puissances ξ de l'équation (1) égaux à zéro et résolvons le système des équations linéaires obtenu.

Déterminons ensuite les déplacements élastiques à la limite de la section de la galerie, en utilisant la formule de G.V. Kolossov et les conditions (2) :

$$v_1 + i\,v_2 = \frac{\lambda + 2\mu}{\mu(\lambda+\mu)}\,\phi(Z) - \frac{\lambda}{2(\lambda+\mu)}\,\varepsilon_{33}\,Z \qquad (5)$$

Pour trouver l'angle de la déviation de la normale η quand la limite est courbée, calculons la différence entre les angles d'inclinaison de la limite avec des déplacements et sans déplacements :

$$\eta = \operatorname{arctg}\frac{d(X_2 + v_2)}{d(X_1 + v_1)} - \operatorname{arctg}\frac{d\,X_2}{d\,X_1} = \frac{\lambda + 2\mu}{\mu(\lambda+\mu)}\,\frac{1}{2i}\left[\phi'(Z) - \overline{\phi'(Z)}\right] \qquad (6)$$

3. LES CORRECTIONS DUES A L'INFLUENCE DE LA SURFACE DE LA TERRE.

Nous considérons la distance du centre de la galerie à la surface libre comme plus grande que ses dimensions transversales, mais plus petite que ses dimensions longitudinales. Nous trouverons par la méthode des approximations successives les corrections des fonctions non-perturbées $\phi(Z)$ et $\psi(Z)$ dues à l'influence de la surface de la Terre. A grande distance les fonctions non-perturbées sont égales asymptotiquement à :

$$\phi(Z) = \frac{1}{4}TZ + \frac{\theta_1}{Z} + o\left(\frac{1}{Z}\right), \quad \psi(Z) = -\frac{1}{2}TZ + \frac{\theta_2}{Z} + o\left(\frac{1}{Z}\right) \qquad (7)$$

Nous obtenons la première approximation de la condition limite sur la surface de la Terre :

$$\psi + \psi_1 + \bar{Z}(\phi' + \phi_1') + \bar{\phi} + \bar{\phi}_1 = \text{const} \qquad (8)$$

Si la surface de la Terre est à la distance h de l'origine des coordonnées, alors $\bar{z}=z-2ih$. Partant de ce que les fonctions de la première approximation ϕ_1 et ψ_1 ne peuvent pas avoir de singularités plus bas que la surface de la Terre, nous trouverons :

$$\phi_1(Z) = -\frac{\bar{\theta}_2}{Z-2ih} + \frac{\bar{\theta}_1}{(Z-2ih)^2}, \quad \psi_1(Z) = -\frac{2\bar{\theta}_1 + \bar{\theta}_2}{Z-2ih} + \frac{2\bar{\theta}_1 Z}{(Z-2ih)^2} \qquad (9)$$

Près du périmètre de la section transversale de la galerie, posant la relation $|Z|/h$ beaucoup plus petite que l'unité, nous trouvons :

$$\phi_1 = -\frac{Z}{4h^2}(\bar{\theta}_1 + \bar{\theta}_2) + o\left(\frac{1}{h^2}\right), \quad \psi_1 = -\frac{Z}{4h^2}(4\bar{\theta}_1 + \bar{\theta}_2) + o\left(\frac{1}{h^2}\right) \qquad (10)$$

Nous trouverons la seconde approximation qui n'a pas de singularités hors l'orifice, partant de la condition sur sa limite :

$$\psi_2 + \bar{Z}\phi_2' + \bar{\phi}_2 = -\psi_1 - \bar{Z}\phi_1' - \bar{\phi}_1 = \frac{Z}{4h^2}(4\bar{\theta}_1 + \bar{\theta}_2) + \frac{\bar{Z}}{4h^2}(\theta_1 + \theta_2 + \bar{\theta}_1 + \bar{\theta}_2) \qquad (11)$$

En utilisant la représentation conforme, comme nous l'avons exposé plus haut, nous trouverons les corrections dues à l'influence de la surface de la Terre.

4. LA DISCUSSION.

Les angles calculés des écarts de la normale η et de la perturbation des déplacements horizontaux Δv_1 dûs à la présence d'une cavité sont donnés dans les tableaux 1 et 2. Pour l'uniformité de l'exposé, nous donnons dans ces tableaux la valeur Δv_2^* qui détermine les perturbations des déplacements verticaux :

$$\Delta v_2 = \Delta v_2^* + \frac{2(\lambda + \mu)}{\lambda + 2\mu} q X_2.$$

Ici, nous introduisons $q = \frac{\lambda+2\mu}{4\ \mu(\lambda+\mu)}\ T = \varepsilon_{11} + \sigma\ \varepsilon_{33}$ qui est déterminée par les composantes du tenseur de déformation ε_{11} et ε_{33} théoriques ou mesurées et par le coefficient Poisson $\sigma = \frac{\lambda}{2(\lambda+\mu)}$. La valeur a est partout la moitié de la base, H est la hauteur de la section. Le commencement de la lecture se trouve dans l'angle gauche inférieur de la section. Si la réflexion des points par rapport à l'axe vertical de symétrie d'une section sont symétriques, les valeurs η et $\Delta\ \mathscr{v}_1$ changent de signe, et la valeur $\Delta\ \mathscr{v}_2$ ne change pas.

Nous avons calculé les écarts de la normale en milli-secondes d'arc et les déplacements en microns pour montrer les valeurs de l'effet de cavité pour l'onde M_2 dans les galeries à sections carrées et à sections en voûte (fig. 2 - 5). Nous avons adopté : pour les calculs, une galerie orientée E-W, à la latitude 49°, le nombre de Love h = 0,617, le nombre de Shida ℓ = 0,090, la moitié de la largeur de chambre a = 8m, le coefficient de Poisson σ = 0,11.

La particularité principale de l'effet de cavité est l'insignifiance de la déviation de la normale sur le côté horizontal de la section par rapport au côté vertical et l'existence de quelques points sur le côté horizontal où l'effet de cavité pour les inclinaisons devient zéro. Dans les galeries à section allongée horizontalement, l'effet de cavité est plusieurs fois plus petit que dans les galeries à la section allongée verticalement. L'effet de cavité perturbe essentiellement la composante de déformation à travers la galerie. Dans une longue galerie loin de ses extrémités les composantes des inclinaisons et des déformations le long de la galerie ne sont pas perturbées par l'effet de cavité. L'influence de la surface de la Terre sur l'effet de cavité diminue en raison inverse du carré des distances du centre de la gal rie à cette surface et est égale à peu près à 10 % de cet effet aux distances de la hauteur de la galerie du plafond de la galerie à la surface terrestre.

Pour conclure, ce nous est un agréable devoir de remercier le licencié des sciences physiques et mathématiques V.G. Balenko et le licencié des sciences techniques V.G. Boulatsen de leurs conseils utiles.

LITTERATURE

1. Мусхелишвили Н.И. Некоторые основные задачи математической теории упругости. М., изд-во АН СССР.1949.635 с.
2. Савин Г.Н. распределение напряжений около отверстий.К., "Наукова думка", 1968, 887 с.
3. Хасилев Л.Е. Эффект полости в земноприливных наблюдениях.- Сб."Вращение и приливные деформации Земли". вып.10,К., "Наукова думка".1978(в печати).
4. Хасилев Л.Е., Баленко В.Г., Булацен В.Г. Эффект полости в штольнях некоторых сечений. - Сб. "Вращение и приливные деформации Земли", вып. 10, К.,"Наукова думка",1978 (в печати).
5. KING G.C.P., BILHAM R.G. Tidal Measurements in Europe. Nature, 1973, 243, p. 74-75.
6. BAKER T.F., LENNON G.W. Tidal Tilt Anomalies. Nature, 1973, 243, p. 75-76.
7. ITSUI I U.I., BILHAM R.G. and others. Tidal Strain Enhancement Observed Across a Tunnel. Geophys. J.R. astr. Soc., 1975, 42, p. 555-564.
8. LECOLAZET R., WITTLINGER G. Sur l'influence perturbatrice de la déformation des cavités d'observation sur les marées clinométriques. C.R. Acad. Sc. Paris, 1974, 278, Série B, p. 663-666.
9. HARRISON J.C. Cavity and Topographic Effects in Tilt and Strain Measurements. J. Geophys. Res., 1976, 81, 2, p. 319-328.

TABLEAU 1

Effet de cavité sur la base de la galerie.

	Sections rectangulaires									section en demi-cercle, H : a = 1			section en voûte, H : a = 2,76		
	H/a = 2			H/a = 6,4			H/a = 0,62								
	η/g	$\Delta v_1/ag$	$\Delta v_2^*/ag$	η/g	$\Delta v_1/ag$	$\Delta v_2^*/ag$	η/g	$\Delta v_2/ag$	$\Delta v_2^*/ag$	η/g	$\Delta v_1/ag$	$\Delta v_2^*/ag$	η/g	$\Delta v_2/ag$	$\Delta v_2^*/ag$
0,0a	4,14	-1,09	1,75	5,01	-2,39	6,02	3,02	-0,50	0,51	2,38	-0,66	0,47	4,37	-1,50	2,28
0,1	-0,36	-0,73	1,72	0,69	-1,78	5,99	-0,13	-0,32	0,52	-0,03	-0,44	0,51	0,68	-0,98	2,34
0,2	-0,32	-0,59	1,70	-0,58	-1,34	5,94	-0,15	-0,24	0,52	-0,28	-0,32	0,49	-0,36	-0,72	2,32
0,3	-0,18	-0,49	1,67	-0,70	-1,09	5,86	-0,08	-0,20	0,51	-0,20	-0,25	0,47	-0,51	-0,54	2,28
0,4	-0,06	-0,42	1,66	-0,63	-0,86	5,82	-0,01	-0,17	0,50	-0,07	-0,21	0,46	-0,46	-0,42	2,25
0,5	0,03	-0,36	1,66	-0,54	-0,66	5,79	0,04	-0,15	0,51	0,03	-0,18	0,46	-0,39	-0,31	2,21
0,6	0,08	-0,29	1,67	-0,43	-0,51	5,74	0,07	-0,12	0,51	0,09	-0,15	0,47	-0,31	-0,23	2,18
0,7	0,10	-0,22	1,67	-0,32	-0,38	5,71	0,08	-0,10	0,52	0,11	-0,12	0,48	-0,23	-0,16	2,16
0,8	0,09	-0,14	1,69	-0,21	-0,25	5,69	0,07	-0,07	0,52	0,10	-0,08	0,48	-0,16	-0,11	2,14
0,9	0,05	-0,07	1,70	-0,11	-0,13	5,69	0,04	-0,03	0,53	0,06	-0,04	0,49	-0,08	-0,05	2,14
1,0	0,00	0,00	1,70	0,00	0,00	5,69	0,00	0,00	0,53	0,00	0,00	0,49	0,00	0,00	2,13

TABLEAU 2

Effet de cavité sur le côté vertical de la galerie

	sections rectangulaires									section en demi-cercle, H : a = 1			section en voûte, H : a = 2,76		
	H : a = 2			H : a = 6,4			H : a = 0,62								
	η/g	$\Delta u_1/ag$	$\Delta u_2^*/ag$	η/g	$\Delta u_1/ag$	$\Delta u_2^*/ag$	η/g	$\Delta u_1/ag$	$\Delta u_2^*/ag$	η/g	$\Delta u_1/ag$	$\Delta u_2^*/ag$	η/g	$\Delta u_1/ag$	$\Delta u_2^*/ag$
0,0H	4,14	-1,09	1,75	5,01	-2,39	6,02	3,02	-0,50	0,51	2,38	-0,66	0,47	4,37	-1,50	2,28
0,1	2,02	-1,78	1,46	2,22	-5,00	5,08	1,96	-0,68	0,41	1,88	-0,93	0,29	1,89	-2,30	1,83
0,2	1,24	-2,10	1,12	1,33	-5,69	3,91	1,06	-0,77	0,32	0,48	-1,06	0,10	1,06	-2,70	1,35
0,3	0,79	-2,33	0,76	0,84	-6,91	2,64	0,59	-0,82	0,21	-0,26	-1,13	-0,09	0,59	-2,68	0,87
0,4	0,40	-2,42	0,38	0,42	-7,31	1,32	0,26	-0,85	0,11	-0,75	-1,16	-0,28	0,22	-3,05	0,33
0,5	0,00	-2,45	0,00	0,00	-7,44	0,00	0,00	-0,86	0,00	-1,10	-1,16	-0,47	-0,17	-3,04	-0,17
0,6	-0,40	-2,42	-0,38	-0,42	-7,31	-1,32	-0,26	-0,85	-0,11	-1,35	-1,11	-0,67	-0,66	-2,95	-0,70
0,7	-0,79	-2,33	-0,76	-0,84	-6,91	-2,64	-0,59	-0,82	-0,21	-1,51	-1,02	-0,86	-1,35	-2,73	-1,23
0,8	-1,24	-2,10	-1,12	-1,33	-5,69	-3,91	-1,06	-0,77	-0,32	-1,55	-0,88	-1,05	-2,16	-2,36	-1,77
0,9	-2,02	-1,78	-1,46	-2,22	-5,00	-5,08	-1,96	-0,68	-0,41	-1,35	-0,65	-1,25	-2,30	-1,81	-2,32
1,0	-4,14	-1,09	-1,75	-5,01	-2,39	-6,02	-3,02	-0,50	-0,51	0,00	0,00	-1,44	0,00	0,00	-2,92

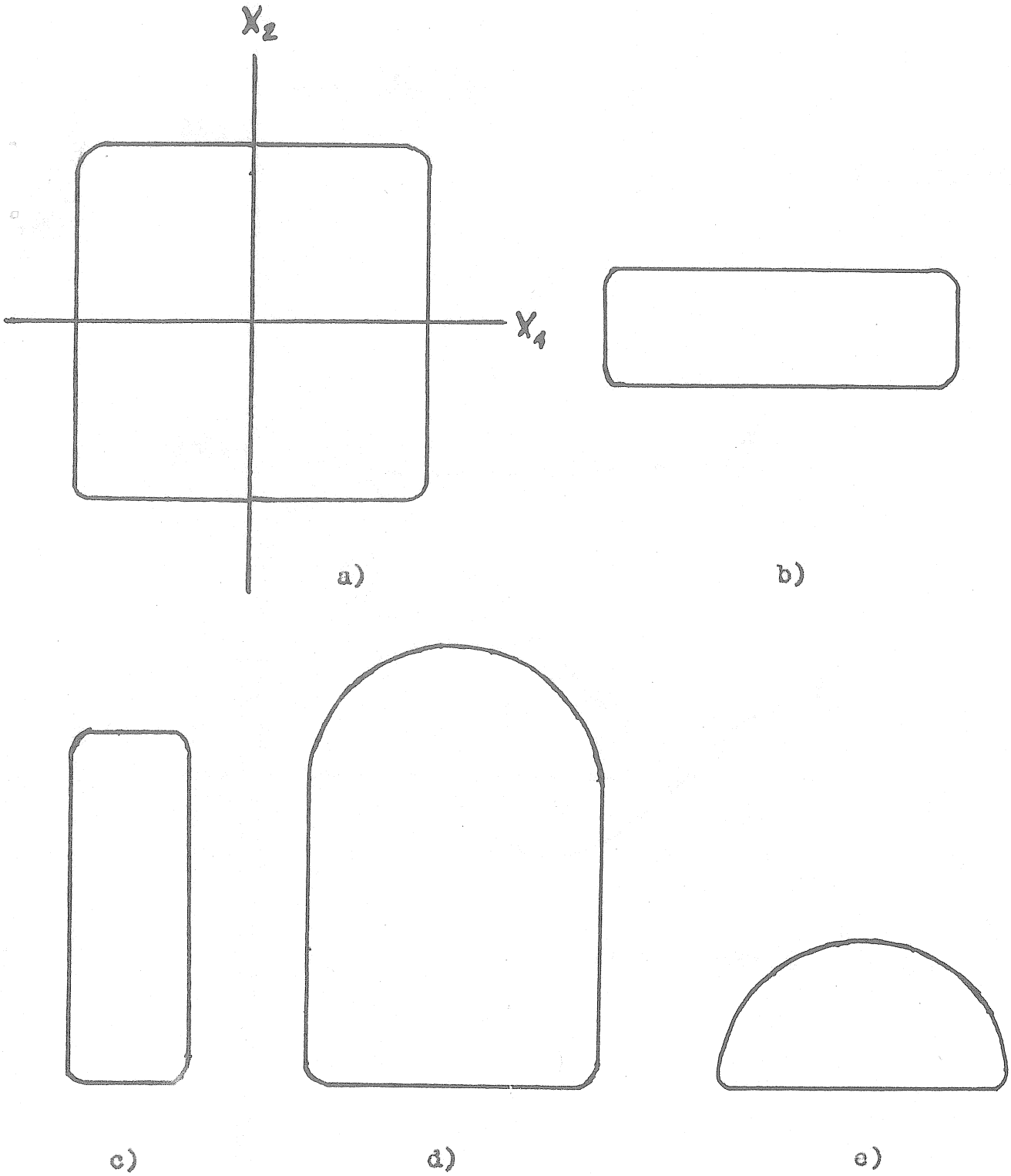

Fig. 1. Sections transversales des galeries :

a) carré
b) rectangle de côtés en relation 3,2:1
c) rectangle de côtés en relation 1:3,2
d) voûte
e) demi-cercle.

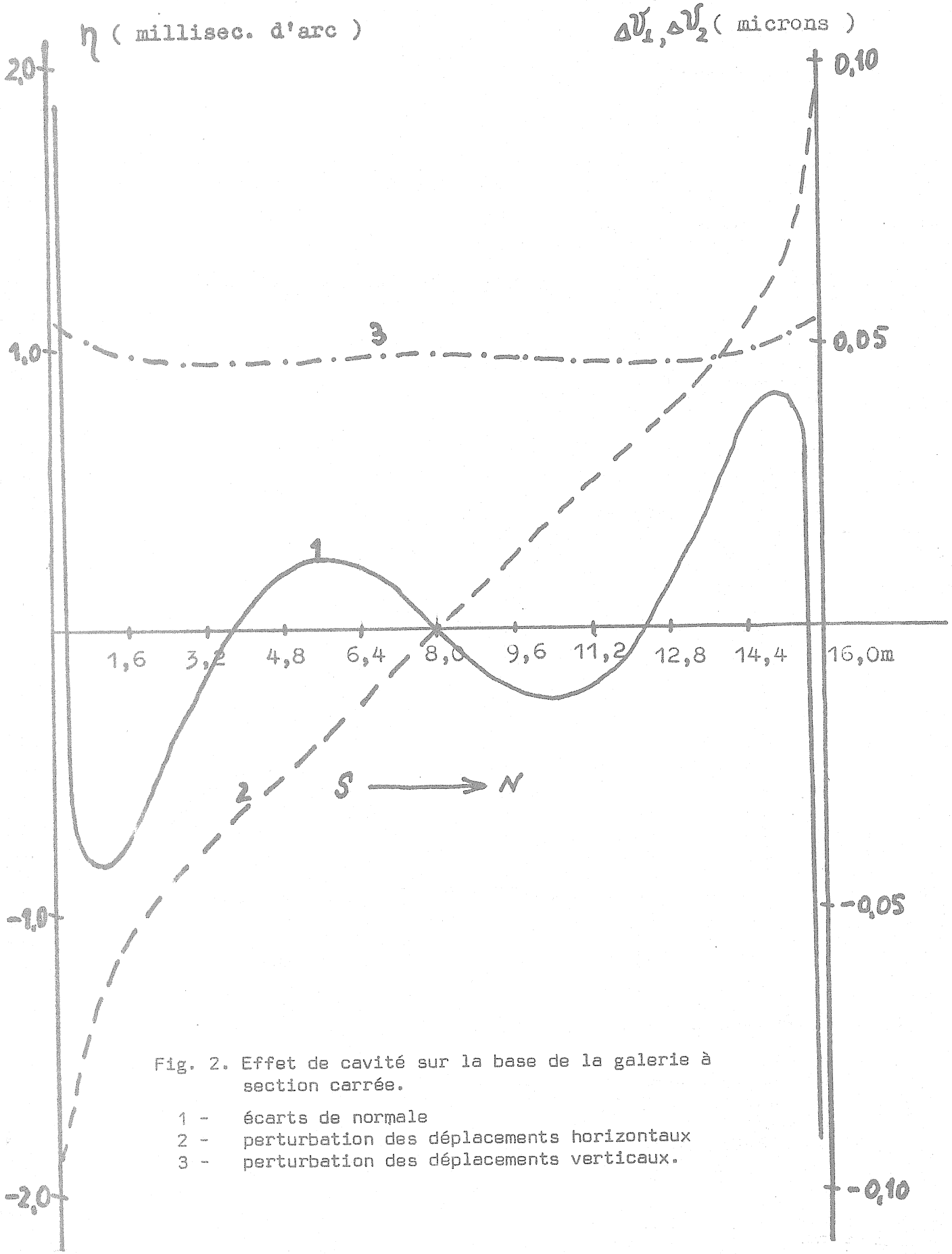

Fig. 2. Effet de cavité sur la base de la galerie à section carrée.

1 - écarts de normale
2 - perturbation des déplacements horizontaux
3 - perturbation des déplacements verticaux.

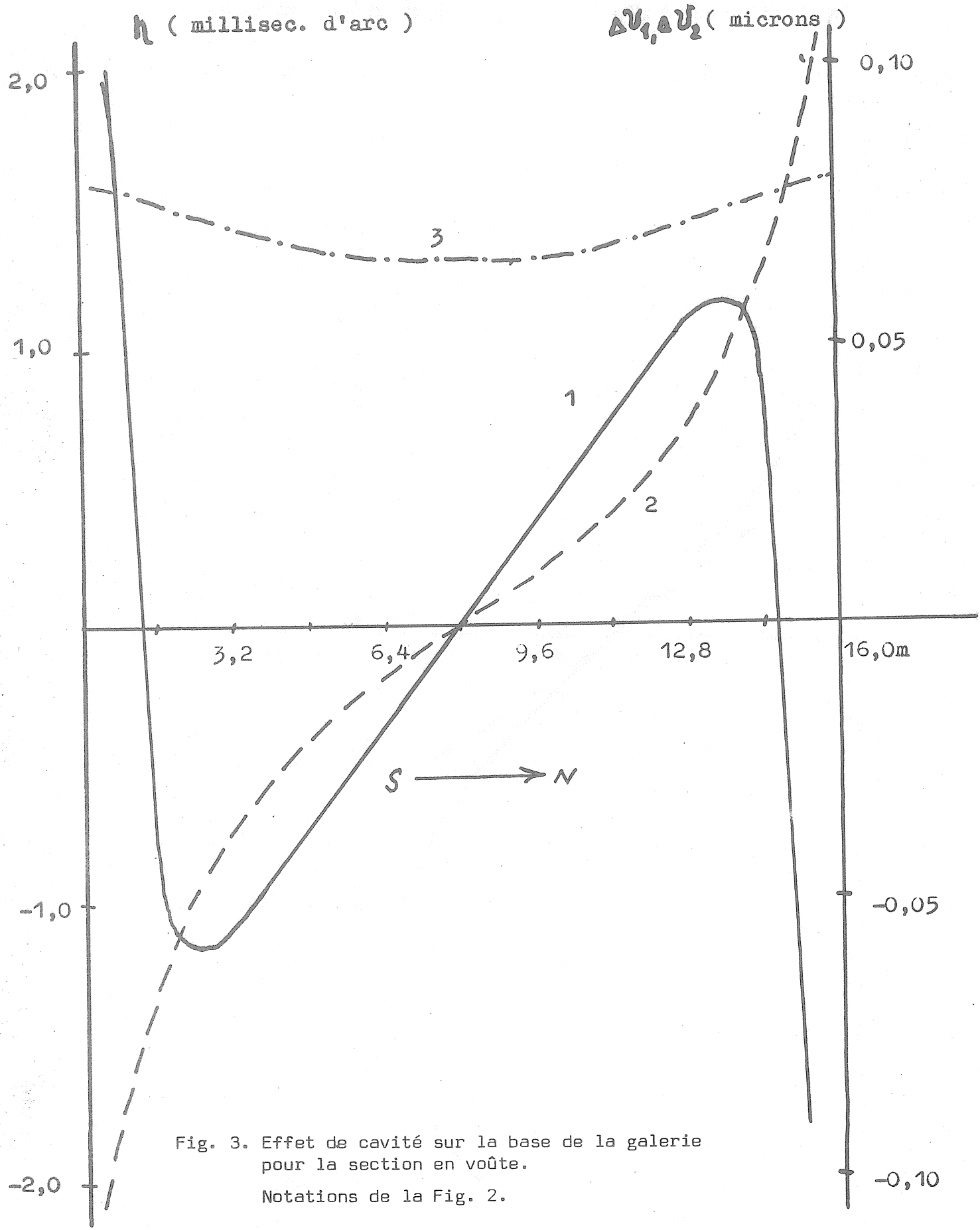

Fig. 3. Effet de cavité sur la base de la galerie pour la section en voûte.

Notations de la Fig. 2.

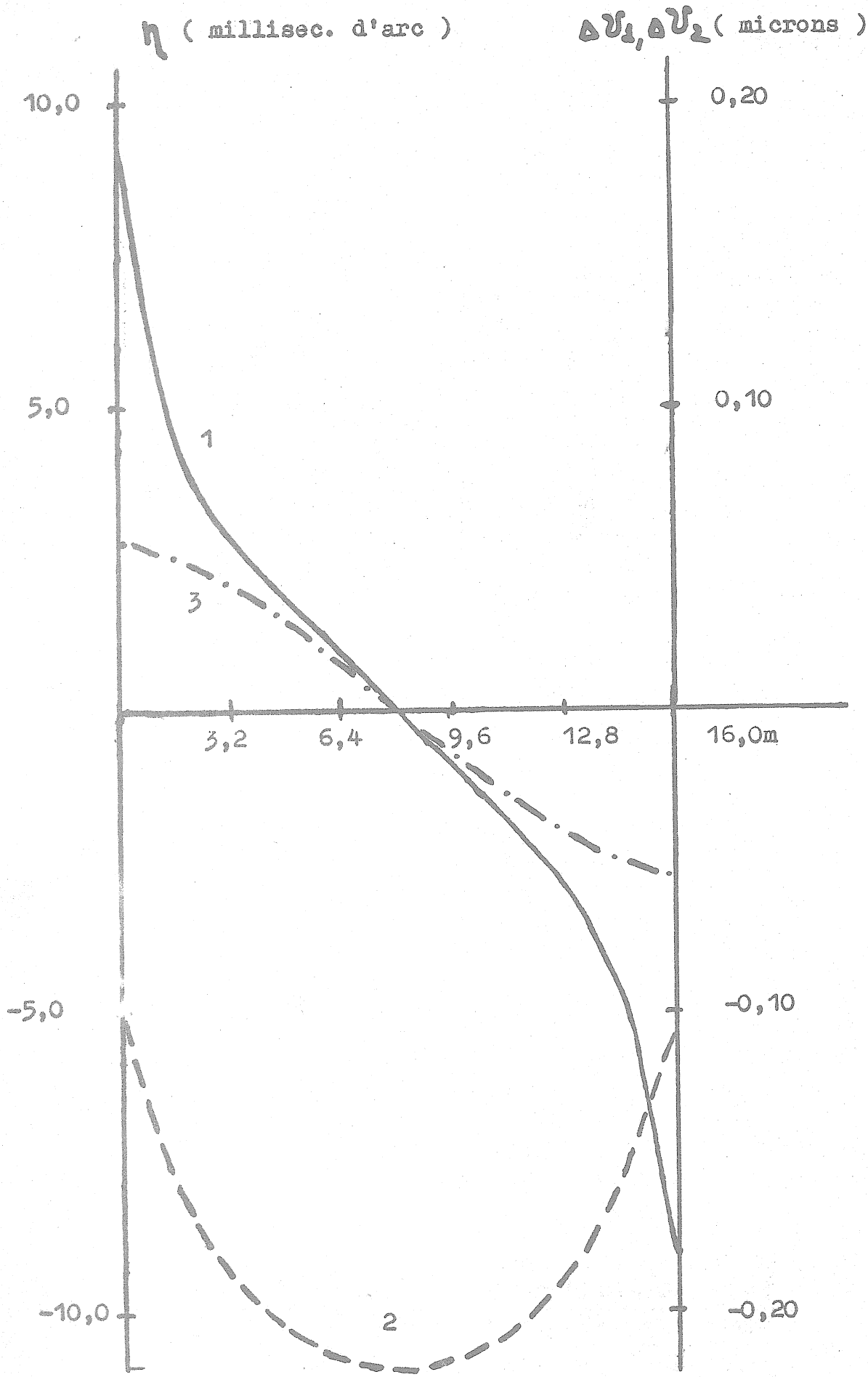

Fig. 4. Effet de cavité sur le côté vertical de la galerie à section carrée. Notations de la Fig. 2.

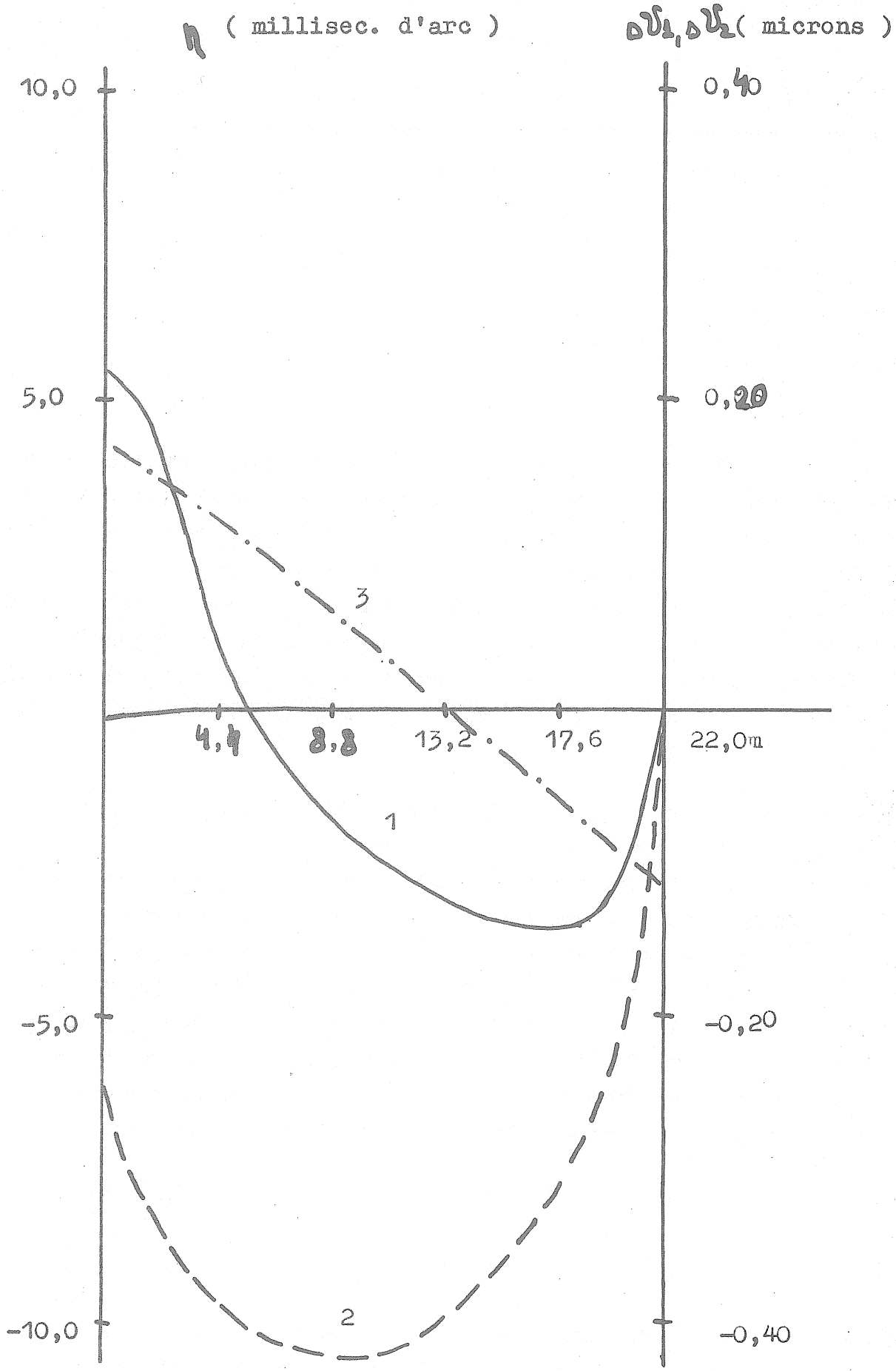

Fig. 5. Effet de cavité sur le côté vertical de la galerie pour la section en voûte.
Notations de la Fig. 2.

THE EFFECT OF INERTIAL FORCES UPON EARTH TIDE OBSERVATIONS.

N.N. PARIISKY, B.P. PERTSEV

Observations of tidal variations of gravity and tilts of the Earth's surface are performed upon a rotating and deformable Earth. In view of periodical displacements of the observation station due to tidal forces of the Moon and the Sun the gravitymeter or tiltmeter records not only the Earth tides, but also the inertial forces of relative motion, variations of the centrifugal force and the force of Coriolis. These forces are small, but the present everincreasing accuracy of tidal measurements makes it necessary to take into account the effect of inertial forces for geophysical interpretation of the results of observations.

The effect of vertical relative accelerations upon tidal gravity recordings has been discussed previously (Pariisky, 1960).

But besides vertical displacements all points of the Earth's surface undergo horizontal periodical motions. These displacements are also of tidal origin and can be presented as motions along the meridian and the prime vertical. These motions, occuring on a rotating Earth, give rise to Coriolis inertial forces which affect not only the readings of gravitymeters but also tiltmeter recordings. Besides, the vertical motions and displacements along the meridian lead to variations in the distance of the apparatus from the axis of rotation and thus to changes in the value of the centrifugal force.

The observed value of the gravity factor δ, $-\delta_o$ is equal to

$$\delta_o = \frac{\Delta g_T + F_{iz}}{\Delta g_o} = \delta_T + \frac{F_{iz}}{\Delta g_o} = \delta_T - \Delta\delta$$

where Δg_T and δ_T are the unknown values of Δg and δ, Δg_o - the tidal variation of the force of gravity for a rigid Earth, and F_{iz} - the vertical component of all inertial forces

$$\bar{F}_i = \bar{F}_{ir} + \bar{F}_{ic} + \bar{F}_{icf}$$

The tidal displacement of the point of observation is determined by vector

$$\bar{S} = U\bar{i} + V\bar{j} + W\bar{k}$$

where $\bar{i}$, $\bar{j}$, $\bar{k}$ are unit vectors in the south, east and vertical directions respectively.

This displacement, as we know, can be expressed by the tide-generating potential $W_n^{(m)}$ and Love and Shida numbers h and

$$\bar{S} = \frac{l}{g}\frac{\partial W_n^{(m)}}{\partial \phi}\bar{i} + \frac{l}{g\cos\phi}\frac{\partial W_n^{(m)}}{\partial \lambda}\bar{j} + \frac{h}{g}W_n^{(m)}\bar{k}$$

where

$$W_n^{(m)} K_{nm} \sum_i A_i \cos(\sigma_i t + \chi_i + m\lambda)$$

i - is the wave index. A_i, σ_i and χ_i are the amplitude, frequency and phase, given in the tables of Cartwright.

For tidal waves of the second degree (n=2) we have:

a) for semidiurnal waves

$$m = 2 \qquad K_{22} = D\cos^2\phi$$

b) for diurnal waves

$$m = 1 \qquad K_{21} = D\sin 2\phi$$

c) for longperiod waves

$$m = 0 \qquad K_{20} = -\frac{1}{2}D(3\sin^2\phi - 1)$$

D is the Doodson constant

$$D = 26277$$

and S - the latitude of the station. The constant D is valid for both the lunar and solar waves. The difference is accounted for in the amplitude coefficients in the Doodson and Cartwright tables.

The inertial forces can now be written in the following form.

The inertial force of relative motion:

$$\bar{F}_{ir} = -\ddot{U}\bar{i} - \ddot{V}\bar{j} - \ddot{W}\bar{k}$$

The Coriolis inertial force:

$$\bar{F}_{ic} = -2\left[\bar{\omega}\times\dot{\bar{S}}\right] = 2\begin{vmatrix} \bar{i} & \bar{j} & \bar{k} \\ -\omega\cos\phi & 0 & \omega\sin\phi \\ \dot{U} & \dot{V} & \dot{W} \end{vmatrix}$$

Variation in the centrifugal force:

$$\bar{F}_{icf} = \omega^2(U\sin^2\phi + W\cos\phi\sin\phi)\bar{i} + \omega^2(U\sin\phi\cos\phi + W\cos^2\phi)\bar{k}$$

The correction $\Delta\delta$ to the observed value δ_o will be

$$\Delta\delta = -\frac{F_{iz}}{\Delta g_o} = \frac{1}{\Delta g_o}\left[\ddot{W} - \omega\cos\phi\,\dot{V} - \omega^2(U\sin\phi\cos\phi + W\cos^2\phi)\right]$$

Corrections to the observed values of γ(N - S) and γ(E - W) can be received in just the same manner.

Without reproducing here elementary and monotonous calculations we shall give the final formulas for determining the corrections to the values of δ for longperiod, diurnal, semidiurnal and terdiurnal waves and to the values of γ for diurnal and semidiurnal waves. To account for the effect of inertial forces the corrections $\Delta\delta$ and $\Delta\gamma$ should be added to the values of δ and γ received from the analysis of observations.

1. Semidiurnal waves (n = 2)

$$\Delta\delta = -\frac{a}{2g}\left\{h\sigma^2 - 4\ell\sigma\omega + \omega^2\left[h - (h - 2\ell)\sin^2\phi\right]\right\}$$

$$\Delta\gamma\ (N\text{-}S) = \frac{\ell\, a\,\omega^2}{g}\left[\frac{h}{2\ell} + \left(\frac{\sigma}{\omega}\right)^2 - 2\left(\frac{\sigma}{\omega}\right) - \left(\frac{h}{2\ell} - 1\right)\sin^2\phi\right]$$

$$\Delta\gamma\ (E\text{-}W) = \frac{h\, a\,\omega^2}{g}\left[\frac{\sigma}{\omega} - \left(\frac{\sigma}{\omega}\right)^2\frac{\ell}{h} - \frac{\sigma}{\omega}\left(1 - 2\frac{\ell}{h}\right)\sin^2\phi\right]$$

2. Diurnal waves (n = 2)

$$\Delta\delta = -\frac{a}{2g}\left\{h\sigma^2 - 2\ell\sigma\omega + \omega^2\left[(h-\ell) - (h-2\ell)\sin^2\phi\right]\right\}$$

$$\Delta\gamma\ (N\text{-}S) = \frac{\ell\, a\,\omega^2}{g}\left\{-\left(\frac{\sigma}{\omega}\right)^2 + \left[\left(\frac{h}{\ell} - 1\right) - 2\frac{\sigma}{\omega} - \left(\frac{h}{\ell} - 2\right)\sin^2\phi\right]\frac{\sin^2\phi}{\cos 2\phi}\right\}$$

$$\Delta\gamma\ (E\text{-}W) = \frac{h\, a\,\omega\sigma}{g}\left[2\left(1 - \frac{\ell}{h}\right) - \frac{\ell}{h}\frac{\sigma}{\omega} - 2\left(1 - 2\frac{\ell}{h}\right)\sin^2\phi\right]$$

3. Longperiod waves (n = 2)

$$\Delta\delta = -\frac{a}{2g}\left\{h\sigma^2 + \omega^2\,\frac{\cos^2\phi\,[h - 3(h-2\ell)\sin^2\phi]}{1 - 3\sin^2\phi}\right\}$$

4. Terdiurnal waves (n = 3)

$$\Delta\delta = -\frac{a}{3g}\left\{h\,\sigma^2 - 6\ell\sigma\omega + \omega^2\left[h - (h-3\ell)\sin^2\phi\right]\right\}$$

In these formulas

σ - wave frequency in rad. / sec.

ω - angular velocity of the Earth's rotation in rad. / sec.

a - radius of the Earth in cm

g - force of gravity in gal.

ϕ - geocentric latitude of the point of observation.

h and ℓ are the Love and Shida numbers.

In view of their small magnitude variations in the velocity of the Earth's rotation can be neglected.

As can be seen from the formulas separate components have different signs and therefore partly cancel each other in the total corrections. The values of inertial corrections for the main waves of each tidal group and selected latitudes are given in the following table. In their calculation it was assumed that h = 0.60 and ℓ = 0.08.

CORRECTIONS FOR INERTIAL FORCES TO THE VALUES OF δ AND γ ($\times 10^4$)

Wave	M_2			K_1		
ϕ	0°	45°	90°	0°	45°	90°
$\Delta\delta$	-38	-34	-31	-16	-13	- 9
$\Delta\gamma$(N-S)	-10	- 6	- 2	- 3	∞	0
$\Delta\gamma$(E-W)	+30	+15	0	+33	+18	+ 3
	M_f			M_3		
ϕ	0°	35°26	90°	0°	45°	90°
δ	-10	∞	0	-49	-47	-44

The infinite values of the corrections $\Delta\delta(M_f)$ at ϕ = 35°26 and Δ (N - S) of the diurnal waves at ϕ = 45° are the result of zero amplitudes of the waves at those latitudes. In other words, the observations at these latitudes in the frequency of the mentioned waves should show only the inertial effects and possibly the indirect effects of the oceans and atmosphere.

The curves in fig. 1 and 2 show the corrections for the main tidal waves to δ_o and γ_o as functions of latitude of the tidal station.

REFERENCES

PARIISKY N.N., Correction des accélérations verticales lors des observations des variations de marées de la force de pesanteur.
Gravimetrical Res. 1, Moscow 1960 also
BIM N°69 Bruxelles 1974.

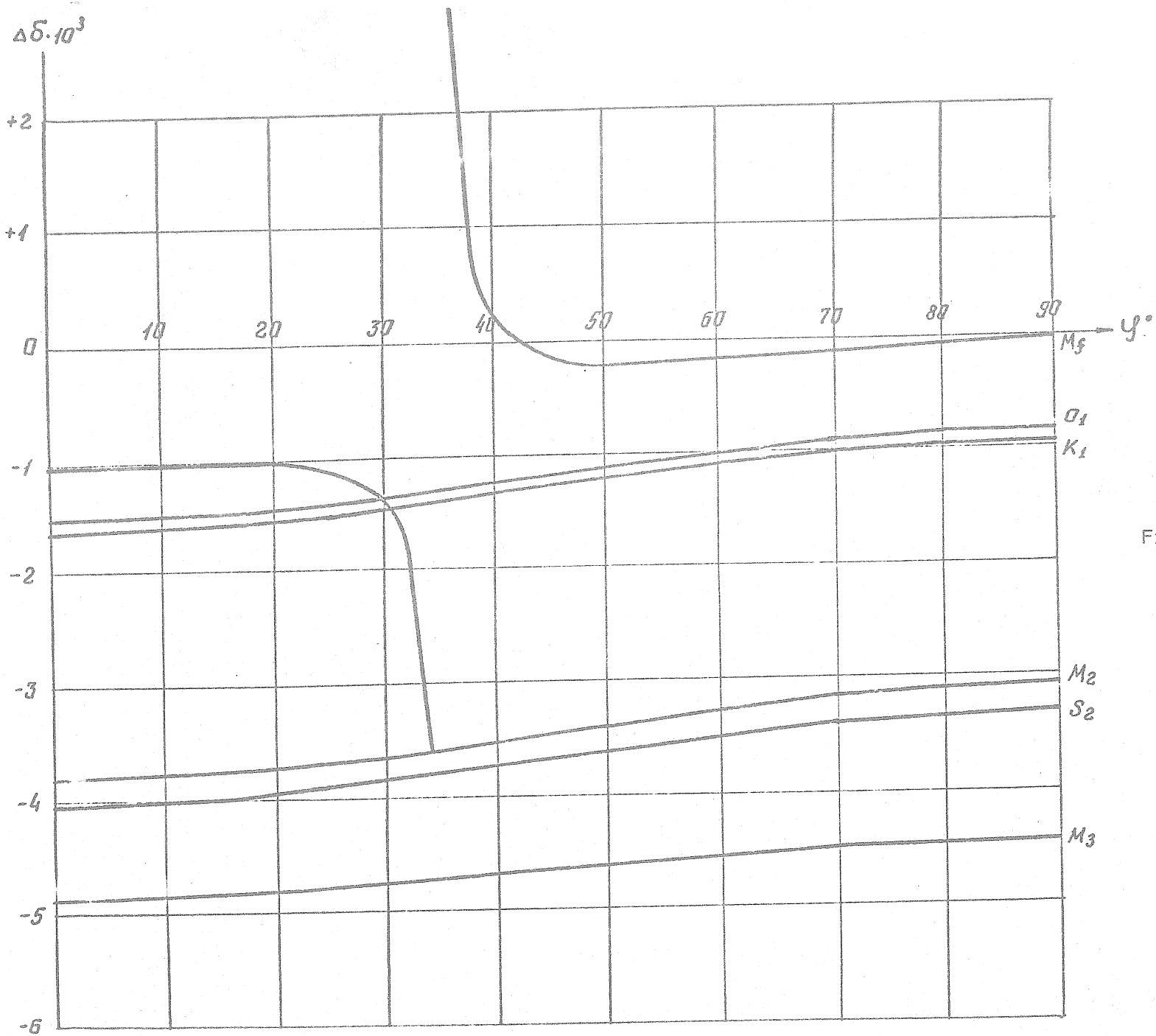

Fig. 1: Corrections to observed values of δ for the effect of inertial forces.

4868

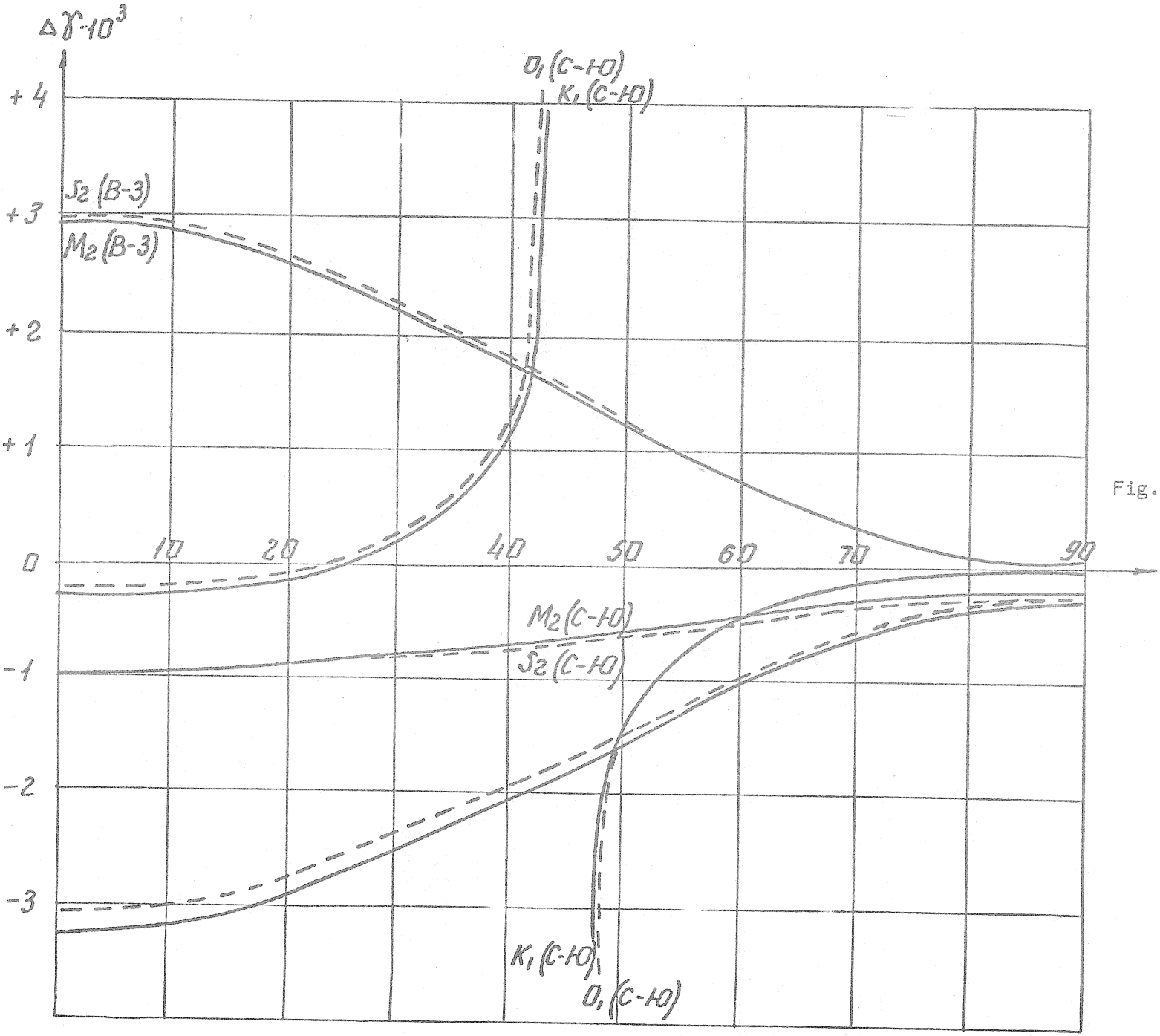

Fig. 2: Corrections to observed values of Δγ for the effect of inertial forces.

4869

VERTICAL DISPLACEMENTS OF THE EARTH'S SURFACE IN EUROPE CAUSED BY OCEAN TIDE LOADING

B.P. PERTSEV, M.V. IVANOVA

Periodical radial or vertical displacements of the Earth's surface caused by tide-generating forces and ocean tide loading can not as yet be measured directly. These displacements reveal themselves in tidal variations of gravity and tilts of the Earth's surface. But in both cases the effect of vertical displacements is to a large degree compensated by variations of the gravitational potential due to the deformation of the Earth. So that the total effects does not give a true notion about the relative values of separate components. Vertical displacements of the Earth's surface due to the effect of Earth and sea tides may also be of interest in mareographic research and in high-precision measurements of distances to artificial satellites and to the Moon.

Vertical displacements caused by Earth tides may be easily calculated by taking global values of Love coefficient h_2 determined from Earth-tide measurements or from theory. The part which is due to the loading effect of ocean tides can be determined by the same method as the ocean-tide corrections to Earth-tide gravity and tilt measurements.

In the case of vertical displacements the effect of a uniform layer of density $\rho = \rho_o H$, covering a spherical cap of radius α will be equal to

$$\Delta h = \frac{2\pi G \rho a}{g} \sum_n \frac{h'_n}{2n+1} \left[P_{n-1}(\alpha) - P_{n+1}(\alpha) \right] P_n(\psi)$$

where α is the radius of the Earth, g - acceleration of the force of gravity, G - the gravitational constant and h'_n - load coefficient of degree n.

The total effect is reached by adding the effects of all caps covering the oceans and seas for which cotidal charts are available.

By this method we have calculated vertical displacements of the Earth's surface in Europe due to the loading effect of ocean tides in the M_2 frequency. According to tidal gravity measurements and calculated corrections for the indirect effect of ocean tides (Pertsev B.P., 1977) tidal deformations of the Earth's crust in this region are not anomalous. And therefore we can expect that the calculated amplitudes of vertical displacements under the influence of ocean tides will also give for the European continent a reliable picture of the phenomenon. The calculations were based upon the global cotidal charts of Bogdanov C.T. and Magarik V.A. (1967) slightly corrected to conserve the mass of tidal water. Moreover we have taken into account the tides in the North Sea (Hansen W., 1952) the Mediterranean sea (Chiaruttini C., 1976) and in other seas and sea regions distant from Europe.

Calculations were performed for a large number of points. On this basis a map of amplitudes of vertical displacements in Europe has been drawn. All available cotidal data up to about 100 km from each point were taken into account in the calculations. For this reason lines of equal amplitudes are not extended up to the coastline. As can be seen from the map, amplitudes of vertical displacements due to the loading effect of ocean tides for only one wave M_2 can reach 10 mm even at a distance of hundreds of km. from the coast. Near the coast the displacements can exceed this value by a large amount. The amplitudes of vertical displacements decrease with the distance from the Atlantic ocean and the North sea to about 3 mm in eastern Europe. The Mediterranean sea does not contribute much to the total effect. The tides in the Black sea and the Baltic are very small. The unaccounted tides in some Arctic seas may of course have an influence on the vertical displacements in eastern Europe. The lines of equal amplitudes stretch roughly in the North-South direction parallel to the Atlantic ocean.

It is well known that the amplitude of vertical displacements due to Earth tides in the frequency of separate waves depend only upon latitude. If we put $h_2 = 0.6$ then for M_2 the amplitudes of vertical displacements at latitudes 45° and 50° are equal respectively to 73 and 60 mm. Thus the vertical displacements of the Earth's surface due to the loading effect of ocean tides equals in continental parts of western Europe up to about 15% of Earth-tide displacements. In view of smaller amplitudes of Earth tides in higher latitudes the relative contribution of the loading effect in total vertical displacements will be much greater. In the gravity tide in this region (Pertsev B.P., 1977) the effect of the seas accounts only for 3-4% of the total tidal variations of gravity.

The amplitudes of vertical displacements which we have received for western Europe are about two times smaller than those given in D. Bower's (1969) map. In our opinion this difference is explained not only by the difference in cotidal data, but also by the fact that the map of D. Bower was calculated according to the method of Boussinesq for an elastic halfspace.

Only the amplitudes of vertical displacements due to ocean tidal loading are shown in the figure. The total radial displacements of the surface due to Earth and sea tides are naturally represented by a sum of two vectors and are therefore dependant on the difference of phases of these two motions. It should be noted that the phases of the load component can adopt all possible values and can therefore be different at different points of the Earth's surface. It is well known that the phases of Earth tides differ very little from the phases of the tide-generating potential. In view of the relatively big contribution of the ocean tide loads in the total effect the phases of real displacements at some points may differ substantially from the theoretical values of the phases of radial deformations.

Thus it is necessary to take account of the indirect effect of ocean tides in evaluating the tidal radial displacements of the Earth's surface. This is especially important for points located at small distances from the sea coast or at high latitudes, where the effect of ocean-tide loading can be comparable in size with Earth tide deformations.

REFERENCES

BOGDANOV K.T., MAGARIK V.A. (1967) Numerical solution of the problem of semi-diurnal tidal waves propagation in the World Ocean. Doklady AN SSSR, vol. 172 n°6.

BOWER D. (1969) Some numerical results in the determination of the indirect effect. Sixième Symposium International sur les Marées Terrestres-Strasbourg.

CHIARUTTINI C. (1976) Tidal loading on the Italian peninsula. Geophys. J. R.A.S. vol. 46 n°3

HANSEN W. (1952) Gezeiten des Meeres. Landolt-Bornstein Zahlenwerte und Funktionen vol. 3

PERTSEV B.P. (1977) M_2 ocean-tide corrections to tidal gravity observations in western Europe. Annales de Géophysique fasc. I/2 t.33

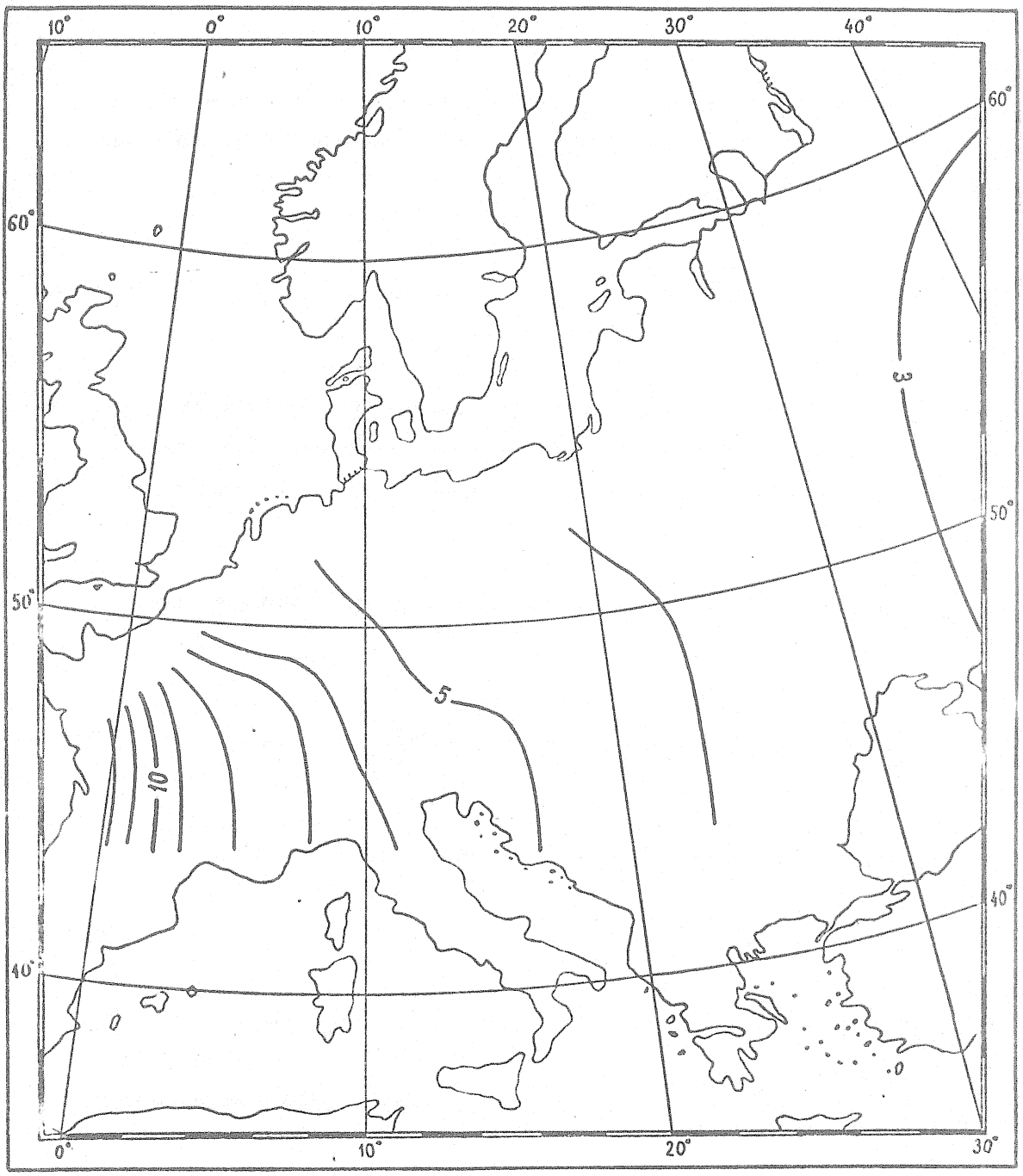

Amplitudes (in mm.) of vertical displacements of the Earth's due to ocean tide loading in the M_2 frequency

ON THE ASYMPTOTICALLY EFFICIENT ESTIMATION OF THE TIDAL GRAVITY VARIATION SPECTRUM

I.E. NIKOLADZE

Let y(t) be a given function which may be represented as a sum of sinusoids whose periods do not form a harmonic sequence for the given interval of time (-L, L) :

$$\sum_{i=1}^{N} A_i \sin(\omega_i t + \phi_i) = \sum_{i=1}^{N} (a_i \sin \omega_i t + b_i \cos \omega_i t) = y(t) \qquad (1)$$

Here y(t) is given for equidistant points of the time argument t_j, j=0,1,2 ..., the frequencies ω_i are known, or is known in advance that they do not form a harmonic sequence for the (-L, L). The problem is to estimate the parameters A_i, ϕ_i or a_i, b_i.

As is generally accepted the estimates a_i, b_i must satisfy the condition :

$$\int_{-L}^{L} \left[\sum_{i=1}^{N} (a_i \sin \omega_i t + b_i \cos \omega_i t) - y(t) \right]^2 dt = \min. \qquad (2)$$

This leads to two normal systems of linear equations :

$$ca = h, \quad cb = h' \qquad (3)$$

Where the matrix $\{c_{iK}\} = \left[\sin(\omega_i - \omega_K) L\right] / (\omega_i - \omega_K) L$ is the same for both equations (3) if the interval (-L, L) satisfies the condition : $\left[\sin(\omega_i + \omega_K) L\right] / (\omega_i + \omega_K) L \simeq 0$. The components of the right-side vectors are :

$$h_i = \frac{1}{L} \int_{-L}^{L} y(t) \sin \omega_i t \, dt , \quad h'_i = \frac{1}{L} \int_{-L}^{L} y(t) \cos \omega_i t \, dt \qquad (4)$$

The main difficulty arising in studying amplitude-phase spectrum of tides is that the equations (3) are too "oblique-angled", even for a one and

half year interval. This is due to the fact that the tidal harmonics are very close in regard to frequencies. Therefore, the estimates of a_i and b_i, obtained by direct solutions of these systems, are irregular.

In order to obtain correct estimates of harmonic parameters it is necessary to have a longer interval of time (-L, L) or to increase the accuracy of the readings of y(t). But these requirements are connected with technical difficulties.

The problem is how to transform y(t) so as to obtain maximum possible information on the sought harmonic parameters for the given limited interval of time and accuracy of readings. Notwithstanding the large number of techniques evolved for the solution of this problem it still remains unsolved.

A know scheme of transformation of the initial function is suggested in the present paper with a view of obtaining a correct solution of the system of equations (3).

Instead of the interval (-L, L) we shall consider (0, 2L). Let $2L_i < 2L$, $T_i = 2\pi/W_i$. We take $2L_i$ such that T_i should enter in $2L_i$ in integer times. Let us consider the following sequence of sub-intervals of time $(t_m, t_m + 2L_i)$, were $t_1 = 0$, $t_2 = \alpha_1$, $t_3 = 2\alpha_1 \ldots t_m = 2L - 2L_i$. The cosine transformation for the given frequency ω_i for the first sub-interval has the form :

$$A_i \sin \phi_i + \frac{\sin (\omega_i-\omega_1) L_i}{(\omega_i- \omega_1) L_i} A_1 \sin \left[(\omega_i-\omega_1) L_i + \phi_1 \right] + \ldots = \frac{1}{L_i} \int_0^{2L_i} y(t) \cos \omega_i t \, dt \tag{5}$$

Performing analogous transformations for all sub-intervals we obtain :

$$A_i \sin (\omega_i t_j+\phi_i) + \frac{\sin(\omega_i-\omega_1) L_i}{(\omega_i - \omega_1) L_i} A_1 \sin \left[\omega_1 t_j+\phi_1' \right] + \ldots = \frac{1}{L_i} \int_0^{2L_i} y(t) \cos \omega_i t \, dt$$

$$= h_1 (t_j) \tag{6}$$

Therefore, after a single use of the sliding cosine transformation for the given frequency ω_i we have $y(t) \to h_k(t)$, where $h_k(t)$ is the sum of the same harmonics, but it is important that the amplitude and the phase sought harmonic remain constant while the amplitudes of all the other waves are

suppressed, as $\left[\sin (\omega_i - \omega_K) L_i \right] / (\omega_i - \omega_K) L_i \leq 1$. Repeating this transformation k times we obtain :

$$A_i \sin (\omega_i t_j + \phi_i) + \left[\frac{\sin(\omega_i - \omega_1) L_i}{(\omega_i - \omega_1) L_i} \right]^K A_1 \sin (\omega_1 t_j + \phi'_1) + \ldots = h_K(t_j) \quad (7)$$

The interval of any k new function $h_K(t)$ is decreased by $2L_i$, for each stage of transformation. Therefore, the maximal number of transformation is entier (L/L_i) for the interval 2L.

Hence, the recursive transformation gives the amplitude coefficients :

$$\rho_{ikj} = \left[\frac{\sin (\omega_i - \omega_j) L_i}{(\omega_i - \omega_j) L_i} \right]^k \quad (8)$$

Usual transformation would give such amplitude coefficients :

$$\alpha_{ij} = \frac{\sin (\omega_i - \omega_j) K L_i}{(\omega_i - \omega_j) K L_i} \quad (9)$$

Comparison of this coefficients is shown on the fig. 1

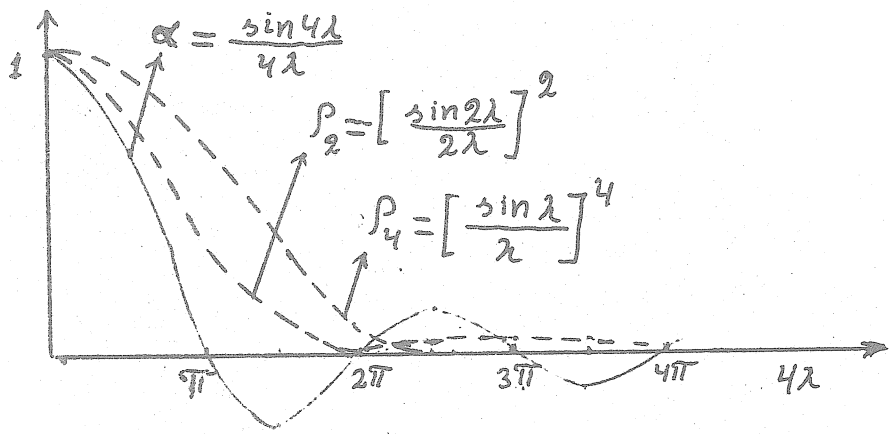

Fig. 1. The amplitude coefficients.

Comparison of these coefficient shows that this recursive transformation excludes the harmonics whose frequencies sufficiently differ from the W_i under investigation. This advantage of recursive transformation is very important for the investigation of tidal phenomena, for this process involves waves greatly differing in amplitudes. Furthermore, instrumental drift is approximated by long-period waves. The frequencies of these harmonics differ considerably from the diurnal, semi-diurnal and terdiurnal ones. Therefore, the amplitude coefficients for them will be very small. Thus, the influence of drift is practically eliminated from estimation value.

As is known, there are other methods of eliminating fictitious waves (1,2). E.g. the use of the weighted functions (Gipp's and Gan's). But in using these transforms the prescribed function y(t) must be available in the form of readings without gaps. However, this is technically difficult.

An advantage of the suggested recursive transformation it is feasible to use data having gaps of any length.

Let us consider the first stage of recursive transformation. Let any subinterval contain a gap. Then we shall subdivide this interval into small nonintersecting intervals of the length T_i. We shall fill this subinterval so that the period T_i enter $2L_i$ the same number times as the interval without gaps. Then, it can be easily demonstrated that the accuracy of the transformation will not be inferior to the case in which gaps are absent.

In the study of tides the parameters $\delta_i = \tilde{A}_i^\circ / \tilde{A}_i^T$ and $\chi_i = \phi_i^\circ - \phi_i^T$ are estimated. Here A_i° and ϕ_i° are observed amplitudes and phase, A_i^T, ϕ_i^T being the theoretical ones.

The suggested recursive transformation allows to estimate the parameters δ_i and χ_i without solving the system of equations (3) obtained through transformation of (7). The graph shows that amplitude coefficients ρ_{ikj} are practically zero for harmonics whose frequencies are not very close. If we combine separate harmonics the frequencies of which are close as practised in other methods (3) and if we assume that the parameters δ_i, χ_i are the same for each component of this group, then the transformation of (7) gives :

$$\tilde{a}_i^\circ = \delta_i \left[A_i \cos(\phi_i + \chi_i) + \rho_{ik1} A_1 \cos(\phi_1' + \chi_i) + \ldots \right] \qquad (10)$$

$$b_i^\circ = \delta_i \left[A_i \sin(\phi_i + \chi_i) + \rho_{ik1} A_1 \sin(\phi_1' + \chi_i) + \ldots \right]$$

After simple transformations we obtain :

$$\tilde{a}_i^{\circ} = \delta_i \left[(A_i \cos \phi_i + \rho_{ik1} A_1 \cos \phi_1' + \ldots) \cos \chi_i - (A_i \sin \phi_i + \rho_{ik1} A_1 \sin \phi_1' + \ldots) \sin \chi_i \right] , \tag{11}$$

$$\tilde{b}_i^{\circ} = \delta_i \left[(A_i \sin \phi_i + \rho_{ik1} A_1 \sin \phi_1' + \ldots) \cos \chi_i + (A_i \cos \phi_i + \rho_{ik1} A_1 \cos \phi_1' + \ldots) \sin \chi_i \right] .$$

Similar operations are carried out for the theoretical function describing the given process in the same interval of time. Then $\delta_i^T = 1$, $\chi_i^T = 0$ and we obtain the homological values of the parameters

$$\tilde{b}_i^h = A_i \sin \phi_i + \rho_{ik1} A_1 \sin \phi_1' + \ldots , \quad \tilde{a}_i^h = A_i \cos \phi_i + \rho_{ik1} A_1 \cos \phi_1' + \ldots \tag{12}$$

Then the expression (11) may be written thus :

$$\begin{aligned} \tilde{a}_i^{\circ} &= \delta_i \left[\tilde{a}_i^h \cos \chi_i - \tilde{b}_i^h \sin \chi_i \right] , \\ \tilde{b}_i^{\circ} &= \delta_i \left[\tilde{a}_i^h \sin \chi_i + \tilde{b}_i^h \cos \chi_i \right] . \end{aligned} \tag{13}$$

Hence we obtain

$$\delta_i = \tilde{A}_i^{\circ} / \tilde{A}_i^h ,$$

$$\cos \chi_i = \frac{\tilde{a}_i^{\circ} \tilde{a}_i^h + \tilde{b}_i^{\circ} \tilde{b}_i^h}{\delta_i (\tilde{A}_i^h)^2} , \qquad \sin \chi_i = \frac{\tilde{b}_i^{\circ} \tilde{a}_i^h - \tilde{a}_i^{\circ} \tilde{b}_i^h}{\delta_i (\tilde{A}_i^h)^2} \tag{14}$$

Therefore, if the assumation that the parameters δ_i and χ_i are the same for harmonics of close frequencies is valid then, it is not necessary to solve the equation (7) in respect to a_i and b_i. The expressions (14) may be used in this case.

The following are the basic advantages of this algorithm of estimation of a spectrum of Earth tides :

1. the estimations obtained by this algorithm satisfy the basic condition (2),
2. the transformation of the given function is linear, therefore the sinusoidal spectrum of the process is not distorted,
3. it is possible to use data with gaps.

This algorithm has been tested with models.

REFERENCES

1. Blackman R.B. and Tuckey J.W. (1959) : The measurement of power spectra. New York.

2. Anderson T.W. (1971) : The statistical analysis of time series, New York.

3. Lecolazet R. (1956) : Application à l'analyse des observations de la marée gravimétrique, de la méthode de H., et J. Labrouste, dite par combinaisons linéaires d'ordonnées. Ann. de Géoph., t. 12, fasc. 1.

OBSERVATIONS OF TIDAL TILTS IN BORE-HOLES

I.A. SHIROKOV, K.M. ANOKHINA

The tiltmeter technique of study of the Earth crust's deformations is presently going through the stage of instrumental and methodical renovation. The unwieldy and relatively simple tiltmeters with mechanical amplification are being substituted by instruments with electronic amplification, having automatic calibration, digital recording, and remote monitoring. The progressively distinct current trend in technique is the substitution of observations in the arbitrarily placed stations by more strict and effective system of profile observations being characterized by the versatile and conventional procedure of the tiltmeter's installation at any given point of a profile (1). This trend corresponds to the character of the international geophysical projects in which observations of the Earth tides play an important role.

The precision of measurements of the tidal and secular tilts essentially depends upon a noise level inherent to the specific procedure of the tiltmeter's installation : in adits, in prospect-holes, or in prospect-pits. Also a noise level for the different tidal station isn't the same and is likely to change for a year. Therefore the precision of determination of the tidal tilts is now being improved due to development of the procedure of the tiltmeter's installation and due to experience of continuous observations in as much as possible large number of stations. At present the main tidal waves are being determined with a precision of about 1 % in certain stations (2).

When interpreting the profile or areal tidal observations, the most difficulties arise owing to inadequate representation of the individual results, this term denoting here the requirement for obtaining of the observed values γ and χ ressembling in error limits at the points falling close together. The Earth tides as a global phenomenon capturing the deepest regions of the Earth have to be characterized by the almost identical parameters observed on the broad area places and, in any case, at the points 20-30 m apart. The perturbing effect of the local tectonic situation on the results of observations at these points is assumed the same.

But many instances are available when the tidal waves' parameters at the points falling close together are different one from another more than it follows from an estimate of their internal precision. In our view, the inadequate representation of such results is due to lack of an effective conventional procedure of the tiltmeter's installation.

From this point of view the results of the tiltmeter observations in the bore-holes falling close together, carried out near Moscow, are of certain interest.

The tiltmeter observations in bore-holes in the USSR were began to carry out from 1972 by the Institute of Physics of the Earth at the Polushkino tidal station with Askania-borehole tiltmeters, and, beginning from 1974, with modified Ostrovsky tiltmeters (3). It is to be noted that until recently observations of the Earth tides in bore-holes failed by horizontal pendulums, mainly, because of high requirements to a construction of an instrument and of a bore-hole. When resolving this problem, the suitable procedure of lowering, azimuthal orientation, and adjustment of a bore-hole instrument have been developed.

The Polushkino tidal station has three identical bore-holes 30 m deep and 10-15 m apart. Three Ostrovsky tiltmeters (NN 4, 51, 78) installed at bore-hole had been used in the observations. Regardless of low times of sets of the simultaneous observations we held it possible to use their for determination of representative values of the tidal parameters as well as for comparison of the procedures of the tiltmeter's installation at bore-holes and -pits.

Tables 1 and 2 present the values of the amplitudinal factor γ and of the phasal delay χ in conjunction with the estimate of precision for four the most major waves M_2, S_2, K_1, O_1. To obtain the representative values γ and χ for these waves the weighted mean values were calculated for a group of the bore-holes. The coefficients inversely proportional to squares of standard errors were used as a weight.

The maximum deviation from the weighted mean value $\gamma(M_2)$ was obtained for the bore-hole 1 (0.8 %). The relatively large standard error of the result is accounted for by low time of the set of observations at the bore-hole 1.

The result for the bore-hole 2 was obtained with less error since the time of the set of observations at it was almost three times as large as one at the bore-hole 1. At the bore-holes 1 and 2 the Ostrovsky horizontal

pendulums were installed close to the face at the same deep approximately.

The least error of an amplitudinal factor was obtained for the tiltmeter installed in the middle of the bore-hole 3. Where the value γ (M_2) was 0.726 with the deviation of 0.15 % from the weighted mean.

For the wave S_2 the maximum deviation of a factor γ from the weighted mean value was obtained at the bore-hole 2 (2 %). The similiar deviations for the bore-holes 1 and 3 were 0.3 and 1 %, respectively.

The diurnal waves have been determined with less precision than the semi-diurnal ones since the higher periodic noise level is observed on these frequencies. The investigations (4) have showed that the main noises at the Polushkino station is the local temperature periodic tilts and the barometric loading effects.

The weighted mean value γ (K_1) for the group of the bore-holes was 0.687. The maximum deviation from it amounts to 1.5 % at the bore-hole 1, and the values γ (K_1) at the bore-holes 2 and 3 are differ one from another and from the weighted mean value no more than 0.5 %.

For the lunar wave O_1 the weighted mean value γ (O_1) is 0.751, and the deviation of the results for the separate bore-holes from it doesn't exceed 1 %.

Thus, the amplitudinal factors correlating for each of the examined waves with the precision of 1-2 % have been determined for three bore-holes falling close together. It is indicative of the representation of the obtained results for the studied ground.

The observed stable difference between γ for the various waves is attributed to the perturbing effect of the periodic noises at all bore-holes.

The delay of a tidal tilt's phase is determined with relative confidence for the wave M_2. The weighted mean value χ (M_2) was - 1°.8. The most value χ (M_2) reaching - 5°.6 was obtained for the bore-hole 1. It seems to be accounted for by less accurate tiltmeter's orientation carrying out by means of a magnetic compass at the bore-hole 1. Excluding the result for the bore-hole 1 from consideration the phasal delay of the wave M_2 is -0°.9 ± 0.7.

Let us compare the tidal parameters obtained from the observations at the group of bore-holes and at the group of bore-pits near Moscow (2). For the wave M_2 Table 3 gives the results of the bore-hole observations at the

Polushkino station and the results of the bore-pit observations at the stations Syanovo, Khatun', and Novlinskoye. Each of the latter stations has the near-lying bore-pits 15-20 m apart and 10-12 deep.

Table 3 shows that the values γ (M_2) for the bore-holes correlate better than ones for the bore-pits. The error of the mean value γ (M_2) for the bore-holes is 0.5 % only, and the least one for the bore-pits is 1.5 % (the Syanovo station). The value of a phase delay χ (M_2) for the bore-holes is markedly less than this one for the bore-pits, too. Thus, the tidal observations at the bore-holes are more representative than the ones at the bore-pits.

REFERENCES

1. Schmitz-Hübsch H., Das Oberbayerische Testnetz für Erdgezeiten der Abteilung I des Deutschen Geodätischen Forschunginstituts München, 3. Internationalen Symposium "Geodäsie und Physik der Erde". Weimar im Oktober 1976.

2. Ostrovsky A.E., Matveyev P.S., Tidal Tilts of the Earth's Surface Observed in the USSR. Sbornik "Izuchenie Prilivnykh Deformatsii Zemli" (in "Study of Tidal Deformations of the Earth"). "Nauka", 1973.

3. Schirokov I.A., Anokhina K.M., Local, Temperature Tilts of the Earth's Surface. Sbornik "Vrashchenie i Prilivnye Deformatsii Zemli" (in "Rotation and Tidal Deformations of the Earth", VII). "Naukova dumka", 1975.

4. Shirokov I.A., Anokhina K.M., The Technique and Results of the Tiltmeter Observations in the Bore-holes. Sbornik "Sovremennye Dvizheniya Zemnoy Kory" (in "Recent Motions of the Earth's Crust"). Novosibirsk, 1976.

TABLE 1

Results of harmonic analysis of the tiltmeter observations at the bore-holes of the Polushkino tidal station.

(The method of analysis - by Venedikov;
component E-W;
the instrument - Ostrovsky tiltmeter)

semi-diurnal waves

	Point of observation	Instrument N°	Depth of installation	Time of observation	Wave M_2		Wave S_2	
			meters	days	γ	χ	γ	χ
1.	bore-hole 1	NF-51 (TP-51)	28	40	0.719 31	-5°.6 1°.8	0.709 76	4°.9 4°.4
2.	bore-hole 2	NF-4 (TP-4)	30	116	0.729 22	0°.6 1°.6	0.721 62	1°.7 4°.0
3.	bore-hole 3	NF-78 (TP-78)	17	40	0.726 11	-2°.3 0°.6	0.701 24	1°.9 1°.5
4.	weighted mean				0.725 3	-1°.8 0°.7	0.707 5	2°.4 1°.2

TABLE 2

Results of harmonic analysis of the tiltmeter observations at the bore-holes of the Polushkino tidal station.

(The method of analysis - by Venedikov;
component E-W;
the instrument - Ostrovsky tiltmeter)

Diurnal waves

	Point of observation	Instrument N°	Depth of installation	Time of observation	Wave K_1		Wave O_1	
			meters	days	γ	χ	γ	χ
1.	bore-hole 1	NF-51 (TP-51)	28	40	0.676 73	-12°6 4°2	0.760 122	11°6 7°0
2.	bore-hole 2	NF-4 (TP-4)	30	116	0.692 79	6°7 4°5	0.744 96	12°5 5°5
3.	bore-hole 3	NF-78 (TP-78)	17	40	0.690 25	-0°1 1°4	0.750 45	2°4 2°6
4.	weighted mean				0.687 5	-1°4 1°2	0.751 6	6°8 3°7

TABLE 3

Values of γ and χ for the wave M_2 by observations of the Earth's tilts at the bore-holes and -pits in the tiltmeter stations near Moscow

Tiltmeter stations of the Institute of Physics of the Earth near Moscow.

Polushkino			Syanovo			Khatun'			Novlinskoye		
Point N°	γ	χ	Point N°	γ	χ	Point N°	γ	χ	Point N°	γ	χ
bore-hole 1	0.719	-5°.6	bore-pit III	0.675	-5°	bore-pit IV	0.733	-5°.7	bore-pit I	0.692	-5°.2
bore-hole 2	0.729	0°.6	bore-pit VII	0.680	-4°	bore-pit V	0.715	-3°.3	bore-pit II	0.768	-7°.6
bore-hole 3	0.726	-2°.3	bore-pit VIII	0.698	-5°.3	bore-pit VI	0.707	-4°.0			
mean	0.725 3	-1°.8 0°.7	mean	0.684 9	-4°.8 0°.5	mean	0.718 10	-4°.3 0°.9	mean	0.729 37	-6°.4 1°.2

THE TILTMETER OBSERVATIONS BY AN ASKANIA VERTICAL PENDULUM IN A BORE-HOLE NEAR MOSCOW

I.A. Shirokov, K.M. Anokhina

The observations of tidal tilts were run by the Askania vertical pendulum.

N°9 in the test station Polushkino near Moscow at the depth of 45m. The construction and technology of making of the bore-hole were carried out according to recommendations of the Askania firm.

The purpose of observations was determination of an amplitude factor and a phase delay of waves of a tidal tilt. The recording of tidal tilts was began from August, 1974 and was continued steadily during six months. Tilts were recorded by an point compensograph Siemens 288 x 288.

The orientation of the Askania tiltmeter at the borehole was carried out by means of the device developed especially a long the azimuths N-S and E-W with a precision of about 0°3. The scaling factors of recording were computed from the data of multiple calibrations by a ball and were: $K_{E-W} = 0.341.10^{-3}$ sec. arc/mm and $K_{N-S} = 0.303.10^{-3}$ sec.arc/mm. The stability of this factors was hot worse than 0.6%.

The zero point's drift was calculated by Pertsev's combination. As is seen from Fig. 1, the drift is monotonous and doesn't exceed 0.1 sec.arc/ month. The total value of the drift for six months of observations had amounted to 0.55 and 0.48" for E-W and N-S, respectively. The drift of a zero point doesn't correlate with temperature variations in the borehole at the depth of 45m.

The tide released from a drift was subjected to harmonic analysis by Pertsev's and Venedikov's methods. Tables 1 and 2 present the resultats of the analysis. The values γ and χ obtained by different methods agree within error limits. The exception is the waves N_2 and O_1 along the N-S azimuth with

disagreement amounting to 1.9%. For the wave N_2 this appears to be attributed to the procedre of smoothing in calculations of independent values and by Pertsev's method.

While correcting for the effect of ocean tides according to B.P. Pertsev's estimation, the azimuthal inequality $\gamma_{N-S} < \gamma_{E-W}$ for the wave M_2 disappears since the values of corrections for N-S and E-W components are +0.053 and 0.015, respectively. The phase delay of the wave M_2 is $\chi_{E-W} = -1°.5$ and $\chi_{N-S} = +1°.0$ taking into account the indirect effect. For the remaining semi-diurnal waves the correction for ocean wasn't estimated.

However, the amplitude factors of semi-diurnal waves (Table 1) have the more high values than the ones obtained so far in the other stations near Moscow /1/. In particular, the observations in the Polushkino station carried out with Ostrovsky's horizontal pendulums at three boreholes 10m distant from the borehole with the Askania tiltmeter had given three independent factors γ_{E-W} (M_2) with the mean value of 0.725, resembling with a precision of 1% /2/. This difference of 7% appears to be account to availability of a systematic error in observations by the Askania tiltmeter. The effect of a systematic error on the results of determination of diurnal waves is reflected less markedly.

To find the causes of the observed disparity of the results it is assumed to carry out observations by the Askania tiltmeter at three adjacent boreholes mentioned above.

REFERENCES

1. OSTROVSKY A.E., MATVEYEV P.S. Tidal tilts of the Earth's surface by observations in the USSR. In: "Izuchenie Prilivnych Deformatsii" ("Study of Tidal Deformations of the Earth"). "Nauka", 1973.

2. SHIROKOV I.A., ANOKHINA K.M. The technique and results of tiltmeter observations in boreholes Proceedings of the Conference on Recent Motions of the Earth's Crust. Novosobirsk, 1976.

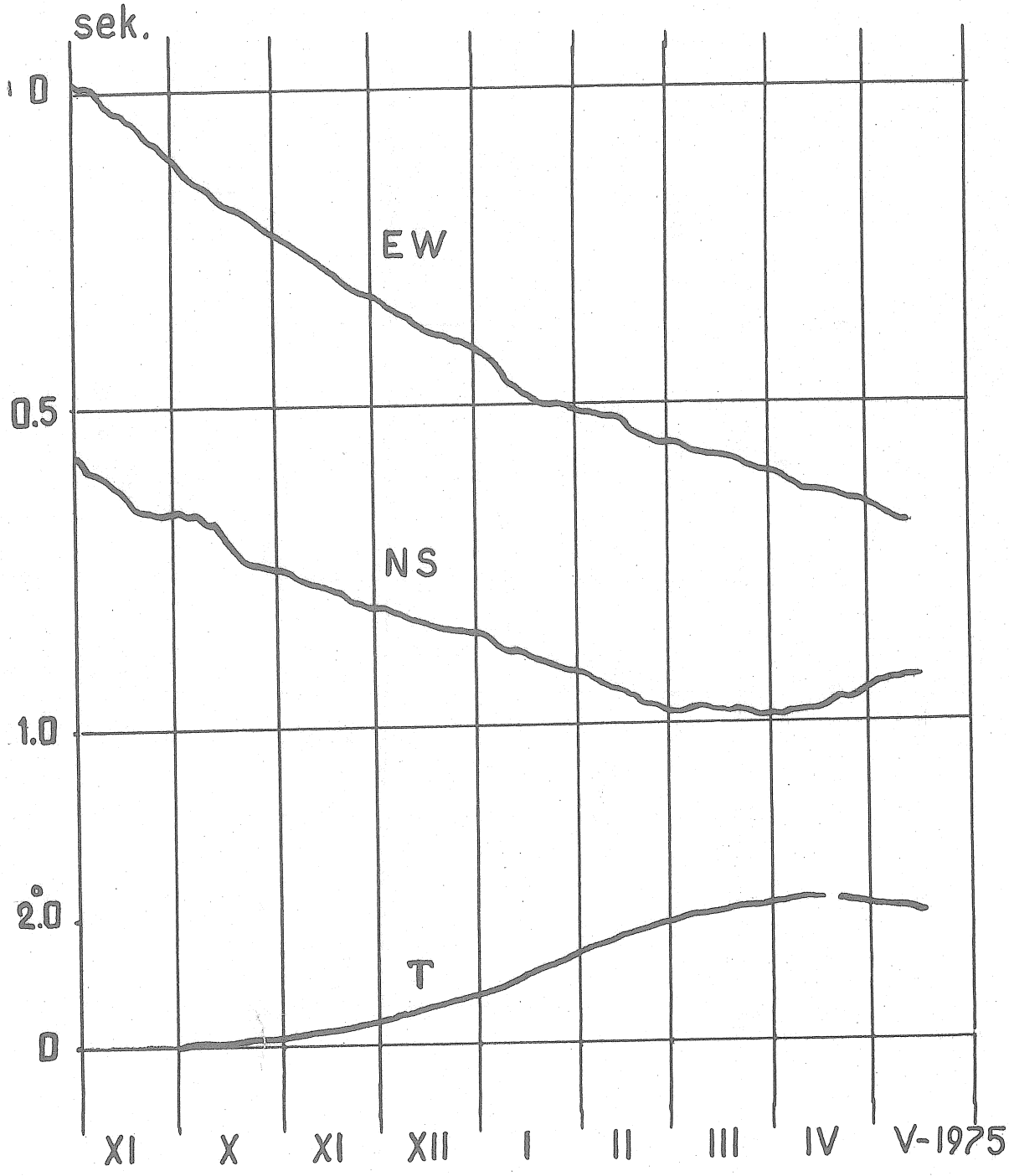

Fig. 1

The drift of zero point of the Askania borehole tiltmeter.

TABLE I. RESULTS OF HARMONIC ANALYSIS OF OBSERVATIONS OF TIDAL TILTS BY AN ASKANIA BOREHOLE TILTMETER

Semi-diurnal waves

WAVES		M_2	S_2	N_2	$2N_2$	L
H_T, msec. arc		8.93	4.16	1.71	0.27	0.25
Parameter		Y X	Y X	Y X	Y X	Y X
E-W	V	0.777 -3.5 3 2	0.784 -2.2 6 3	0.797 -2.5 15 8	0.654 -8.2 78 5	0.871 19.7 164 9.4
	P	0.773 -3.5 5 2	0.781 -2.0 8 5	0.799 -2.1 17 4	- -	- -
H_t msec. arc		7.36	3.42	1.41	0.23	0.21
N-S	V	0.744 1.4 4 2	0.745 0.1 7 4	0.722 -0.9 18 1.0	0.838 -7.5 97 5.5	1.023 2.5 188 10.7
	P	0.742 1.4 5 5	0.757 2.3 5 1.4	0.736 -2.0 18 1.8	- -	- -

TABLE 2

Diurnal waves

WAVES		K_1	O_1	Q_1	M_1	J_1	OO_1
H_t, msec. arc		7.56	5.37	1.03	0.42	0.42	0.23
Parameter		γ χ	γ χ	γ χ	γ χ	γ χ	γ χ
E-W	V	0.681 -4.3 8 5	0.666 -2.0 12 7	0.677 -3.3 63 3.6	0.650 9.2 126 7.2	0.874 14.8 144 8.2	0.751 20.2 265
	P	0.684 -4.0 18 5	0.663 -4.3 18 1.5	- -	- -	- -	- -
H_t, msec. arc		3.29	2.34	0.45	0.18	0.18	0.10
N-S	V	0.763 -2.1 19 1.1	0.729 5.9 29 1.6	0.645 9.2 159 9.1	0.435 35.0 288 16.5	1.459 -5.4 392 12.4	0.743 11.1 644 16.9
	P	0.788 -3.0 18 3.1	0.737 5.0 25 1.6	- -	- -	- -	- -

THE RISE OF PRECISION AND THE AUTOMATION OF TILTMETER MEASUREMENTS

M.J. BAGMET, A.E. OSTROVSKY, A.L. BAGMET

In the USSR measurements of tilts of the Earth's surface for decision of problems of geophysics and engineering geology mainly carry out by tiltmeters with photoelectric magnification (1). Experience of many years of work with these instruments had showed their reliable performance, convenience for field observations, high sensitivity, large stability of the null-point, and high precision of measurements of tidal and slow tilts with error of no more than 1 %.

The problem of rise of precision of tilts' measurements permanently confronts the geophysicists. To this end the numerous studies were carried out of recent years. But it is clear that the most essential results can be reached by development of automatic tiltmeters of stable sensitivity, giving results of measurements of tilts in the form of suitable for direct introduction into electronic computer without preliminary treatment.

This work presents the results of studies in the direction, carried out at the Laboratory of Tilts of the Institute of Physics of the Earth (Moscow).

The symbols

$\varepsilon \left[S^{-1}\right]$ - the constants of the tiltmeter's pendulum;

$\eta \left[S^{-1}\right]$ -

$L_o \left[m\right]$ - the reduced length of the pendulum;

$\Delta\theta \left[\text{sec.arc}\right]$ - the angular deviation of the pendulum from the equilibrium position;

$g \left[m/S^2\right]$ - gravity acceleration;

$\psi \left[\text{sec.arc}\right]$ - the tilt of the base on which the tiltmeter was placed relative to the plumb line;

$L_k \left[H\right]$ - the inductance of the pendulum's coil placed in a field of constant magnet;

$R_k \left[\Omega\right]$ - the resistance of the coil;

$T_k = \frac{L_k}{R_k}$ - time constant of the circuit of the coil;

$T_1 = R_1 \cdot C_1$ - time constant of a differentiating unit;

$T_2 = R_2 \cdot C_2$ - time constant of an integrating unit;

K_2 - transmission gain of the transducer of a shift of the pendulum into electric signal;

K_3, K_4 - transmission gains of amplifying gains;

I_o (μA/sec.arc) - electrodynamic constant of the tiltmeter;

K_6 - transmission gain of the voltage divider in the feedback circuit;

K_5 - transmission gain of the correcting gain (the coil);

$U_o \left[v\right]$ - an initial voltage of integration.

The tiltmeter

The improvement of metrological characteristics of a tiltmeter (as well as any measuring instrument) can be achieved by transfer of it into a regime of automatic control (2). For a tiltmeter NF (with photoelectric magnification) it is relatively simply to carry out as the mechanical system of the pendulum can be remained invariable, using another transducer only. The fact is that an existing transducer (photocells with a galvanometer) have low output signal (of about 0.1 mv per an amplitude of a tidal tilt). It doesn't allow directly to use it in the system of automatic control and requires to use complex amplifiers of direct current without a drift.

Therefore the new photoelectric transducer, in which the photocells were lighted by alternating luminous flux and the alternating current was amplified, was developed.

The work of the transducer is to be described in another report. Here we note the following :

a) the null-point's drift of the transducer is negligible low as the amplification is carried out by an alternating current;

b) the amplification is carried out by more high frequency relative to the one of useful signal, allowing to obtain very low noise level (70 db);

c) the value of an output signal is 5 v per an amplitude of a tidal tilt (0,02 sec. arc).

Fig.1 shows a fragment of a record chart with the recording of a tidal tilt obtained in Obninsk by an usual tiltmeter with the foregoing transducer.

Having a large output signal of the transducer, one can transfer the tiltmeter's pendulum in a regime of automatic control. In our case it is reasonably to use the mode of control by deviation, i.e. to build the system with a closed feedback. Fig. 3 presents the block diagram of the tiltmeter with automatic control by deviation.

An input value (command) is an angle of a tilt of the base $\Delta\psi$ vs time. The tiltmeter converts $\Delta\psi$ into an angular deviation of the pendulum from the equilibrium position ($\Delta\theta$), and an output voltage of the transducer (ΔU_1) appears. This voltage arrives to a controller involving two amplifying units 3 and 6, an integrating unit 5, a differentiating unit 4, and an adder 7. The output voltage of the adder arrives to a correcting element (the coil) through a voltage divider with the transmission gain K_6. The current flowing through the coil compensates the deviation of the pendulum $\Delta\theta$, caused by tilt of the base on the angle $\Delta\psi$.

Let us consider the dynamics and the static of the tiltmeter NF in the regime of automatic control.

The equation of the motion of the pendulum affected by harmonic tilts for an opened feedback is :

$$\ddot{\Delta\theta} + 2\varepsilon\dot{\Delta\theta} + n^2\Delta\theta = \frac{q}{L_o} \cdot \sin\Delta\psi \; . \qquad (1)$$

Standing for $\frac{L_o}{g} = K$ and taking into account that angles are low, we obtain :

$$\Delta\ddot{\theta} + 2\varepsilon\Delta\dot{\theta} + n^2\Delta\theta = \frac{1}{K}\Delta\psi. \qquad (2)$$

Upon closing the feedback the equation of motion of the pendulum will be :

$$K\Delta\ddot{\theta} + 2K\varepsilon\Delta\dot{\theta} + Kn^2\Delta\theta = \Delta\psi - \Delta_1\psi \ , \qquad (3)$$

or in the operator form :

$$\Delta\theta\,(Kp^2 + 2K\varepsilon p + Kn^2) = \Delta\psi - \Delta_1\psi \qquad (4)$$

The equation of dynamics of the system according to the equivalent diagram presented in Fig. 2 will be :

$$\Delta\theta = (Kp^2 + 2\varepsilon Kp + Kn^2) + K_2\left(K_3 + pT_1K_4 + \frac{1}{pT_2}\right)\frac{K_5}{1+T_k} = \Delta\psi. \qquad (5)$$

This is the equation describing dynamics of automatic control of the tiltmeter's pendulum.

In the case of static or quasi-static tilts ($p = 0$) we obtain :

$$\Delta\theta = 0 \qquad (6)$$

Hence, in the case of slow tilts of the base the control system will retain the pendulum at the zero position. The input voltage of the summation unit (ΔU_6) will be the electric analog of the input command, i.e. of a tilt $\Delta\psi = f(t)$.

The transfer function of a closed system of control ($W = \frac{\Delta U_6}{\Delta\psi}$) is :

$$W = \frac{K_2K_3 + K_2K_4T_1p + \frac{K_2}{pT_2}}{Kp^2 + 2K\varepsilon p + Kn^2 + \left(K_2K_3 + K_2K_4T_1p + \frac{K_2}{pT_2}\right)\cdot\frac{K_5}{1 + pT_k}} \qquad (7)$$

From here one can find the sensitivity of the tiltmeter to static tilts ($p = 0$) :

$$K_t = \frac{\Delta U_6}{\Delta\psi} = \frac{1}{K_5} = \frac{1}{K_6\,I_o} \qquad (8)$$

Thus, the sensitivity of the tiltmeter with automatic control depends only on the transmission gain of the feedback circuit, i.e. on K_6 and I_o, and doesn't depend on variation of the sensitivity of the transducer.

For a year I_o varies less than by 0.2 %. By use of modern high-stable wire-wound resistors in the feedback circuit we obtain the stability of the sensitivity of the tiltmeter with automatic control of no worse than 0.2 % for a year that makes it superfluous to carry out a periodic control of sensitivity of the tiltmeter.

Now let us find the frequency responses of the tiltmeter.

By ignoring the time constant of the coil, we write the expression of the transfer function (7) as

$$W = -\frac{K_2K_3 + K_2K_4T_1p + \frac{K_2}{pT_2}}{Kp^2 + 2K\varepsilon p + Kn^2 + K_2K_3K_5 + K_2K_4K_5T_1p + \frac{K_2K_5}{pT_2}} \qquad (9)$$

The tiltmeter with automatic control built by us on the basis of the conventional instrument NF has the following values of the constants :

$K_2 = 10^2$ v/sec.arc;

$K_3 = 10$;

$K_4 = 10^{-2}$;

$K_5 = 10^{-2}$ sec.arc/v;

$T_1 = 10s$;

$T_2 = 33s$;

$K = 10^{-1}$;

$\varepsilon = n = 2.5$.

The main unit of the controller is the integrator 5 which must have a minimum drift of the null-point, a large dynamic range, a high linearity of integration, a large time constant (dozens of seconds). The studies had showed that, by making use of high-precise microwire-wound resistors and capacitors of synthetic dielectric, such a integrator can be built on the basis of usual operational amplifiers of extensive application.

No special requirements to the residual units are.

Taking into account the numerical values of the constants, we write the equation (9) in the complex form :

$$W = \frac{10j\omega + \frac{3}{j\omega} + 10^3}{0.1\,\omega^2 + 0.6j\omega + \frac{0.03}{j\omega} - 10.6} \qquad (11)$$

Taking the module and the argument (10), we obtain the amplitudinal and phasal frequency characteristics (Fig. 4a,b).

The amplitudinal characteristic, i.e. the dependence of the sensitivity of the tiltmeter $(\frac{\Delta U_6}{\Delta\psi})$ on the period of tilts of the base, is the straight line parallel to X-axis within the range of low frequencies (T < 6s). It means that within this range and up to T = ∞ the sensitivity of the tiltmeter is constant and is 100 v/sec.arc in this case.

Within the range of high frequencies (T < 6s) the sensitivity of the tiltmeter falls. By comparing the amplitudinal characteristics of an usual tiltmeter (1) and the tiltmeter with automatic control it is clearly seen that the drop of the sensitivity begins by lesser periods (6s against 100s) and the rate of the drop is far less. On the one hand, it allows to record tilts of more high frequency with constant sensitivity and, on the other hand, it requires to use a low-pass filter for recording tidal tilts to suppress seismic noises.

Figs. 5 and 6 present the diagram of such a filter and its amplitudinal frequency characteristic obtained experimentally by means of an infra-low generator, respectively. For periods of T > 100s the filter introduces negligible low phasal distortions and effectively suppresses seisms of high frequency.

Fig. 4b shows the phasal frequency characteristic of the tiltmeter. Unlike a conventional tiltmeter the phasal distortions begin to increase by rather more frequencies (T < 10s). It is resulted from both lack of a galvanometer giving an essential phase shift (1, Table 3) and general features of measuring instruments with automatic control having more high metrological characteristics relative to usual ones.

Now we show as were selected the constants of the tiltmeter providing its stability by pulse commands. The compution of stability was carried out by Hurwitz criterion, as this system of automatic control is of fourth order. The stability margin was studied by Mikhailov criterion (2).

The equation of dynamics (5) can be written as :

$$\Delta\theta\,(a_4p^4 + a_3p^3 + a_2p^2 + a_1p + a_o) = \Delta\psi \qquad (11)$$

where a_1 is adequate combinations of the constants K_i, T_i, , and n.

According to Hurwitz criterion the system of automatic control is stable if the Hurwitz determinator of the characteristic equation :

$$a_4 p^4 + a_3 p^3 + a_2 p^2 + a_1 p + a_o = 0 \qquad (12)$$

and its diagonal minors Δ_3, Δ_2, and Δ_1 are positive, i.e.

$$\Delta_4 = \begin{vmatrix} a_3 & a_1 & 0 & 0 \\ a_4 & a_2 & a_o & 0 \\ 0 & a_3 & a_1 & 0 \\ 0 & a_o & a_2 & a_o \end{vmatrix} > 0,$$

$$\Delta_3 = \begin{vmatrix} a_3 & a_1 & 0 \\ a_4 & a_2 & a_0 \\ 0 & a_3 & a_2 \end{vmatrix} > 0, \qquad (13)$$

$$\Delta_2 = \begin{vmatrix} a_3 & a_1 \\ a_4 & a_2 \end{vmatrix} > 0,$$

$$\Delta_1 = a_3 > 0.$$

From these conditions the constants of the tiltmeter were selected.

The stability margin was evaluated by Mikhailov's procedure of graphic analysis. Let us present the left part of the characteristic equation (12) as a function of p :

$$F(p) = a_4 p^4 + a_3 p^3 + a_2 p^2 + a_1 p + a_o.$$

By replacing $p = j\omega$ we obtain the equation of a complex vector :

$$F(j\omega) = a_4\omega^4 - ja_3\omega^3 - a_2\omega^2 + ja_1\omega + a_o = x(\omega) + jy(\omega), \qquad (14)$$

its end drawing the Mikhailov's curve :

$$x(\omega) = a_4\omega^4 - a_2\omega^2 + a_o$$

$$y(\omega) = -a_3\omega^3 - a_1\omega \qquad (15)$$

by variation of ω from 0 to ∞.

According to Mikhailov criterion a system of automatic control of fourth order will be stable if the Mikhailov's curve successively passes through all four quadrants without crossing an origin (the stability limits). It can be achieved, varying some constants (e.g., K_2). The Mikhailov's curve for the tiltmeter built by us is shown in Fig. 7. It is seen that the system has a sufficient stability margin.

Fig. 8 gives the fragment of the record chart with the recording of a tidal tilt by the tiltmeter with automatic control in the Obninsk station.

The digital recording of tilts

Having a tiltmeter with constant sensitivity and large output signal, one can essentially increase the precision of recording of tilts, applying a digital recording in the form of suitable for direct introduction into a computer (3).

It was decided to build the digital system of recording of tilts on the basis of widespread integral microcircuits of medium-scale integration rather than of factory-made instruments (digital voltmeter, etc.). It allows to create the relatively simple inexpensive digital recorder (class of precision - 0.1) without unnecessary units.

The punched tape was selected as a information carrier. For direct introduction of it into a computer it must also contained a necessary service information.

The block diagram of the instrument is shown in Fig. 8.

The exchange assures an alternate connection of 8 tiltmeters. Its error is no more than 10 μv.

The voltage coder is built by standard microcircuits and have a dynamic range of 60 db and the error of coding of less than 0.1 %. The studies showed that the lasting drift of the null-point of the coder was less than 0.1 % for half a year.

The digital integrator permits to obtain the mean of 10 measurements with an interval of 1s. So the effect of seismic noises on precision of measurements of tilts is reduced.

The following information takes out in a punched tape :

1) the beginning of a cycle of measurement;

2) the channel's item No;

3) tiie of measurement;

4) the current value of output signals of tiltmeters - the mean of 10 measurements with an interval of 1s;

5) if required, the sigh of calibration of tilts, i.e. the calibration information;

6) The signal of proper work of a punch (the inspection of parity of a quantity).

The technical features of the instrument of digital recording of tilts are the following :

1) The number of channels - 8.

2) The time of one measurement - 10s (depending on time of digital integration).

3) The dynamic range - 60 db.

4) The error of measurement - 0.1 %.

5) Weight - 6 kg.

6) Intake power - 15 w.

The studies showed that the ordinates of tilts read from a punched tape agreed with the ones obtained as a result of its treatment within experiment error limits.

The punched tape is suitable for a direct introduction into a computer without a preliminary treatment.

Two tiltmeters with automatic control and the digital system of measurement of tilts are presently working in Obninsk. The results of these studies are to be published.

REFERENCES

1. A.E. Ostrovsky. A tiltmeter with photoelectric recording. Sbornik "Izuchenie Zemnykh Prilivov" (in "Studies of Earth's Tides"). Publ. House Acad. Sci. of USSR, Moscow, 1961.

2. V.A. Ivanov, B.K. Tchemodanov, V.S. Medvedev. "Matematicheskie osnovy avtomaticheskogo regulirovaniya" ("Mathematical Principles of Automatical Control") "Vysshaya Shkola", Moscow, 1971.

3. M.J. Bagmet. Digital recording of tilts of the Earth's surface. Sbornik "Sovremennye Dvizheniya Zemnoy Kory" (in "Recent Motions of the Earth's Crust"). Novosibirsk, 1976.

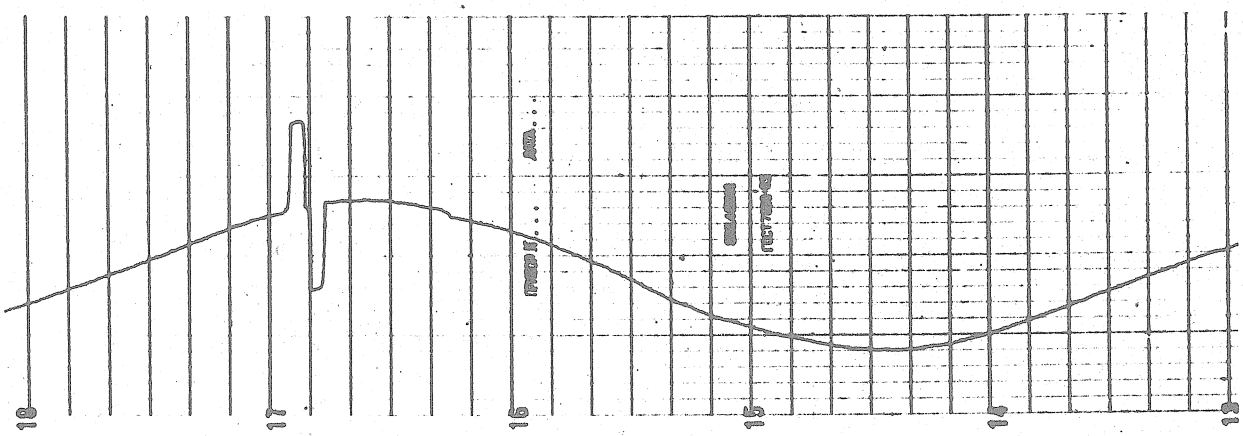

Fig. 1.

The fragment of a recording chart with a recording of a tidal tilt by the tiltmeter with new photoelectric transducer. The tilt's amplitude conforms to the output voltage of 5V..

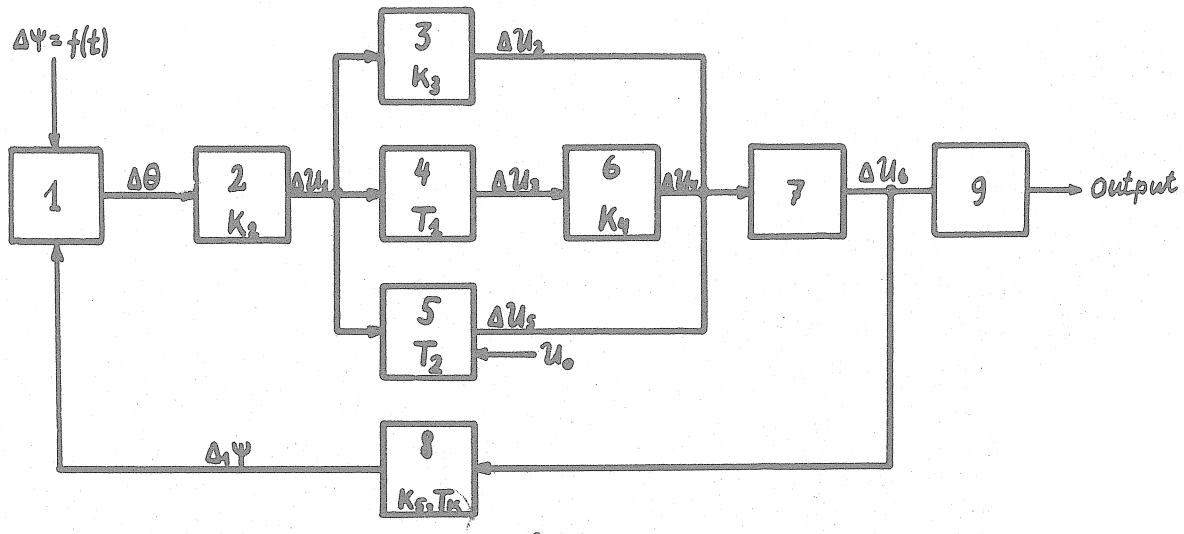

Fig. 2

The block diagram of the tiltmeter with automatic control.
1- the controlled object (horizontal pendulum);
2- the transducer of a pendulum's shift into electric signals;
3- the amplifying unit;
4- the differentiating unit;
5- the integrating unit;
6- the amplifying unit;
7- the summation unit;
8- the correcting element (coil);
9- the output L.F. filter;
ΔU_1 - ΔU_6 - the output voltages of units;
U_o - the initial voltage of integration.

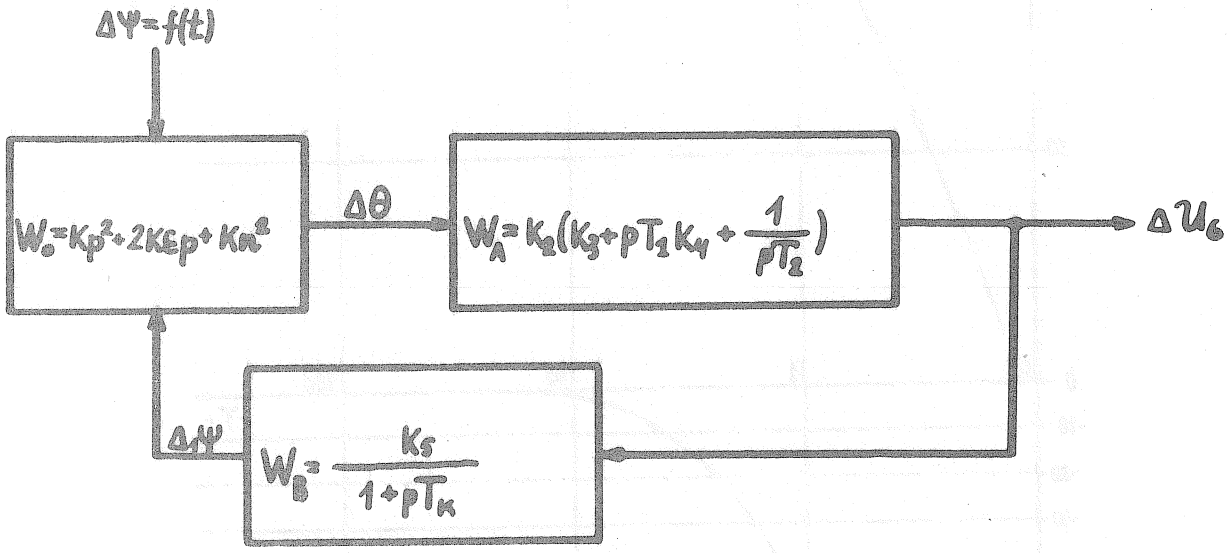

Fig. 3

The equivalent block diagram of the tiltmeter.

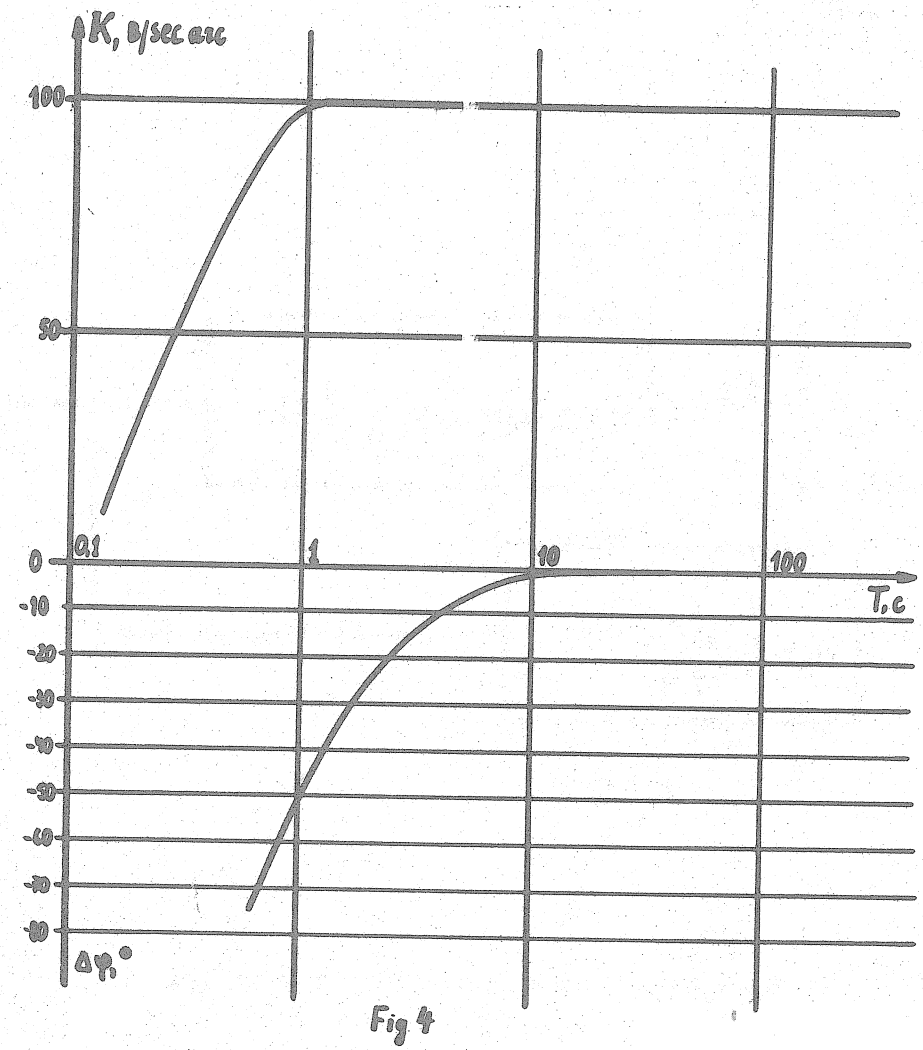

Fig 4

The frequency characteristics of the tiltmeter with automatic control:

a) amplitudinal

b) phasal.

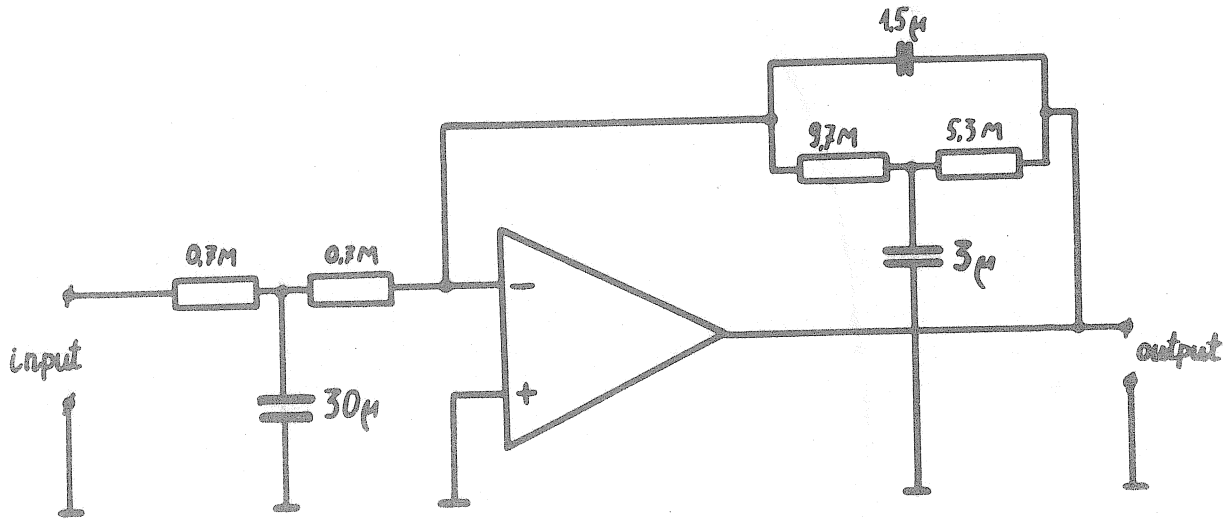

Fig. 5

The circuit diagram of the output L.F. filter.

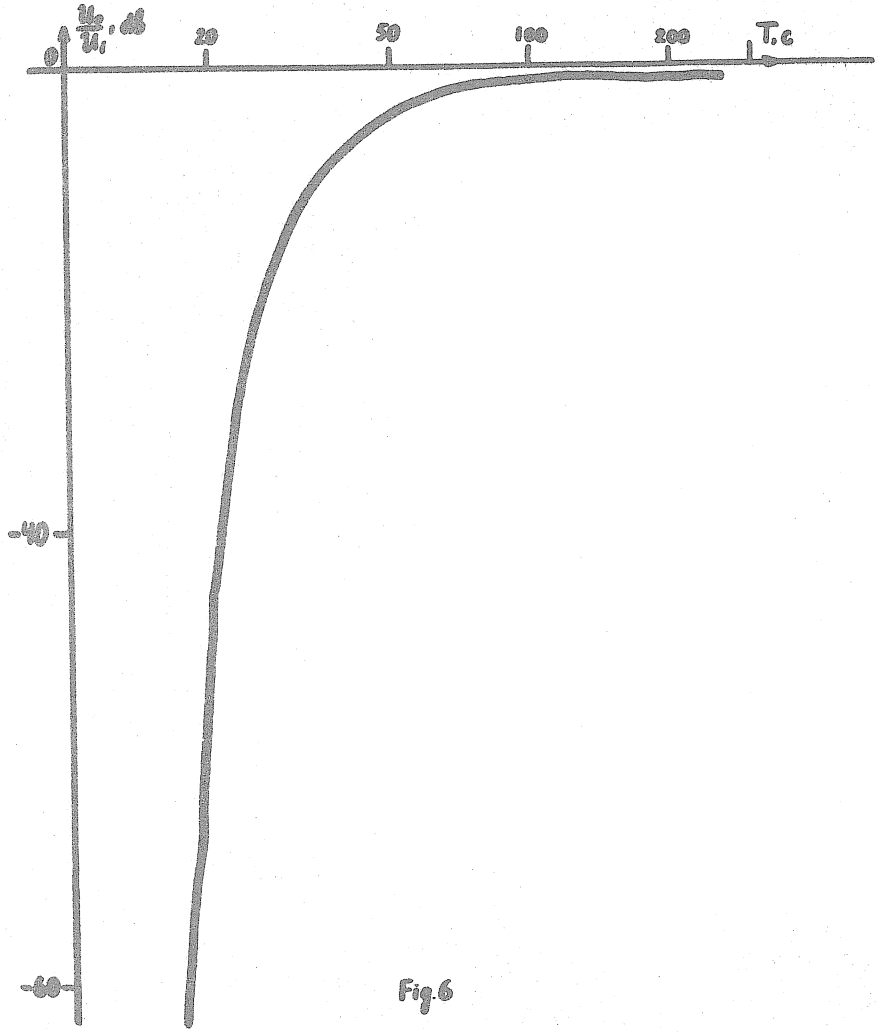

Fig.6

The amplitudinal frequency characteristics of the L.F. filter.

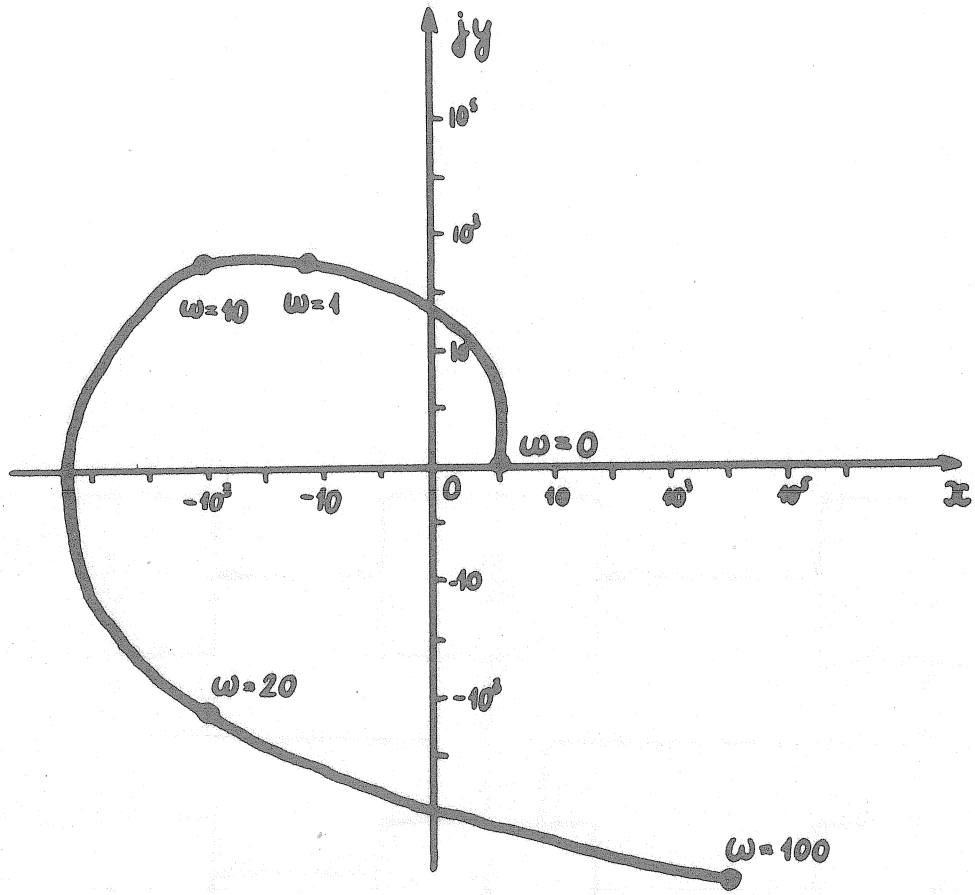

Fig.7

The Mikhailov's curve for the tiltmeter with automatical control.

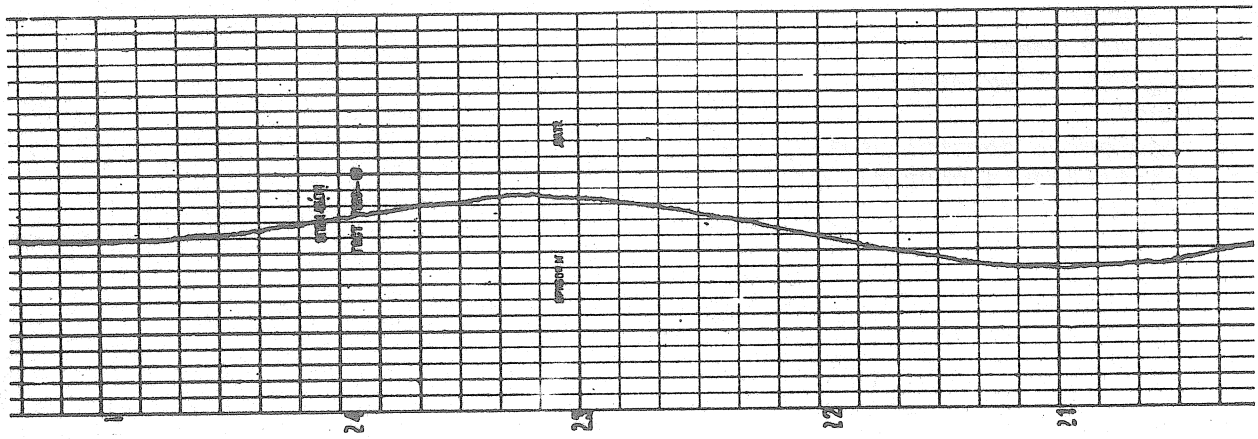

Fig.8

The fragment of a recording chart with a recording of a tidal tilt by the tiltmeter with automatic control. The tilt's amplitude conforms to the output voltage of 10 V. The Obninsk station.

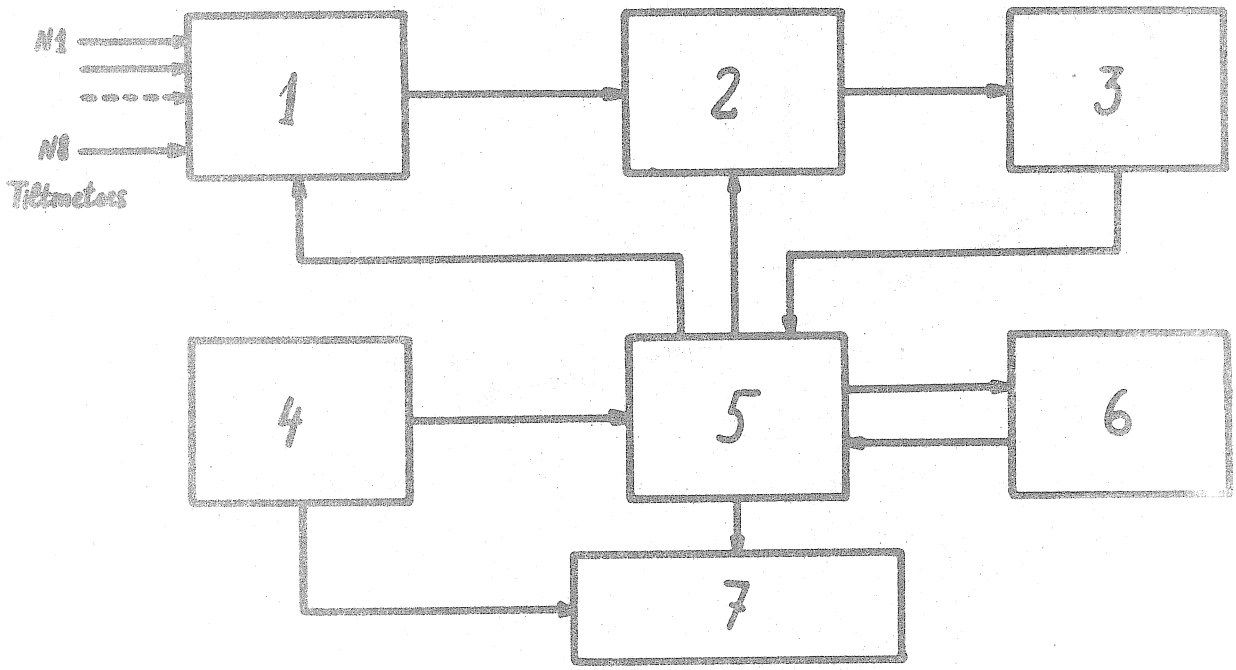

Fig. 9

The block diagram of the digital recorder of tilts.

1- the exchange;
2- the voltage coder;
3- the digital integrator;
4- the timer;
5- the recorder's control unit;
6- the calibration's control unit;
7- the punch.

INVESTIGATION OF TILTS AND DEFORMATIONS OF THE EARTH'S CRUST IN THE ZONE OF A TECTONIC FAULT

B.K. Balavadze and V.G. Abashidze

The area of construction of the Inguri power station (Western Georgia) is located in the zone of high tectonic activity. One of the faults, besides, lies in the base of the arch dam. That is why the detection of the intensity and behaviour of tectonic movements of some structural blocks separated by faults is of primary importance both before the construction of the dam and in the process of laying of the dam's body and filling of the reservoir by water.

To solve these problems the Institute of Geophysics of the Academy of Sciences of the Georgian SSR has since 1967 been carrying out tiltmeter and extensometer investigations on the site of the high-altitude arch dam of the power station under construction on the Inguri River.

It is known that photoelectric tiltmeters of A.E. Ostrovsky's system possess high sensitivity and equally with tidal tilts permit to obtain necessary information on the nature of deformations taking place in the Earth's crust in time. However, the base of these instruments is small, so a question arises as to the representativeness of the results of observations. Taking into account this fact as well as the complexity of the region under investigation in seismoactive aspect, hydrostatic levelling-boxes and quartz extensometers were used.

The paper gives the basic results of tiltmeter and extensometer observations.

Since 1970, in the immediate proximity to the dam, comparative tiltmeter and other observations have been carried out in three tunnels, two of them - N° 183 and N° 3413 being on the right bank of the Inguri while the third one - N° 160 - on the left bank of the river. The left bank tunnels intersect the fault lying in the base of the arch dam (Fig. 1) at different levels.

Chambers for tiltmeters are separated from the recording sections by several thermoinsulating screens. The tiltmeters are mounted on teschenite slabs firmly secured to the bed-rock with a cement solution. The slabs in the right bank tunnels are arrauged on the main walls (edges) of the fault. In the left bank tunnel N° 160 the slabs are 40 metres away from each other.

The tilts of the Earth's crust were recorded by tiltmeters of A.E. Ostrovsky's system in E-W and N-S directions. To control the readings of the instruments in the process of observation, they were set parallel to each other, mutually replaced and turned 180°. The sensitivity of tiltmeters was adjusted according to the background interferences and varied in the range of 800-400 arc mm/sec.

Observations of the temperature regime in the tunnels were carried out with the aid of resistance thermographs inserted in the set of tiltmeter apparatus of A.E. Ostrovsky's system. The temperature in the chambers was kept constant to the precision of a few units of millidegrees.

For visual demonstration of tilt variations in the building ground of the dam Fig. 2 presents vector diagrams for each point of observation.

Figure 2 shows quite definite tendency of tilt variations in time on the area under investigation.

Thus, for example, on the right bank of the Inguri the outer block of the right bank fault (the front one from the gorge side) tilts towards the fault - to SW-SE (azimuth 145°-165°). The inner block earlier had been tilting towards the fault, that is, to NW, but in 1975-1976 changed its direction and began to tilt to SW.

The Inguri's left bank according to observation data 1972-1974 was oriented to NE and since 1975 tilts to SE.

To make clear possible causes of the earth surface tilt variations observed at dam's building ground since 1975, Fig. 2 gives comparisons of curves of tilt variations with ground water variations and concrete pouring in the body of the dam. Here we see a good agreement of tilt variations recorded by one and the same components of the instruments placed in different tunnels at the outer (a) and inner (b) blocks of the fault.

There is no evident correlation between earth surface tilts and the change of water level in piezometer placed in the entrance of the tunnel N°3413. The same can be said about earth surface tilts and air temperature and baric field variations. As for precipitations, in case of heavy showers, though they cause fluctuation in tilts these changes are of instant origin and can be easily eliminated during data processing.

Then, consequently, remains the problem of technogenic process connected with the sinking of the basin and concrete pouring into the body of the dam.

We have no data on the basin's working. It is only known that from the dam's base about $2,5 \times 10^6$ m^3 ground was excavated. It must be taken into account that tiltmeter observations at the dam's building ground were commenced when the main excavation works had already been finished. Hence it is difficult to determine their influence upon the tilt variations. As for concrete pouring it was started in 1972 and proceeded in time in the way as shown on Fig. 2 (the lower curve). It appears from the graph that by end of 1976 $1,2 \times 10^6$ m^3 concrete had been poured into the body of the dam this making up nearly 3×10^6 tons. It is not unlikely that the change of tilts direction is connected with the effect of concrete pouring. Definitive answer to this question may be given by posterior observations.

At the beginning of 1974 in the tunnel N° 3413 two parallel extensometers were installed. They were arranged in a cross-strike direction to the fault, N 8° W. Recordings were carried out by an photooptic method. The base of the instruments was 22,5 m., sensitivity to displacement -6,7 μ/mm, sensitivity to deformation $(0,7 - 0,8) \times 10^{-8}$ 1/mm.

Fig. 3 shows the trend of displacements and linear deformations from 1974 up to 1976. Here also are plotted the curve of air temperature variations and data on precipitation.

Judging from the nature of deformations, there occurs the interchange of extension and compression of the fault's walls, or edges. Against a general background of deformations the process of extension is prevailing, though from time to time the calm ensues and the grouth of displacements and deformations is almost not observed (IX-XI, 1974; XI-XII, 1975 and VIII-XII, 1976).

A general trend of displacements and deformations becomes complicated by seasonal phenomena: precipitations and air temperature change. Rainfalls stir up rock deformation and cause a short-term compression.

It is with this fact, that toothed character of the curve is connected, reflecting displacement and deformation variations.

Readings of the both extensometers served as the basis for calculation of the intensity of rock displacement for each month, and for years. During the last 2,5 years a general displacement according to the first extensometer D_I is 160 μ, according to the second one D_{II} - 140μ. The difference between them do not exceed 10-15% which points to the reliability of these data.

Mean value of displacements for 2,5 years is equal to 150μ or 60μ per year. Linear rock deformation is equal to $27,10^{-7}$ a year.

The study of recent tectonic movements in the vicinity of the arch dam of the Inguri pover station has led us to the conclusion as follows:

The rock massif on the territory under study undergoes constant movements and deformations this being the cause of rock tension variations. These changes are engendered both by natural causes of tectonic character and by technogenic processes connected with the construction of the dam.

The values of tilt vectors throughout the construction site are small, exibit a tendency towards decrease and according to 1976 data do not exceed 3-4 angle sec/year.

The outer block of rightbank fault tilts to SW-SE, that is, towards the fault.

The inner block has changed tilt direction from NW to SW as well as the left bank changed its direction from NE to SE. Observations with the aid of quartz extensometers have revealed the domination of an extension process of rock which make up the fault adges or walls. The value of displacement is equal to 60μ, while the linear deformation -27×10^{-7} per year.

Rain falls are accompanied by the actuation of deformation rocks surrounding the body of the future dam.

REFERENCES

1. (Balavadze B., Abashidze V.) Балавадзе Б.К., Абашидзе В.Г., Наклономерные исследования современных тектонических движений земной коры в районе строительства плотины Ингури ГЭС. Сообщ. АН ГССР, т.71, № 3, Тбилиси, изд."Мецниереба", 1973.

2. Balavadze B.K., Abashidze V.G., Investigation of Recent Tectonic Movenemts of the Earth Crust by means of Tiltmeters Изд. АН Венгрии, Будапешт, 1974.

3. (Balavadze B.K., Ostrovsky A.E., Abashidze V.G., Latynina L.A. et al.) Балавадзе Б.К., Островский А.Е., Абашидзе В.Г.,

Латынина Л.А. и др. Исследование современных дифференцированных тектонических движений земной коры в районе строительства плотины Ингури ГЭС сб. Современные движения земной коры, Новосибирск, Институт геологии и геофизики СО АН СССР, I976.

4. (Latynina L.A., Karmaleeva R.M.) Латынина Л.А., Кармалеева Р.М., Измерения горизонтальных смещений на земной поверхности экстензометром. Сб. Современные движения земной коры. Изд. АН ЭССР № 2, Тарту, I965.

5. (Ostrovsky A.E.) Островский А.Е., Наклономер с фотоэлектрической регистрацией, Сб. Изучение земных приливов УШ разд. № 2, изд. АН СССР, Москва, I96I.

6. (Shirokov I.A., Abashidze V.G., Bagmet A.E., Yakovlev V.N.) Широков И.А., Абашидзе В.Г., Багмет А.Л., Яковлев В.Н., Изменения наклонов в районах строительства плотин. Симп. по обмену опытом наклон. наблюдений и крит. рассмотрению их физ. смысла, М., I969.

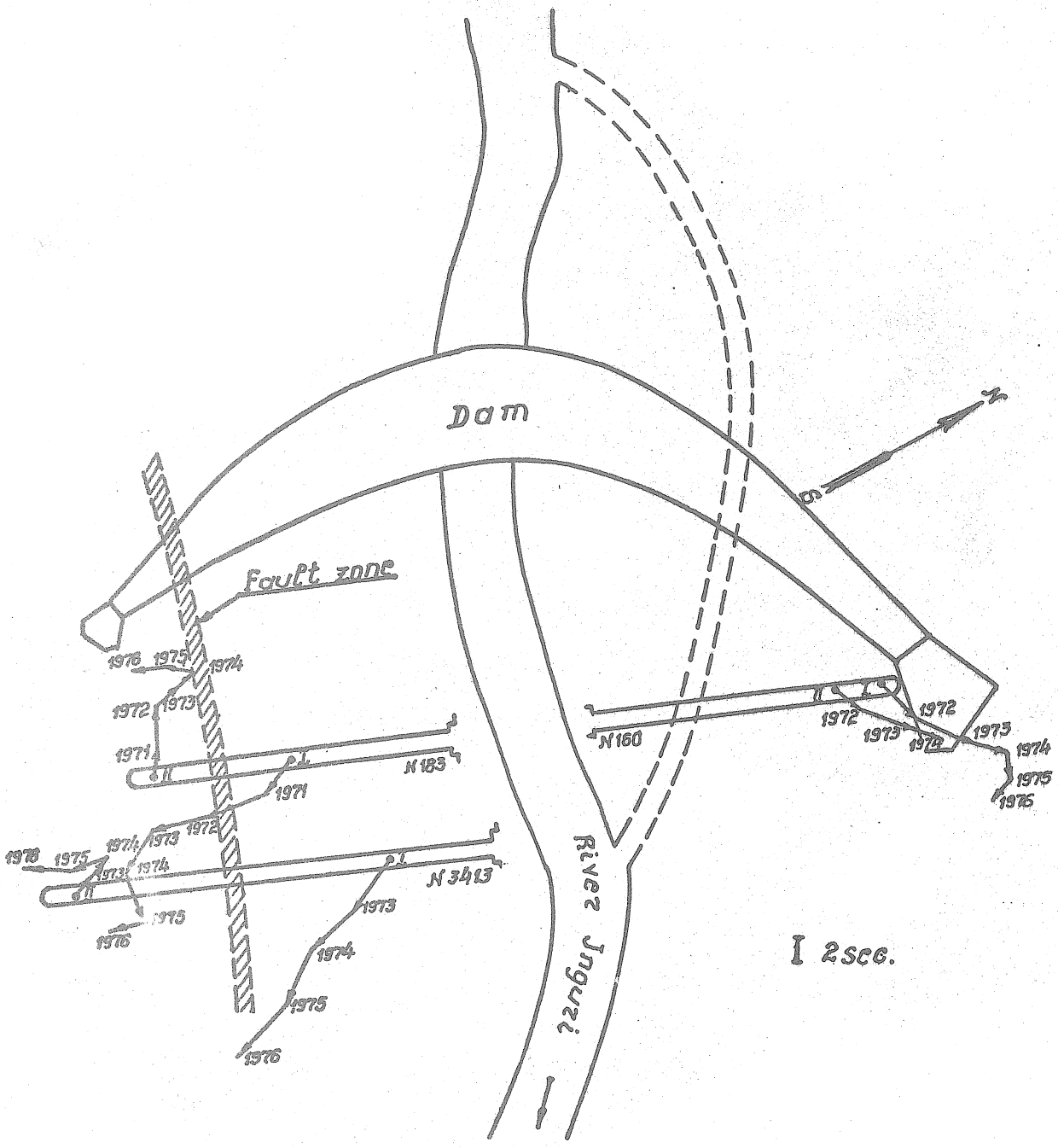
Dam
Fault zone
N
S
N 160
N 183
N 3413
1971
1972
1973
1974
1975
1976
River Inguri
I 2 sec.

Fig. 1

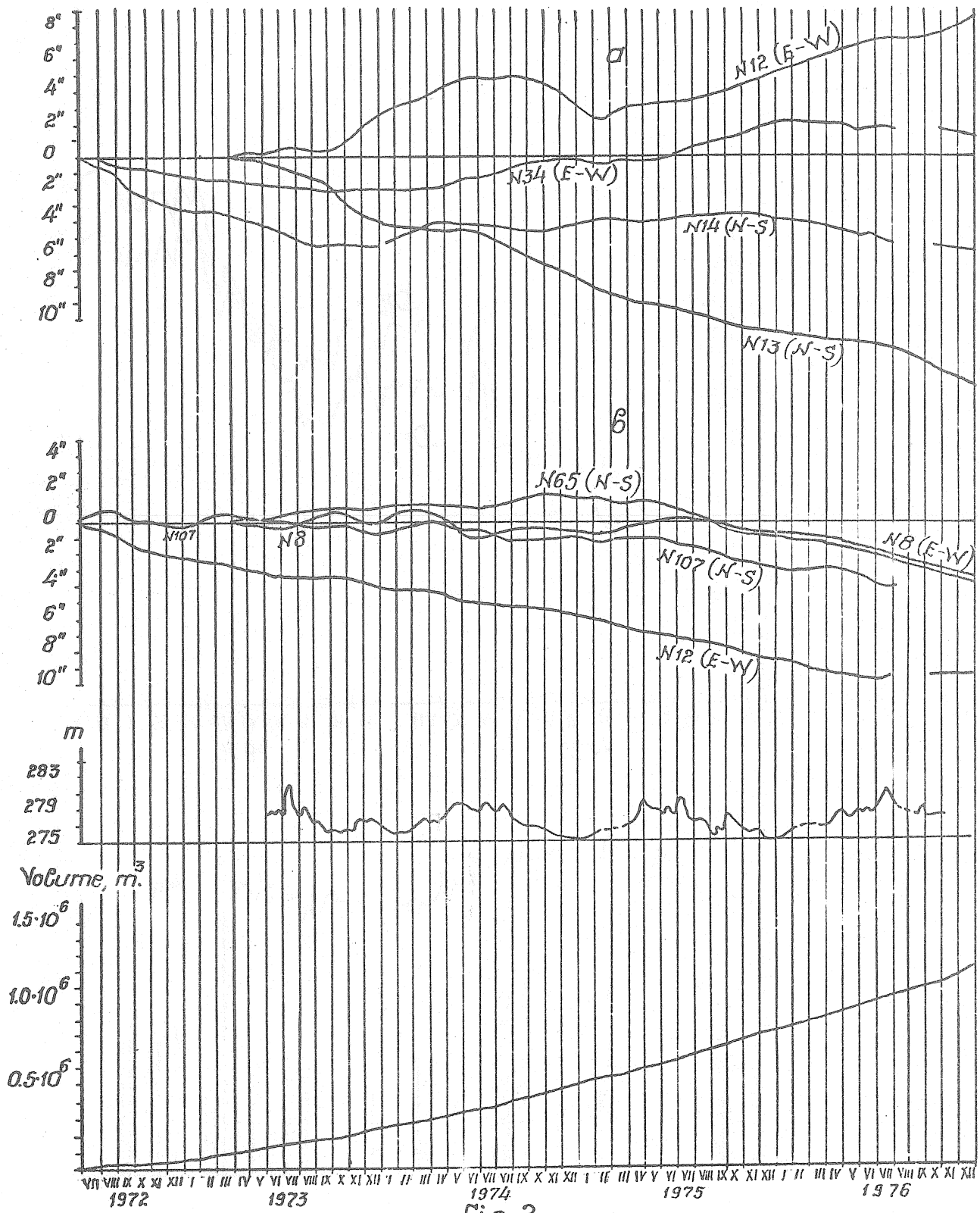
a
N12 (E-W)
N34 (E-W)
N14 (N-S)
N13 (N-S)
8"
6"
4"
2"
0
2"
4"
6"
8"
10"
б
N65 (N-S)
N107
N8
N8 (E-W)
N107 (N-S)
N12 (E-W)
4"
2"
0
2"
4"
6"
8"
10"
m
283
279
275
Volume, m³
1.5·10⁶
1.0·10⁶
0.5·10⁶
1972
1973
1974
1975
1976

Fig. 2

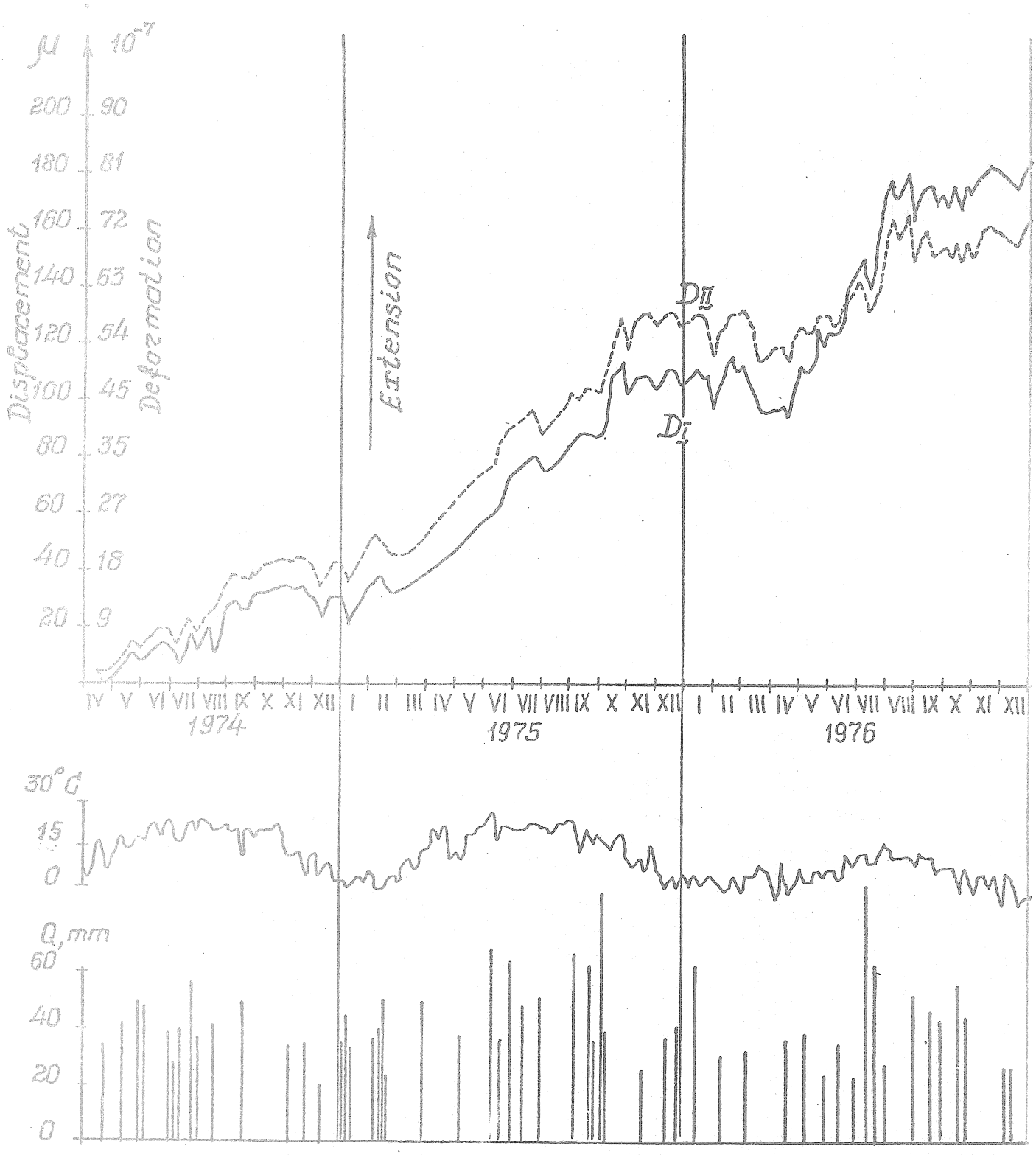
Displacement
μ
200
180
160
140
120
100
80
60
40
20
Deformation
10⁻⁷
90
81
72
63
54
45
35
27
18
9
Extension
DII
DI
IV V VI VII VIII IX X XI XII I II III IV V VI VII VIII IX X XI XII I II III IV V VI VII VIII IX X XI XII
1974
1975
1976
30°C
15
0
Q, mm
60
40
20
0

Fig.3

TIDAL INFORMATIONS ON AN ACTIVE FAULT

L.A. LATYNINA

During the last decade indirect effects of the Earth's tides as a source of information on horizontal inhomogeneities of the Earth upper layers draw the attention of researchers. (Kuo J.T. et al., 1970; Melchior, 1976; Matveyev et al., 1976). the use of tidal linear deformations of the Earth's surface is promising for the study of the block structure of the Earth's crust and tectonic faults (Latynina et al., 1976).

The mechanism of faults affecting linear deformations can be easily understood by the following schemes. Let two relatively rigid blocks A and A divided by the zone B of low elasticity modelling the fault zone be affected by extending or compressing forces P (Fig. 1). Deformation within the limits of A and B volumes far from their boundaries has the nature of monoaxial extension or compression and is equal to P/E_1 and P/E_2 where E_1 and E_2 are Young modul of elasticity of A and B volumes respectively. Thus, deformation in the "fault" zone is E_1/E_2 times as much as within the "block".

Let the abc band, consisting of parts considered above, be subjected to elongation by the $2\,\Delta\ell$ value. This elongation is accomplished mainly by means of deformation of B zone and the more so the greater is the E_1/E_2 ratio. Deformation in the A area is less in this case than in that of a homogeneous band with the same value of elongation.

We have estimated the values of the fault effect showing that if its depth equals the block length deformation in the middle part of the block equals approximately half the elongation which would exist under the same conditions in an undisturbed medium (Latynina, 1976) D. Harrison computed distribution of deformations and the Earth's surface inclination angles within the contact area between the rigid structure and an extended depression filled in with soft sediments (Harrison, 1976) (Fig. 2). The Young modulus decreases four times with the transition from rigid to soft structure.

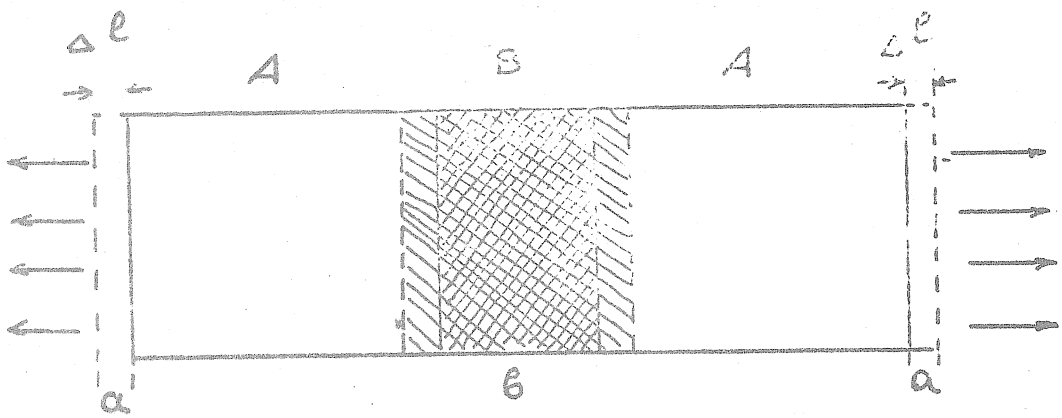

Fig. 1. A scheme illustrating an increase of linear deformations in the zones of minor elasticity.

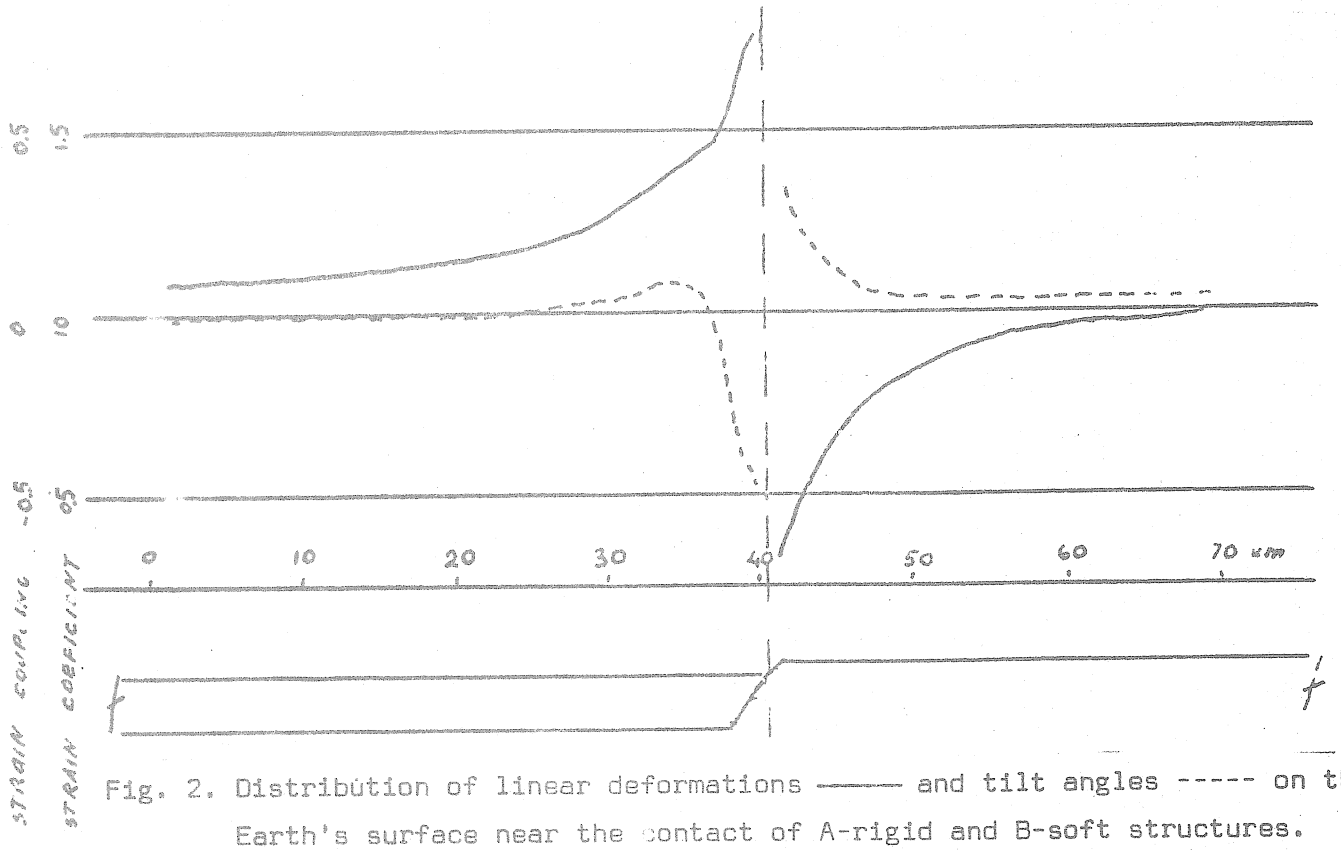

Fig. 2. Distribution of linear deformations ——— and tilt angles ----- on the Earth's surface near the contact of A-rigid and B-soft structures. Data by Harrison.

The computation was made under the assumption that the medium deformation at large distances from the discontinuity boundary is homogeneous. Close to the boundary linear deformations are obtained to be equal: in the area of minor rigidity 170% of their normal value and in the area of great rigidity -37% (Fig.2) Variations of the Earth's surface inclination angles are somewhat less in value and are concentrated in a zone move narrow if compared with linear deformations. The considered geological structure may be a model of the extended fault zone.

The nature of the fault effect on deformation linear component normal to the fault striking is generally clearly seen from the schemes. This deformation is great in the fault zone and small in the adjacent relatively rigid areas if compared with its value in an undisturbed medium. All the above said refers to deformations of any origin. The use of tidal deformations when studying the Earth's crust structure is advantageous in comparison with deformation of another origin because in a homogeneous undisturbed medium distribution of tidal deformations is known. The periodic character of tidal phenomena allows to define tidal harmonics by the data obtained experimentally with sufficient reliability.

Study of distribution of tidal deformations on the Earth's surface and their anomalies opens possibilities for the solution of a number of geological -tectonic tasks: 1) to discover active faults, 2) to define the fault zone boundaries, 3) to define fault characteristics: its depth, effective elasticity, 4) to distinguish between active and healed non-active faults.

By the example of the Garm region, Tadjik SSR we illustrate the character of distribution of tidal deformations in the region crossed by a large tectonic fault. This region is at the juncture of two global tectonic structures: the Pamirs and Tien Shan mountain systems. These structures are divided by the system of deep Guissar-Kokshaal faults a segment of which within the limits of the studied region - the Surkhob fault - is shown on the tectonic scheme of the Garm region (Fig. 3).

Tidal deformations are registered in four points: at the observatories of Garm, Sari-Pul, Tchusal and Tchil-Dora.

Registration of tidal deformations is carried out by quartz extensometers with bases from 9 to 27 metres equipped with optical and photoelectric recording devices. Fig. 3 shows orientation of extensometers at each of the enumerated stations. All the stations but that of Sari-Pul have extensometers installed in horizontal underground galleries made in the slopes of mountain ranges at the distance from the day surface on the order of 30-50 metres. The Sari-Pul station is in a trench at the depth of about 10 metres.

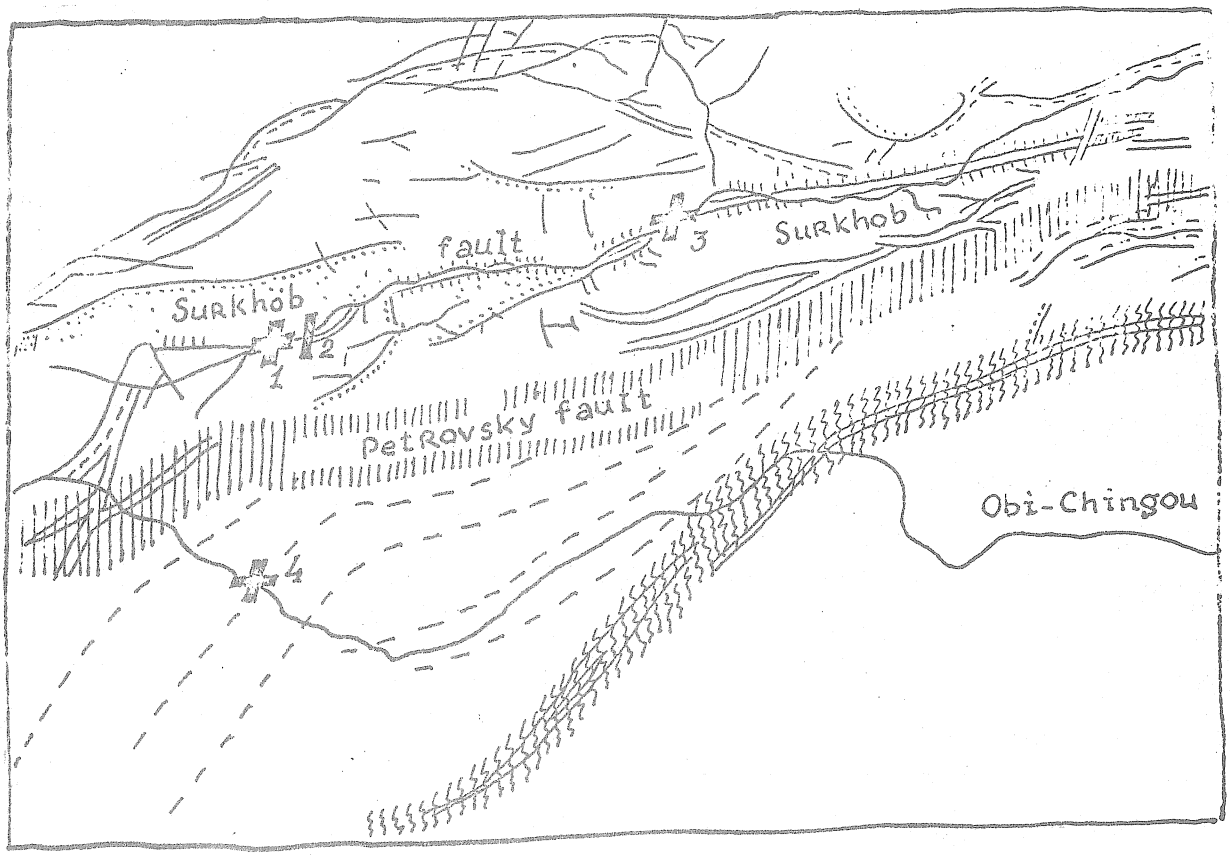

Fig.3. A tectonic scheme of the Garm region. Straight lines show extensometer orientation at the stations.
The observatories: Garm - 1, Sari-Pul-2
Tchusal-3, Tchil-Dora-4.

The Sari-Pul station is directly in the zone of the Surkhob fault in the valley of the Surkhob river where steeply-falling faults are traced separating the Guissar range of Tien-Shan from the pre-mountain foredeep and a system of gentle thrusts along which the Pamirs rocks were displaced northwards having overlapped the frontal zone of the Guissar range. The Garm station is at the distance of 2 km westwards of the Sari-Pul station (and along the direction normal to the fault striking at the distance on the order of 500 metres) at the slopes of the Guissar range. The station underground galleries are located in a granite horst upwards along the Surkhob fault. The horst slopes are strongly destroyed. The fault zone boundary passes along the horst surface. The third station of the testfield-Tchusal- is on the slopes of the Guissar range at the distance of 30 km eastwards of Garm. Station underground galleries are at the distance of 1 km from the Surkhob river valley. The main Surkhob fault passes along the river valley and its branches cross the northern slopes of the Guissar range so that the station is located somewhere within the region of fault flattening. The fourth station of the test-field-Tchil-Dora- is situated within the Pamirs, 20 km southwards of Garm. The system of Guissar-Kokshaal faults is northwards of the station.

In the station area crustal invisible faults of the North-eastern striking are assumed to be located (Gubin, 1960).

We shall dwell upon the peculiarities of distribution of tidal deformations in the zone of an active tectonic fault and its surroundings. From tidal deformations defined experimentally one should eliminate the values caused by indirect effects of the ocean, relief and underground gallery to establish the connections of the observed anomalous tide with faults. The effect of the oceanic tide in the region of Central Asia is negligible and it can be ignored. The underground gallery effect can lead to an increase of deformation by 1-2% (Harrison, 1976). Extensometers are mounted in tunnels at some distance from heading sides of the gallery. Therefore the cavity effect can be ignored as well. The Earth's surface relief effect can appear to be essential. Observations are carried out in the conditions of a mountain area with great falls of heights. The station galleries are on the slopes of mountain ranges at the height of 20-30m from the valley level. We have not computed topographic effects of the tide for the concrete conditions of the station. According to the results of computation of deformation distribution on the range slopes (Harrison, 1976; Levina et al., 1976) under the conditions of Garm stations one must expect the linear deformation component to be decreased in the direction normal to the range slope if compared with its value on the flat Earth's surface. The second deformation component registered along the range is not subjected to any noticeable effect of its slopes. It is more representative when we analyse the connections of tide anomalies with tectonics.

Let us give the data on amplitudes of main lunar waves M_2 and O_1 at all the enumerated stations (Tables I-IV). Processing of extensometer data was carried out by the 29-day Pertsev method with series shift by 24 hours (Pertsev, 1958). Instrument bases and their orientation are shown in the tables while a * sign indicates those instruments which are oriented along the range and for which the topographic effect is insignificant.

Sari-Pul (Latynina et al., 1977). At this station registration was made by two parallel devices with bases of about 27 metres. At one of the extensometers four recording devices were installed which allowed to register relative displacements at several bases. According to the Table 1 data the M_2 wave amplitude taken as the mean one out of 17 poorly dependent series is equal to $3.67.10^{-8}$ and is almost three times more than the "normal" value theoretically computed for the observational point. The O_1 wave amplitude equals $1.82.10^{-8}$ and exceeds the normal value 36 times. Determination errors of mean amplitudes as seen from Table I comprise 2-3%.

The Sari-Pul station is installed in a trench not deep and with rather considerable temperature variations. Therefore a question arises whether the obtained tidal anomalies are the result of big temperature errors. By other tidal wave amplitudes we can judge on the effect of temperature disturbances. For M_2, O_1, S_2, N_2, K, waves the ratio of experimental amplitudes of tidal waves to their theoretical values is equal to 2.87, 3.64, 2.76, 3.75 and 3.27 respectively. For S_2 and K_1 waves most of all subjected to the effect of diurnal processes this ratio is of the same order of value as for the M_2 wave. Hence the conclusion is drawn on a minor effect of temperature variations.

The relief effect can not either explain the anomalies so great as the observed ones. The station is situated within the limits of rather a wide river valley. The nearest range slope is a gentle one. According to computational data (Harrison) deformation increase by tens per cent can be anticipated here.

Thus at the Sari-Pul station in the zone of the deep tectonic fault the amplitude of tidal deformations if three times higher than their "normal" values.

Garm. M_2 and O_1 wave amplitudes in the direction crossing the fault are equal to $0.9 \cdot 10^{-8}$ and $0.4 \cdot 10^{-8}$ respectively and are by 20 and 40% below the norm (Table II). One must take into account that this direction is perpendicular to the range slope so that the obtained decrease of tidal wave intensity can be caused by the effect of the range free surface. In EW direction parallel to the fault striking the M_2 and O_1 wave amplitudes equal to $0.1 \cdot 10^{-8}$ and $0.2 \cdot 10^{-8}$ are also below the norm. The Garm station is at the boundary of the fault zone at the range slopes subjected to elevation along the fault plane. Here tidal wave amplitudes are somewhat lower in comparison with "normal" values.

Tchusal. The M_2 wave amplitude in the direction close to North-South, perpendicular to the Surkhob fault equals $1.0 \cdot 10^{-8}$, its theoretical value being $1.25 \cdot 10^{-8}$. These values can be considered sufficiently close. The O_1 amplitude in the same direction is by 35% below the norm. This direction is parallel to the range slope. In the direction crossing the range slope M_2 and O_1 amplitudes are much lower. Thus at the Tchusal station which is in the zone of the tectonic fault flattening the tidal wave amplitude is somewhat below the norm.

Tchil-Dora. (Zharinov, 1976). M_2 and O_1 amplitudes in two mutually perpendicular directions are considerably, 2.5 times, below the norm. The direction close to N-S is normal to the range slopes. In this direction tidal waves can be considered relatively more intensive since the introduction of the correction due to the range free surface effect will somewhat increase the obtained values of amplitudes. The main peculiarity of tidal waves at this station which is

beyond the zone of the deep fault is their essentially decreased if compared with "normal" amplitude values.

Conclusions

Active tectonic faults in the Earth's crust ssem to be the zones of low effective elasticity separating rigid blocks. Under the effect of tearing or compressing efforts linear deformations in fault zones should be larger - and within the undisturbed block less - than those under the same loads in the conditions of an undisturbed medium. One can expect the tectonic faults to affect linear deformations of tidal origin in the same way also. Tidal deformations can be computed for the set model of the Earth's crust and can be defined with high accuracy by the observational data. Therefore the use of tidal deformations seems to be promising to study the structure of the Earth's crust and that of large faults, in particular.

How the intensity of tidal deformation varies in the region crossed by a deep tectonic fault is shown by the example of data obtained at the stations of the Garm testfield, Tadjik SSR. This fault separates mountain areas of Pamirs and Tien-Shan.

In the fault zone proper the tidal wave amplitude according to the Sari-Pul data is three times higher than its "normal" value. At the Garm station at the distance of 2 km from Sari-Pul at the boundary of the fault zone and the block, tidal wave amplitudes are 4 times less than those at the Sari-Pul station and somewhat below the norm. At the Tchusal station which similar to Garm is situated on the Tien-Shan side of the fault the area of ruptures feathering the Surkhob fault, wave amplitudes are lower. The M_2 wave amplitude in the direction crossing the fault most reliably defined is by 25% below the normal value. Tidal wave intensity beyond the zone of deep fault can be derived from the data of Tchil-Dora station which is within the Pamirs block. Tidal wave amplitudes here are essentially, 2.5 times, less than the normal ones.

Thus, tidal wave amplitudes recorded in four points of the Garm region vary regularly with variation of the distance from the deep fault. This indicates that there is a certain connection between the observed tidal anomalies and the fault zone.

REFERENCES

1. KUO J.T., JACHENS R.G., WHITE C., EWING M. Tidal gravity measurements along a trans-continental profile across the United States
6th Int. Symp. on Earth Tides. Royal Observatory of Belgium, Brussels, 1970.

2. MELCHIOR P. Trans-European tidal gravity profiles. Preliminary experimental results. Proceedings of the seventh Int. Symp. on Earth Tides, Budapest, 1976.

3. MATVEYEV P.S., BOGDAN I. Ju, GOLUBITSKY V.G. Determination of the M_2 constituent from the tilt observations along the profile Sumy-Kherson.
Proceedings of the seventh Int. Symp. on Earth Tides, Budapest, 1976.

4. LATYNINA L.A., KARMALEEVA R.M. On the intensity of lunar-solar tidal deformations under different tectonic conditions.
Sb. "Sovremennye dvizheniye zemnoi kory", Novosibirsk, 1976.

5. HARRISON J.C. Cavity and topographic effects in the Earth's crust and strain measurements. J. Geoph. Res. v. 81, n°2, 1976.

6. LEVINE J., HARRISON J.C. Earth tide strain measurements in the Poorman mine near Boulder, Colorado.
J. Geoph. Res. v. 81, n°13, 1976.

7. LATYNINA L.A. Investigation of faults in the Earth's crust by linear tide strains. Proceedings of the seventh Int. Symp. on Earth Tides, Budapest, 1976.

8. GUBIN I. Ye. Regularities of seismic displays on the territory of Tadjikistan.
Izd-vo AN SSSR, M., 1960, ch.I, gl.7.

9. PERTSEV B.P. Harmonic analysis of elastic tides.
Izv. AN SSSR, Sér. Geoph. n 8, 1958.

10. LATYNINA L.A., SHISHKINA T.P. On the connection of tectonic and tidal Earth's surface movements in the zone of the Surkhob fault. Izv. SSSR, Physika Zemli, 1977.

11. ZHARINOV N.A. On the Earth's surface deformations at the Tchildora station.
sb. "Sovremennye dvizheniya zemnoi kory", Novosibirsk, 1976.

TABLE I Amplitudes of M_2 and O_1 tidal waves at the Sari Pul Station

orientation: North-South

Base in metres	An average day of the series	Amplitudes in 10^{-8} M_2	O_1
	1974		
9.0	10.1	3.18	1.55
	3.II	3.61	1.45
	24.II	3.13	1.82
	8.I	3.31	1.52
17.8	4.II	4.44	1.49
	26.II	3.78	1.63
	4.I	3.24	2.23
22.4	3I.I	3.65	I.98
	25.II	3.09	I.46
M_2	Mean	3.67 ± 0.I0	
	Theoretical	I.28	

Base in metres	An average day of the series	Amplitudes in 10^{-8} M_2	O_1
26.6	1974		
(Instrument I)	23.1	4.49	2.14
	24.II	4.16	1.65
2.6.6	7.1	3.63	2.42
(Instrument II)	3.II	4.24	2.17
	28.II	3.53	2.74
	II.V	3.83	I.58
	I9.VI	3.80	I.77
	II.VII	3.23	I.39
O_1	mean	I.82 ± 0.I0	
	theoretical	0.50	

TABLE II. Amplitudes of M_2 and O_1 tidal waves at the Garm station

orientation base	North-South 27 metres		orientation base	East-West 18 metres	
an average day of the series	amplitude in 10^{-8} M_2	O_1	an average day of the series	amplitude in 10^{-8} M_2	O_1
1972.24.XII	0.78	0.37	1972.4.XII	0.07	0.I7
1973 27.II	0.74	0.22	1972.3I.XII	0.II	0.20
IO.III	0.74	0.I9	1973.8.I	0.IO	0.I6
IO.VI	0.8I	0.30	22.II	0.09	0.20
			22.III	0.IO	0.I7
Mean	$0.77^{\pm}$	$0.27^{\pm}$		$0.09^{\pm}$	$0.I8^{\pm}$
	0.02	0.04		0.01	0.03
Theoret.	I.28	0.50		0.52	0.70

Table III. Amplitudes of M_2 and O_1, tidal waves at the Tchusal station

orientation N 12°E		base in metres 24,6			orientation E 20°S		base in metres 23.8	
	NN of the instrument	an average day of the series	amplitude in 10^{-8} M_2	O_1	NN of the instrument	an average day of the series	amplitude in 10^{-8} M_2	O_1
I.	1972	2I.XII	0.87	0.29	3. 1972.	2I.XII	0.II	0.I6
	1973	I9.I	0.84	0.25	1973	2I.I	0.II	0.I4
		I9.II	0.82	0.29		IO.III	0.I2	0.I4
		I6.III	0.90	0.29				
2.	1972	2I.XII	I.I2	0.39	4. 1972	2I.XII	0.I2	0.I8
	1973	I9.I	I.I4	0.37	1973	2I.I	0.I4	0.I8
		I9.II	I.I3	0.38		2I.II	0.I3	0.20
		I6.III	I.26	0.4I		IO.III	0.I3	0.22
	Mean		I.0I ± 0.06	0.33 ± 0.02	mean		0.I2 ± 0.0I	0.I7 ± 0.0I
	theoret.		I.25	0.5I	theoret.		0.65	0.70

Table IV. Amplitudes of M_2 and O_1 tidal waves at the Tchil-Dora station

Orientation W 15°S base in metres 23.9				Orientation S 15°E base in metres: N°3 - 25.7 N°4 - 24.0			
NN of instruments	an average day of the series	amplitudes in 10^{-8} M_2	O_1	NN of instruments	an average day of the series	amplitudes in 10^{-8} M_2	O_1
I. 19/1	9.II	0.30	0.49	3. 1971	II.III	0.49	0.2I
	I9.IV	0.25	0.47		IO.IV	0.67	0.27
	29.VII	0.25	0.4I		6.VI	0.54	0.I9
	28.VIII	0.27	0.47		2.VII	0.55	0.I8
2. 1971	9.II	0.24	0.48	4. 1971	II.III	0.60	0.I7
	II.III	0.22	0.39		IO.IV	0.56	0.22
	IO.IV	0.I6	0.64		6.VI	0.50	0.20
	29.VII	0.26	0.43		6.VII	0.53	0.I9
	28.VIII	0.25	0.46		5.VIII	0.43	0.I9
Mean		0.24 ± 0.02	0.47 ± 0.03			0.54 ± 0.03	0.20 ± 0.0I
Theoretical		0.6I	0.70			I.33	0.52

OBSERVATIONS OF TIDAL AND SECULAR DEFORMATIONS OF THE EARTH'S SURFACE IN TBILISI

B.K. BALAVADZE, K.Z. KARTVELISHVILI

Observations of the Earth's tides with the aid of extensometers, tiltmeters and gravimeters have been going many years at the Tbilisi Laboratory of the Earth's Tidal Deformations of the Institute of Geophysics of the Academy of Sciences of the Georgian SSR.

The results of the processing of these observations are discussed below.

a) Tiltmeter observations.

Observations by means of four photoelectric tiltmeters were begun in March 1967. The tiltmeter chamber is placed at 100m from the tunnel entrance and at a depth of 60m from the surface. The tiltmeters are placed on a massive basalt basement ($1.5 \times 10 \times 0.8$ m^3). Favourable conditions of observation and considerable duration ensures the required accuracy of determination of γ and χ. The materials of instrument-observations of 5827 days were chosen for processing by the method of harmonic analysis. If during the observation the length of a blank exceeded a day, such material was not considered fit for processing. The rare blanks were restored with the aid of well-known formulae and parallel instrument recordings. The scheme of harmonic analysis developed by P.S. Matveev was used. 228 monthly analyses were made in all, among which 194 series were independent and 34 were processed by the method of partial overlapping.

Though the scheme of harmonic analysis used by us enables to single out eight tidal waves, only waves with maximum theoretical amplitudes were considered in order to obtain the most reliable values of the parameters γ and χ.

Table 1 gives the values of the γ-factor for five main tidal waves M_2, S_2, N_2, O_1 and K_1 in the azimuth E-W and for M_2, S_2, N_2 in the azimuth N-S in as much as diurnal waves in this direction have fairly small amplitudes and are not isolable with required accuracy.

TABLE 1

γ - Values for different waves

Period (Epoch) of observations, n, monthly series	Azimuth	M_2	S_2	N_2	O_1	K_1
31.3.1967 - 19.10.1973	E-W	0.712	0.747	0.766	0.648	0.680
n = 1657 days, 66 series	N 33	± 0.009	0.020	0.044	0.039	0.018
31.3.1967 - 12. 8.1973	E-W	0.706	0.713	0.705	0.684	0.726
n = 1068 days, 46 series	N 85	± 0.014	0.017	0.052	0.014	0.020
A theoret. (m. sec.)		11.794	5.487	2.258	4.336	6.099
$\gamma_{E-W} = \frac{\frac{\gamma_i \cdot l_i}{\varepsilon_i^2}}{\frac{l_i}{\varepsilon_i^2}}$		0.711 ± 0.011	0.731 0.019	0.747 0.047	0.677 0.019	0.696 0.019
31.3.1967 - 8.12.1973	N-S	0.723	0.702	0.640		
n = 1832 days, 74 series	N 45	± 0.006	0.036	0.027		
5.4.1967 - 5. 7.1973	N-S	0.632	0.676	1.214		
n = 1270 days, 42 series	N 87	± 0.015	0.036	1.439		
A theoret. (m. sec.)		7.850	3.652	1.513	0.770	1.084
$\gamma_{N-S} = \frac{\frac{\gamma_i \cdot l_i}{\varepsilon_i^2}}{\frac{l_i}{\varepsilon_i^2}}$		0.714 ± 0.007	0.692 0.036	0.641 0.028		

As is seen from Table 1 for the components E-W the γ-value for diurnal waves (O_1 and K_1) proved to be systematically smaller than for semi-diurnal waves (M_2, S_2, N_2).

No inequality of the amplitude the γ-factor for the M_2 wave in the N-S and E-W directions is observable within the limits of measurement errors $\gamma_{N-S} - \gamma_{E-W} = -0.0033$.

Following the results of the determination of γ for the diurnal waves O_1 and K_1 the mean values of $\gamma_{O_1} - \gamma_{K_1}$ are also obtained characterizing the

effect of the Earth's liquid core on the Earth's tides :

$$\gamma_{O_1} - \gamma_{K_1} = -0,033 \pm 0,028 \quad \text{(N33- E-W)}$$

$$\gamma_{O_1} - \gamma_{K_1} = -0,042 \pm 0,017 \quad \text{(N85 E-W)}$$

These data are in good agreement with the calculations made by M.S. Molodensky, who obtained for the most reliable Earth's models :

$$\gamma_{O_1} - \gamma_{K_1} = -0,046 \quad \text{(model I)}$$

$$\gamma_{O_1} - \gamma_{K_1} = -0,044 \quad \text{(model II)}$$

The values of χ-phase displacements are given in Table 2. The (-) sign corresponds to the observed tide lag calculated theoretically.

TABLE 2

$\chi = \phi_{obser.} - \phi_{theoret.}$ values for different waves.

N° N°	wave / epoch	O_1	K_1	M_2	S_2
N 33 E-W	31.3.67 - 19.10.1973 n = 1657	0°695 ± 1°550	1°254 ± 1°733	-2°992 ± 1°104	-2°173 ± 1°589
N 85 E-W	31.3.67 - 12. 8.1973 n = 1068	-5°402 ± 3°149	-3°603 ± 1°313	-5°388 ± 2°032	-2°194 ± 2°707
E-W	$\chi_{E-W} = \frac{\sum_i \frac{x_i l_i}{\varepsilon_i^2}}{\sum_i \frac{l_i}{\varepsilon_i^2}}$	-1°226 ± 1°764	-1°302 ± 1°512	-3°371 ± 1°251	-3°081 ± 1°791
N 45 N-S	31.3.67 - 8.12.1973 n = 1832			3°371 ± 1°251	
N 87 N-S	5.4.67 - 5. 7.1973 n = 1270			5°675 ± 1°492	
N-S	$\chi_{N-S} = \frac{\sum_i \frac{x_i l_i}{\varepsilon_i^2}}{\sum_i \frac{l_i}{\varepsilon_i^2}}$			4°071 ± 0°860	

For diurnal and semi-diurnal tides the χ-value has the minus sign and for the main wave M_2 in the N-S direction the positive sign. This is explained by the fact that the mountain massiv in which the tunnel is cut extends from East to West and is subject to temperature deformations capable of disturbing the tiltmeters recording in the N-S azimuth.

As is known, materials of the Earth's tide observations are disturbed by the periodical deflection of the Earth's crust under the load effect caused by the oceanic tides. At our request B.P. Pertsev kindly agreed to calculate the oceanic tidal correction for tiltmeter and gravimetric observations in Tbilisi.

The γ and χ values without and with oceanic tidal correction are given below.

TABLE 3

The γ and χ values with and without oceanic tidal correction

component	Paramet. γ or χ	With oceanic tidal effect	without oceanic tidal effect
E-W	γ_{M_2}	0,711 ± 0,010	0,726
	γ_{S_2}	0,731 ± 0,019	0,731
	γ_{O_1}	0,677 ± 0,019	0,675
	γ_{K_1}	0,696 ± 0,019	0,698
	χ_{M_2}	-1°,226 ± 1°,764	-1°,002
	χ_{S_2}	-1°,302 ± 1°,512	-1°,223
	χ_{O_1}	-3°,371 ± 1°,251	-2°,595
	χ_{K_1}	-3°,081 ± 1°,791	-0°,712
N-S		0,714 ± 0,007 4°,071 ± 0°,860	0,723 3°,305

As seen from Table 3 the oceanic tide correction for the γ factor totals approximately 2 % of this factor for the M_2 wave in the E-W and N-S main

directions; this correction is practically insignificant for other waves. For the value of χ corrections for oceanic tides are more considerable but for K_1 it amounts to approximately 2",4.

From the data of Table 3 it is seen that no inequality of the amplitude factor for the M2 wave in the N-S and E-W directions is observable within the limits of measurement errors.

$$\gamma_{N-S} - \gamma_{E-W} = 0{,}003 \text{ (without oceanic tidal effect)}$$
$$\gamma_{N-S} - \gamma_{E-W} = -0{,}003 \text{ (with oceanic tidal effect).}$$

As the main M_2 lunar determaind most accurately we use the results only for this wave in order ot obtain the final value of γ for Tbilisi.

$$\gamma_{E-W} = 0{,}711 \pm 0{,}010$$
$$\gamma_{N-S} = 0{,}714 \pm 0{,}007 \qquad \text{with oceanic tidal effect}$$

$$\gamma_{E-W} = 0{,}726$$
$$\gamma_{N-S} = 0{,}723 \qquad \text{without oceanic tidal effect}$$

Consideration of the drifts of tiltmeters over the period of investigation (1967-1973) as well as the use of the results of repeated annual levellings allows to establish the fact that the mean annual inclination of the given point does not exceed 0".5. The complete inclination for that period in the N-S azimuth in the southern direction is 0",4 and for the E-W azimuth 3".0 in the western direction.

b) Extensometer observations.

Recording of tidal deformations has been carried out with the aid of two interpendicular extensometers, with bases of 42 a 14.5 m each. Till 1976 the recording was carried out by the method of photooptics, and since 1976 with the aid of capacitive transducer. Application of a capacitive transducer allowed to increase the extensometer sensitivity by approximately one order. In Table 4 are given the amplitudes of five main tidal waves for the N 30°W azimuth, obtained from many year's observations by the photooptical method. The same table also gives the same values obtained from 47-day observations with a capacitive transducer. It should be noted that a longer series of observations obtained with the aid of a capacitive transducer with two components are now being processed.

TABLE 4

Mean values of tidal wave amplitudes in mm.

(extensometer N 30°W)

transducer	M_2	S_2	N_2	O_1	K_1
photooptics $K = 0,7 \cdot 10^{-8}$/mm	0,98 ± 0,03	0,50 ± 0,02	0,21 ± 0,03	0,50 ± 0,03	0,48 ± 0,02
Capacitive $K = 0,57 \cdot 10^{-9}$/mm	12,19 ± 0,21	7,53 ± 0,17	2,48 ± 0,23	5,02 ± 0,47	13,18 ± 0,57

During the 1965-1973 period the deformation in the N 60°E direction amounted to $11.9 \cdot 10^{-6}$ (compression) and in the N 30°W direction $-14.7 \cdot 10^{-6}$ (extension).

c) Gravimetric observations.

Since 1976 observations of tidal variations have been resumed. For this purpose gravimeter GS-11 N° 166 with an electronic amplifier (Keithley Instruments 150B) and compensation self-recorder of the firm Kipp and Zonen BD5 are used.

For the present communication we used the data of 72 days observations. The processing was carried out by the monthly method of harmonic analysis developed by P.S. Pertsev according to the running program with central day's displacement in a day. 41 values of $\delta = 1 + h - \frac{3}{2} k$ for the five main tidal waves by these results in Table 5 are given.

$$\delta = 1 - \frac{3}{2} + h \quad (6.IX.1976\text{-}15.XI.1976)$$

$$C = 3,7695 \ \mu gal/mm$$

TABLE 5

	M_2	S_2	N_2	K_1	O_1
without oceanic tidal correction	1,195 ± 0,003	1.133 ± 0,004	1.195 ± 0,014	1.211 ± 0,003	1.118 ± 0,004
with oceanic tidal correction	1,179	1,126	—	1,219	1,123